



International School of Advanced Studies

Area of Neuroscience

Curriculum in Functional and Structural Genomics

Neuronal hemoglobin:  
new insights into the mechanism of  $\alpha$ -synuclein pathogenicity

Thesis submitted for the degree of “Doctor of Philosophy”

Candidate  
Chiara Santulli

Supervisor  
Prof. Stefano Gustincich

26<sup>th</sup> November 2018

## **DECLARATION**

The work described in this thesis was carried out at International School for Advanced Studies (SISSA), Trieste, between November 2014 and November 2018 with exception of Atomic Force Microscopy, that was performed by Pietro Parisse, PhD, and Fabio Perissinotto, PhD, at Elettra Sincrotrone Trieste.

$\alpha$ -syn preparations were kindly provided by Prof. Legname's group.

## TABLE OF CONTENTS

List of figures .....	1
ABSTRACT .....	4
1 INTRODUCTION .....	5
1.1 Synucleinopathies .....	5
1.1.1 Overview .....	5
1.1.2 Epidemiology .....	5
1.1.3 Neuropathological and clinical features .....	6
1.1.4 Aetiology .....	11
1.2 $\alpha$ -synuclein .....	15
1.2.1 $\alpha$ -synuclein structure .....	15
1.2.2 $\alpha$ -synuclein misfolding and aggregation .....	16
1.2.3 Prion-like spreading .....	17
1.2.4 Challenges to the spreading theory and alternative hypotheses .....	20
1.2.5 Function .....	21
1.2.6 Post-translational modifications .....	22
1.3 Hemoglobin .....	29
1.3.1 The globin family .....	29
1.3.2 Hemoglobin: from gene to protein .....	30
1.3.3 Function .....	33
1.3.4 Hemoglobin disorders .....	35
1.3.5 Expression in nonerythroid locations .....	36
2 MATERIALS AND METHODS .....	41
2.1 Production of recombinant human $\alpha$ -synuclein .....	41
2.2 Fibrillation of human $\alpha$ -synuclein .....	41
2.3 Atomic Force Microscopy .....	41
2.4 Cell line .....	42
2.5 Transfection .....	42
2.6 Co-immunoprecipitation .....	42
2.7 Exposure of iMN9D cells to $\alpha$ -syn monomers and fibrils .....	43

2.8	Antibodies validation for quantitative western blot.....	43
2.9	Biotinylated fibrils pulldown .....	43
2.10	Cathepsin D and Calpain inhibitors treatment .....	44
2.11	Cathepsin D activity assay .....	44
2.12	MTT analysis .....	45
2.13	Western Blot .....	45
2.14	Immunocytochemistry .....	46
2.15	Immunofluorescence with labelled a-syn fibrils.....	46
2.16	Statistical Analysis.....	47
3	RESULTS .....	48
3.1	Previous data obtained in the laboratory of Professor Gustincich.....	48
3.2	Experimental model .....	49
3.3	Hb and $\alpha$ -synuclein interact in transfected cells.....	49
3.4	Characterization of $\alpha$ -synuclein preparations .....	51
3.5	Antibodies validation for quantitative western blot.....	52
3.6	Sonicated $\alpha$ -synuclein fibrils are internalized by iMN9D cells and are phosphorylated at serine 129 .....	54
3.7	Cytotoxicity of $\alpha$ -synuclein preparations .....	56
3.8	Hb triggers the accumulation of a C-terminal truncated form of $\alpha$ -syn .....	57
3.9	$\Delta$ C- $\alpha$ -syn accumulation is not mediated by Hb binding.....	59
3.10	Effect of Calpains inhibition on $\alpha$ -syn C-terminal truncated species accumulation .....	60
3.11	Effect of Cathepsin D inhibition on the accumulation of $\alpha$ -syn C-terminal truncated species .....	62
	DISCUSSION .....	64
	BIBLIOGRAPHY .....	67

## List of figures

<b>Figure 1.</b> $\alpha$ -synuclein inclusions found in synucleinopathies. ....	7
<b>Figure 2.</b> Progression of the pathology in the four major clinical phenotypes of PD. ....	8
<b>Figure 3.</b> Progression of the pathology in the two major clinical phenotypes of MSA. ....	9
<b>Figure 4.</b> Human $\alpha$ -syn structure. ....	15
<b>Figure 5.</b> Schematic representation $\alpha$ -syn conformations in physiological and pathological conditions. ....	16
<b>Figure 6.</b> Potential mechanisms of $\alpha$ -syn spreading. ....	20
<b>Figure 7.</b> Schematic outline of vertebrate globins expression, functions and phylogenetic features. <sup>255</sup> ....	30
<b>Figure 8.</b> Developmental switches in globin expression and $\alpha$ - and $\beta$ - globin gene clusters. ....	31
<b>Figure 9.</b> Hemoglobin structure. ....	32
<b>Figure 10.</b> Hb-O <sub>2</sub> binding. ....	33
<b>Figure 11.</b> Atypical localization of Hb and its putative functions. Modified from Rahaman <i>et al.</i> <sup>255</sup> ....	36
<b>Figure 12.</b> Mouse dopaminergic cell line (iMN9D) stably overexpressing $\alpha$ - and $\beta$ -chains of Hb. ....	49
<b>Figure 13.</b> $\alpha$ -syn and Hb binding in iMN9D cells. ....	50
<b>Figure 14.</b> Biochemical analysis and structural characterization of $\alpha$ -syn preparations. ....	52
<b>Figure 15.</b> Linearity of immunodetection of housekeeping and target proteins in iMN9D cell lysates. ....	53
<b>Figure 16.</b> Sonicated $\alpha$ -synuclein fibrils are internalized by iMN9D cells. ....	55
<b>Figure 17.</b> iMN9D cells show pSer129 positive inclusions after $\alpha$ -syn PFFs treatment. ....	56
<b>Figure 18.</b> Cytotoxicity of $\alpha$ -syn preparation in iMN9D cells. ....	57
<b>Figure 19.</b> C-terminal truncated $\alpha$ -syn accumulation in the presence of Hb in cell lysates. ....	58
<b>Figure 20.</b> C-terminal truncated $\alpha$ -syn accumulation in the presence of Hb in cell media. ....	59
<b>Figure 21.</b> Pull down of biotinylated PFFs in iMND cell lysate. ....	60
<b>Figure 23.</b> Effect of Calpains inhibition on $\alpha$ -syn C-terminal truncated species accumulation in Hb cells. ....	61
<b>Figure 24.</b> Effect of Cathepsin D inhibition on $\alpha$ -syn C-terminal truncated species accumulation in Hb cells. ....	63

## **Abbreviations**

Amino acid, aa

C-terminal truncated species of  $\alpha$ -synuclein,  $\Delta$ C- $\alpha$ -syn

Calpain1, Capn1

Calpain2, Capn2

Caspase-1, Cas1

Cathepsin B, CatB

Cathepsin D, CatD

Cellular Prion Protein, PrPC

Cerebellar MSA, MSA-C

Dementia with Lewy bodies, DLB

Dopamine, DA

Glial cytoplasmic inclusions, GCIs

Hemoglobin, Hb

Immunofluorescence, IF

Lewy bodies, LBs

Lewy neurites, LN

Matrix metalloproteinases, MMP

Methemoglobin, methHb.

Multiple system atrophy, MSA

Nitric oxide, NO

Non-amyloid-beta component, NAC

Parkinson's disease, PD

Parkinsonian MSA, MSA-P

Passage 1, P1.

Pepstatin, PepA

Quantitative RT-PCR, qRT-PCR

Reactive oxygen species, ROS

Reverse Transcription, RT

Sonicated  $\alpha$ -syn preformed fibrils, PFFs

Striatum, ST

Substantia nigra pars compacta, SNpc

Substantia nigra, SN

Thiazolyl Blue Tetrazolium Bromide, MTT

Thioflavin T, ThT

Western blot, WB

$\alpha$ -synuclein monomers, Ms

$\alpha$ -synuclein phosphorylated at Serine 129, pSer129- $\alpha$ -syn

$\alpha$ -synuclein,  $\alpha$ -syn

## ABSTRACT

$\alpha$ -synucleinopathies are a subset of progressive neurodegenerative disorders that share several features and, above all,  $\alpha$ -synuclein ( $\alpha$ -syn) accumulation. Lewy bodies and neurites are typical of Parkinson's disease (PD) and dementia with Lewy bodies, while Multiple System Atrophy is characterized by the presence of glial cytoplasmic inclusions. Several mechanisms are involved in the pathogenesis of these diseases, ranging from genetic factors, environment, cellular disfunctions to  $\alpha$ -syn misfolding. An increasing number of studies reported that  $\alpha$ -syn is subjected to post-translational modifications within Lewy bodies. Among them, C-terminal truncation seems to increase its aggregation propensity.

Hemoglobin (Hb) genes expression was recently demonstrated in the central nervous system and evidences suggest a putative role as oxygen reservoir and in mitochondrial respiration. Dysregulation of Hb expression has been associated to several neurodegenerative disorders and, in particular, to PD.

Previous data from the laboratory of Prof. Gustincich showed that Hb alters mitochondrial genes expression<sup>1</sup>, confers dopaminergic (DA) cells' susceptibility to MPP<sup>+</sup> and rotenone *in vitro* and impairs performance associated to motor learning *in vivo*<sup>2</sup>. Interestingly, the presence of Hb -  $\alpha$ -syn complexes in the brain of aging cynomolgus monkeys has recently been demonstrated<sup>3</sup>.

In this study, we aimed to unveil the interplay between Hb and  $\alpha$ -syn and its contribution to synucleinopathies. To this purpose, we took advantage of MN9D-Nurr1Tet-On dopaminergic neuroblastoma cell lines (iMN9D) stably transfected with  $\alpha$  and  $\beta$  chains of Hb<sup>1</sup> and  $\alpha$ -syn preformed fibrils (PFFs) as a model of  $\alpha$ -syn pathogenicity.

We first demonstrate that iMN9D cells internalize PFFs and are therefore a suitable system to study  $\alpha$ -syn pathogenicity. Then, we show that PFFs treatment is toxic to cells and leads to the accumulation of  $\alpha$ -syn C-terminal truncated species ( $\Delta$ C- $\alpha$ -syn) triggered in the presence of Hb. Given the relevance of C-terminal cleavage products in terms of  $\alpha$ -syn aggregation and toxicity, we investigate the intracellular proteases likely involved in  $\alpha$ -syn truncation. Among them, we provide evidence that, in our model, calpains are involved in  $\alpha$ -syn truncation.

In conclusion, taken together, these findings strongly support Hb implication in  $\alpha$ -syn processing and, therefore it exerts a significant role in the pathogenesis of  $\alpha$ -synucleinopathies.

# 1 INTRODUCTION

## 1.1 Synucleinopathies

### 1.1.1 Overview

The synucleinopathies are a subset of progressive neurodegenerative disorders characterized by abnormal accumulation of misfolded  $\alpha$ -synuclein ( $\alpha$ -syn) in neurons or glia. These diseases include Parkinson's disease (PD), dementia with Lewy bodies (DLB), multiple system atrophy (MSA) and other related disorders as pure autonomic failure (PAF). They share clinical characteristics like progressive decline in motor functions, cognitive impairment and alteration of autonomic functions, depending on lesions distributions. Therefore, the differential diagnosis is sometimes difficult. They also share neuropathological features. Indeed, they are characterized by selective neuronal vulnerability, neuroinflammation and, as already mentioned,  $\alpha$ -syn burden.

Intracellular  $\alpha$ -syn inclusions are the neuropathological hallmarks as Lewy bodies (LB) and neurites (LN) are typical of PD and DLB, while glial cytoplasmic inclusions (GCIs) in oligodendrocytes are distinctive in MSA.

The pathogenesis is very similar too, with oxidative stress, proteosomal and lysosomal system dysfunction and reduced mitochondrial activity. The etiology is still unknown but it has been hypothesized that both environmental and genetics factors may be involved. Moreover, recent findings about the prion-like behaviour of  $\alpha$ -syn, raised new questions as well as new possible explanations about the pathological basis of these diseases.

In this chapter, we will try to deepen the most important features of synucleinopathies, underlying common as well as different characteristics. Mechanisms underpinning  $\alpha$ -syn misfolding and spreading, will be discussed in the next chapter, that is focused on an in-depth analysis of the biology of  $\alpha$ -syn, as the protein is widely recognized as central player in these disorders.

### 1.1.2 Epidemiology

PD is the second most common neurodegenerative disorder after Alzheimer's disease. Its prevalence is 0.3 % in the general population in industrialized countries, while it increases to 1 % in people older than 60 and 3 % in those older than 80 years. The median age of onset is 60 years and the mean duration from diagnosis to death is 15 years<sup>4</sup>. The main risk factor is aging and male

gender is also recognized as prominent. Indeed, both incidence and prevalence of PD are 1.5 times greater in men than women<sup>4</sup>.

DLB is characterized by the predominance of dementia, as the major symptoms are hallucinations, fluctuations in cognition, spontaneous parkinsonism, and rapid eye movement (REM) sleep behaviour disorder (RBD)<sup>5</sup>. It accounts for approximately 4 to 30 % of dementia cases<sup>5</sup>. Cases are classified as DLB if dementia occurs within 12 months of the parkinsonism. If dementia occurs one year or later from the diagnosis, then it is classified as PD with dementia (PDD)<sup>6</sup>. PDD and DLB share both neurobiological and clinical characteristics and are likely to represent two ends of a disease spectrum, other than two different diseases.

MSA is a rare sporadic disorder presenting a combination of autonomic, cerebellar, parkinsonian and pyramidal features<sup>7</sup>. Depending on the phenotype, it is classified in parkinsonian (MSA-P) or cerebellar (MSA-C) variant. The prevalence has been estimated to be 7.8 patients per 100000 over 40 years of age<sup>7</sup>. The mean age at onset of the first symptoms is 52-57 years<sup>8</sup>.

### 1.1.3 Neuropathological and clinical features

#### *$\alpha$ -syn inclusions*

The major hallmark of synucleinopathies is  $\alpha$ -syn accumulation. Specifically, LBs were first described by Friedrich Heinrich Lewy as eosinophilic spherical or kidney-shaped inclusions composed of dense granular material and filaments that are 10-15 nm in diameter. They are present in neuronal cell bodies and contain several proteins, including  $\alpha$ -syn, ubiquitin, parkin, UCHL1 and others<sup>9</sup>. LNs instead are axonal accumulation of the same proteins as in LBs.  $\alpha$ -syn adopts  $\beta$ -sheet rich conformation and 90 % of its aggregated form is phosphorylated at serine 129<sup>10</sup>. Moreover, LBs contain C-terminal truncated species of  $\alpha$ -syn ( $\Delta$ C- $\alpha$ -syn), representing 15 % of all  $\alpha$ -syn in the inclusions<sup>11</sup>.

GCI are nonmembrane-bound cytoplasmic inclusions composed of 10-20 nm diameter filaments, similar to those seen in LBs. They can be triangular, sickle, half-moon, oval, or conical in shape and only appear in oligodendrocytes<sup>12</sup>. They also contain mainly  $\alpha$ -syn, both in its full length and truncated forms, ubiquitin and many other proteins<sup>12</sup>.  $\Delta$ C- $\alpha$ -syn has also been found in the brain of healthy individuals<sup>13-20</sup>.

The pathways leading to  $\alpha$ -syn accumulation and spreading will be discussed in the second chapter of this thesis, after a thorough review on  $\alpha$ -syn structure and its misfolding properties.

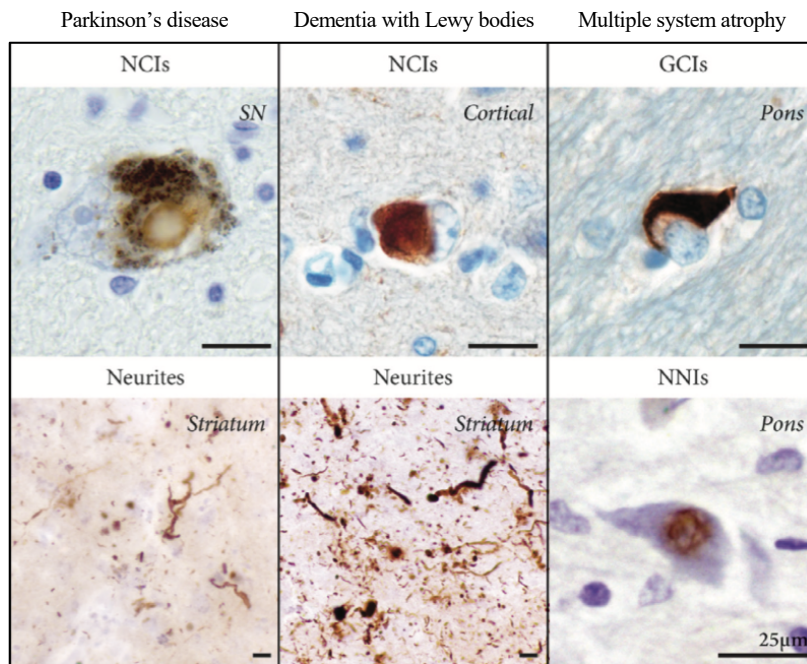


**Figure 1.**  $\alpha$ -synuclein inclusions found in synucleinopathies.

Both PD and DLB have intraneuronal  $\alpha$ -syn inclusions and neurites (LBs and LNs), while MSA has glial cytoplasmic inclusions (GCIs) and neuronal intranuclear inclusions (NNIs).  $\alpha$ -syn immunoreactive structures counterstained with cresyl violet are reported. NCIs, neuronal cytoplasmic inclusions; SN, substantia nigra. Modified from McCann *et al.*<sup>21</sup>

### *Selective neuronal vulnerability*

The principal aspect of PD is the degeneration of DA neurons in the substantia nigra pars compacta (SNpc), resulting in the reduction of dopamine in the basal ganglia in the posterior putamen. Together with disease progression, neuronal degeneration spreads to anterior striatum/caudate, limbic nuclei, and neocortical regions<sup>22</sup>. This leads to the clinical manifestation of the disease: resting tremor, rigidity, bradykinesia and impairment of postural reflexes. Importantly, non-motor manifestations also appear and include impairment of cognition, ranging from mild dysfunction to dementia in the later stages. In particular, non-motor symptoms may precede the formal diagnosis by decades. According to the Braak hypothesis, LBs and LNs are present in multiple location causing pre-motor symptoms prior to their spreading to brain areas, where they cause motor impairment.

In stages I and II, LBs and LNs are present in the olfactory region, dorsal motor nucleus of the vagus nerve and locus coeruleus. This is responsible for autonomic dysfunction, REM sleep behaviour disorder (RBD), depression, and olfactory impairment. In stage III and IV,  $\alpha$ -syn pathology spreads to SNpc, basal forebrain, entorhinal cortex and hippocampus. This coincides with the onset of the typical motor symptoms. Stage V and VI involve temporal, frontal and

parietal cortex and, as consequence, cognitive decline and dementia<sup>23</sup>. Autopsy studies show the presence of  $\alpha$ -syn inclusions at the periphery, including gastrointestinal nerve plexuses and sympathetic ganglia<sup>24,25</sup>. The progression of Lewy-related pathology in DLB occurs in a similar fashion as PD.

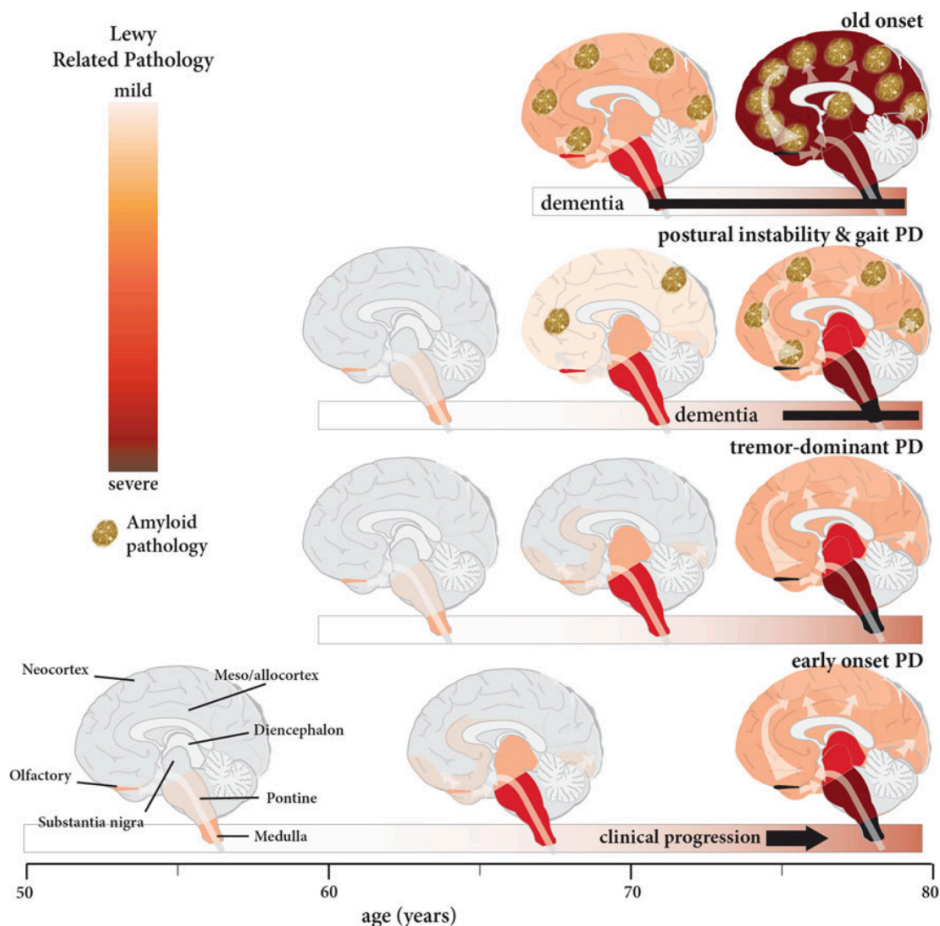


**Figure 2.** Progression of the pathology in the four major clinical phenotypes of PD. Modified from Halliday *et al.*<sup>6</sup>

In the case of MSA, different patterns of neuronal loss can be observed. The relationship between GCIs and neurodegeneration is debated. Striatonigral degeneration is predominant in MSA-P, with loss of DA neurons in SNpc and GABAergic neurons in the caudate-putamen<sup>7</sup>. Akinesia correlates with the grade of the disease in the putamen, globus pallidus and SN, while rigidity correlates with changes in the putamen<sup>6</sup>. In MSA-C, the symptomology is linked to neuronal loss in the inferior olives, pontine nuclei and in Purkinje cells. Neocortical neuronal loss has also been observed and linked to cognitive deterioration<sup>7</sup>.

While a positive correlation between the density of GCIs and neuronal loss has been reported in some cases, no difference in the density of GCIs has been observed in the two forms of the pathology. Moreover, Purkinje cells have never been reported to contain GCIs, indicating that neuronal loss is not simply determined by inclusion formation. Degeneration of the intermediolateral columns and Onuf's nucleus of the sacral spinal cord are characteristics of spinal cord degeneration, leading to autonomic failure<sup>7</sup>. Cognitive impairment is present in 14-18 % of cases but the neuropathological basis are unknown<sup>6</sup>. In addition, severe myelin lesions have been reported to occur predominantly in MSA-C<sup>7</sup>.

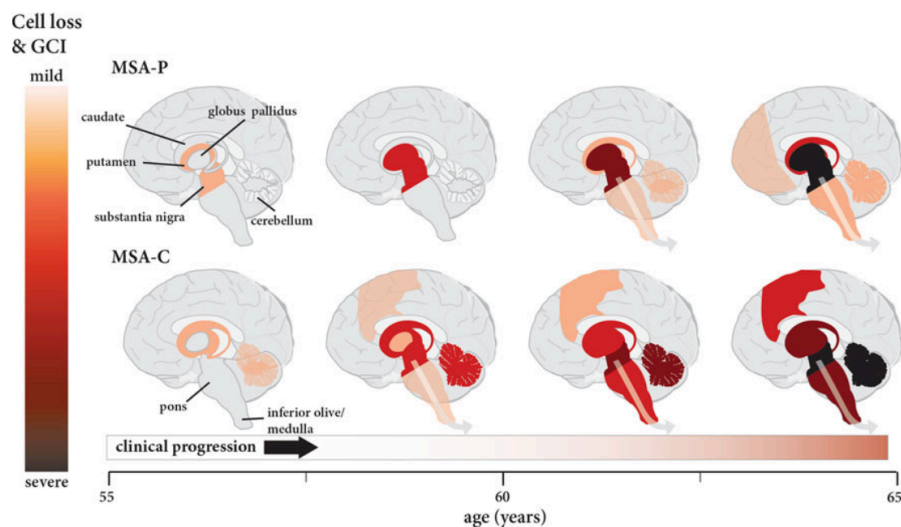


**Figure 3.** Progression of the pathology in the two major clinical phenotypes of MSA. Modified from Halliday *et al.*<sup>6</sup>

Since it is still not clear if  $\alpha$ -syn accumulation precedes cell loss or vice versa, it can be hypothesized that  $\alpha$ -syn inclusions are the toxic agents leading neurodegeneration. On the other hand, they may have a useful role in protecting cells by removing potentially cytotoxic proteins and delaying neuronal loss<sup>26</sup>.

### *Gliosis*

Characteristic features of neuroinflammation include activated microglia, reactive astrocytes within the brain parenchyma and the release of numerous inflammatory mediators. Although previously considered as response to neurodegeneration, neuroinflammation was recently found to be one of the key players of neurodegenerative disorders. Reactive microgliosis and astrogliosis can lead to reactive oxygen species (ROS) and nitric oxide (NO) production, cytokines release

and, therefore, can be detrimental to neurons. Oligodendrocytes are highly vulnerable to oxidative stress and cytokines, resulting in demyelination and cellular dysfunction<sup>8</sup>.

Microglial activation, through the expression of MHC class II molecules, has been observed in all synucleinopathies and in animal model of  $\alpha$ -syn toxicity<sup>27</sup>. While  $\alpha$ -syn immunoreactive astrocytes and oligodendrocytes appear in synucleinopathies<sup>10</sup>, microglial cells don't accumulate  $\alpha$ -syn but degrade it. So on the one hand, microglial cells clear  $\alpha$ -syn and, on the other,  $\alpha$ -syn triggers microglial activation and neuronal death<sup>8</sup>. In PD, activated microglia have been observed in the proximity of degenerating DA neurons and the suppression of activation leads to reduction in neuron degeneration<sup>28</sup>. Several studies show that treatment with exogenous  $\alpha$ -syn leads to inflammatory responses in microglia cultures both from human and rodents. In particular, these studies show that  $\alpha$ -syn is capable of activating microglia and causing ROS and cytokine production<sup>28</sup>. Moreover, evidences have been raised that neuron-released  $\alpha$ -syn binds Toll-like receptor 2 (TLR2), that mediates both the uptake of  $\alpha$ -syn and the signaling leading to inflammation<sup>28</sup>.

Astrocytic gliosis has been shown in  $\alpha$ -syn transgenic mice, corroborating the connection between astroglial pathology and neurodegeneration. On the other hand, astroglial cells also seem to exert a beneficial function as they release neurotrophic factors<sup>8</sup>. An involvement of oligodendrocytes in disease initiation and progression in PD e DLB lacks sufficient evidence at present<sup>8</sup>.

In MSA neuronal inflammation is more prominent than PD. First, oligodendrocytes are considered key players in MSA, due to the presence of  $\alpha$ -syn inclusions. Indeed, they could be the initiators of the disease. Moreover, microglia activation accompanies GCIs pathology in the affected areas of the brain. Microgliosis has been reported in dorsolateral prefrontal cortex, putamen, pallidum, pons and SN<sup>29</sup> and motor-related regions including cerebellar input, extrapyramidal motor and pyramidal motor structures<sup>30</sup>. In mice, microglia activation results in neuroinflammation, oxidative stress and DA neurons loss, similarly to PD. Upregulation of Toll-like receptor 4 (TLR4) has been shown<sup>28</sup>. In contrast to PD and DLB,  $\alpha$ -syn accumulation has not been reported in astroglia. Morphological changes appear leading to enlarged cell bodies and distorted processes. But few data are available at present.

In summary, glia activation may contribute to the progression of PD and DLB as well as MSA.

### *Iron accumulation*

Iron is one of the most abundant element in the human body. It is required for fundamental functions as ATP production, DNA replication and myelin formation. It is also a co-factor of many enzymes as cytochrome c oxidase, catalase and oxygenase. Thanks to its redox properties, it causes the production of ROS through the Fenton reactions, resulting in oxidative stress and peroxidation of membranes<sup>31</sup>. Iron concentration in brain increases with age and it is highly abundant in the nucleus accumbens, deep cerebellar nuclei, red nucleus and parts of the hippocampus as well as the SN. In PD patients, it is particularly high in the SN and the putamen and its accumulation correlates with the disease severity<sup>31</sup>. So it has been suggested to be responsible for nigrostriatal DA neurons degeneration. Iron binds  $\alpha$ -syn in its C-terminal region and increases its propensity to aggregate<sup>32</sup>. Imbalance of iron storage and removal, may also contribute to its accumulation. Moreover, neuromelanin, a reservoir of iron, is present in the SN and has been linked to vulnerability in PD<sup>33</sup>. Similar findings have been reported also in brains of MSA patients<sup>34</sup>, corroborating the notion that iron accumulation and oxidative stress are common features in synucleinopathies.

#### 1.1.4 Aetiology

Aetiology of synucleinopathies is still elusive and probably interactions between genetic and environmental factors are causative.

Sporadic PD represents above 90% of cases while the remaining ones are inheritable<sup>10</sup>. Several loci have been associated to the disease risk and are together classified as *PARK* loci. Gene duplication and triplication of SNCA gene, assigned as *PARK4*, cause autosomal dominant PD with variable penetrance, resulting in individuals carrying either three or four copies of the SNCA gene and, therefore, increased  $\alpha$ -syn protein production. Triplication results in early onset PD of around 40 years, while duplication leads to typical PD with an earlier age at onset<sup>35</sup>.

SNCA point mutations (A53T, A30P and E46K) are assigned as *PARK1*. Patients with A30P mutation manifest symptoms similar to those with sporadic PD, while E46K carriers display a severe parkinsonism and diffuse LB dementia<sup>36</sup>. Recently, other SNCA mutation have been identified (A53E, A18T, G51D, A29S and H50Q). A53T, H50Q, and E46K mutations have been shown to increase  $\alpha$ -syn aggregation, while A30P, G51D and A53E mutations seem to reduce the aggregation properties and inhibit lipids binding<sup>37</sup>. Individuals carrying G51D and A53E mutations have features of both PD and MSA<sup>10</sup>.

The *LRRK2* (*PARK8*) gene encodes a multi-domain protein kinase. At least 128 mutations have been identified in the *LRRK2* gene and are recognized as the most common genetic cause of familial PD<sup>36</sup>. *LRRK2* mutations are also involved in sporadic PD<sup>36</sup>. The neuropathology of *LRRK2* is highly heterogeneous. Elevated kinase and decreased GTPase activities are thought to be responsible of the pathogenicity of *LRRK2* mutations<sup>36</sup>.

*Parkin* (*PARK2*) encodes an E3 ligase associated with the ubiquitin-proteasome system. Its mutations compromise its role as enzyme and are well established risk factors for early-onset PD. Dosage mutations are likely more pathogenic than point mutations<sup>35</sup>. The majority of cases of parkin-related PD are not associated with inclusion formations<sup>36</sup>.

Parkin is involved in removing damaged mitochondria via mitophagy together with *PINK1* (PTEN-induced putative kinase 1), another PD-related gene causing early-onset PD. Deficiency in parkin or *PINK1* function can result in mitochondrial dysfunction, as in several mouse models bearing this mutations, underpinning the importance of mitochondrial homeostasis in PD<sup>36</sup>.

Another mitochondrial related gene associated to PD, is *High-temperature requirement A2* (*HTRA2/OMI*). It is involved in the proteolysis of misfolded and damaged proteins targeted for mitochondrial intermembrane space. Furthermore, it is released from mitochondria in response to apoptotic stimuli and induces apoptosis<sup>38</sup>.

*PARK7* (*DJ-1*) mutations are rare and account for less than 1% of early-onset PD. From a clinical point of view, the phenotype is very similar to those of parkin and *PINK1* mutations, with slow progression and good response to levodopa<sup>36</sup>. *DJ-1* is a molecular chaperone and acts as scavenger of mitochondrial H<sub>2</sub>O<sub>2</sub>. *DJ-1* deficiency predisposes to oxidative stress and can exacerbate neuronal degeneration<sup>36</sup>.

Another evidence for the role of mitochondrial dysfunction in PD, arises from the identification of heterozygous mutation of another mitochondrial related gene. Indeed the *coiled-coil-helix-coiled-coil-helix domain 2* (*CHCHD2*) gene has been found mutated in a Japanese family with autosomal dominant PD. *CHCHD2* binds the subunit 4 of cytochrome C oxidase (*COX4*) and the interaction plays a key role in maintaining energy balance in neurons during hypoxia. Moreover, *CHCHD2* acts as apoptosis regulator by binding to Bcl-xL<sup>38</sup>.

*PARK5* (*UCHL1*) is a deubiquitinating enzyme playing an important role in ubiquitin-dependent proteolysis by recycling polymeric chains to monomeric ubiquitin. I93M mutation has been identified in an autosomal dominant form of PD and leads to decreased hydrolase activity<sup>36</sup>. The S18Y variant is inversely associated with PD, particularly in younger subjects<sup>39</sup>.

An autosomal recessive early-onset forms of PD has been associated to mutations in *vacuolar protein sorting 13C* (VPS13C) gene, but the molecular pathway implicated are currently unknown<sup>38</sup>.

*ATPase type 13A2* (ATP13A2) has been associated with a severe early-onset PD. ATP13A2 encodes for a lysosomal transmembrane protein of unknown function, highly expressed in neurons. Its downregulation in cells, leads to impaired lysosomal proteolysis function, a defect tightly associated with  $\alpha$ -syn accumulation and mitochondrial dysfunction<sup>38</sup>.

*Phospholipase A2 group 6* (PLA2G6) has been identified as causative gene in different neurodegenerative diseases. The encoded protein is involved in phospholipids metabolism. It has been demonstrated that PLA2G6 knocking out leads to defects in remodelling of mitochondrial inner membrane and presynaptic membrane and causes mitochondrial dysfunction, age-dependent degeneration of DA nerve terminals, synaptic dysfunction, and significant iron accumulation in mice brains<sup>38</sup>.

Mutations in the *vacuolar protein sorting 35* (VPS35) gene have been reported as novel causes of autosomal dominant PD. It encoded a core component of the retromer cargo-recognition complex and plays a critical role in cargo retrieving pathway from the endosome to the trans-Golgi network<sup>38</sup>.

*F-box protein 7* (FBXO7) has been identified as causative gene in autosomal dominant early-onset PD, although the exact mechanism by which it contributes to the pathology is unknown<sup>38</sup>.

Interestingly, mutations in *Eukaryotic translation initiation factor 4 gamma, 1* (EIF4G1) gene are also associated to PD. EIF4G encodes for a scaffold protein that acts as key initiator factor in mRNA translation. Therefore, mutations in EIF4G1 could lead to mRNA translation impairment<sup>38</sup>.

CAG repeat expansions within the coding region of *Ataxin-2* (ATXN2) gene have been linked to PD, lately. Recent studies in *Drosophila* suggest that ATXN2 may be involved in mRNA transport and stability in neurons. Mutations in this gene could also lead to mRNA translation impairment and trigger DA neurons degeneration<sup>38</sup>.

*DNAJC6* and *DNAJC13* are involved in endocytosis and transport of clathrin coating of vesicles and mutations in both genes have been reported<sup>38</sup>.

The *SYNJI* gene has been reported to cause juvenile-onset atypical PD. It encodes a presynaptic protein involved in the regulation of synaptic vesicle endocytosis. A recent study in mice showed that *SYNJI* mutations impair the endocytic recycling pathway and therefore result in

the accumulation of proteins at synaptic terminals. This selectively causes in dystrophic DA axon terminals in the dorsal striatum<sup>38</sup>.

Heterozygous mutations of glucocerebrosidase (*GBA*) gene have been linked to increased risk of developing PD<sup>35</sup> and DLB<sup>40</sup>.

Mutations of the *COQ2* gene have been linked to MSA, but only in Japanese families<sup>41</sup>.

Environmental factors are also known to play a role, in particular in PD onset. Indeed exposure to 1-methyl-4-phenyl-1,2,3,6- tetrahydropyridine (MPTP), results in parkinsonism<sup>42</sup>. Exposure to herbicides and pesticides (paraquat and rotenone) is associated with elevated risk of PD<sup>43</sup>. The role of ROS in synucleinopathies pathogenesis has been already analyzed in the previous section.

As regards MSA, limited number of studies on its aetiology is currently available as the disease is rare and underdiagnosed.

## 1.2 $\alpha$ -synuclein

### 1.2.1 $\alpha$ -synuclein structure

$\alpha$ -synuclein ( $\alpha$ -syn) is a 140 amino acid protein that is highly expressed in the nervous system, representing 1% of all cytosolic proteins in brain<sup>44</sup>. It has been classified as an intrinsically disordered protein (IDP), due to the undefined structure of its monomeric form in solution<sup>45,46</sup>. Nevertheless, recent studies provide evidence that endogenous  $\alpha$ -syn exists as an  $\alpha$ -helically folded tetramer under physiological conditions, thus questioning the longstanding notion of the natively unfolded structure of  $\alpha$ -syn<sup>47,48</sup>.

The N-terminal region (1-60 aa) is almost entirely composed of four imperfect 11-aa repeats, each containing a conserved XKTKEGV hexameric motif, which strongly resembles the one found in the  $\alpha$ -helical domain of apolipoproteins. These repeats are responsible for  $\alpha$ -syn-lipid interactions<sup>49–53</sup>. Depending on the membrane curvature, the N-terminus adopts either a single elongated or a broken  $\alpha$ -helical conformation upon binding<sup>54–56</sup>.

The central region (61–95 aa) includes three additional repeats and the non-amyloid-beta component (NAC). The latter is responsible for  $\alpha$ -syn aggregation and  $\beta$ -sheet formation<sup>57–59</sup>.

The C-terminal domain (96-140 aa) regulates fibril formation. In particular, the negatively charged residues 104, 105 and 114, 115 were suggested to be responsible for the reduced aggregation and the lack of seeding of full-length  $\alpha$ -syn<sup>60</sup>. Moreover, it modulates the interactions with membrane<sup>61</sup> and more than 30 different proteins<sup>62</sup> and ions<sup>63</sup>.

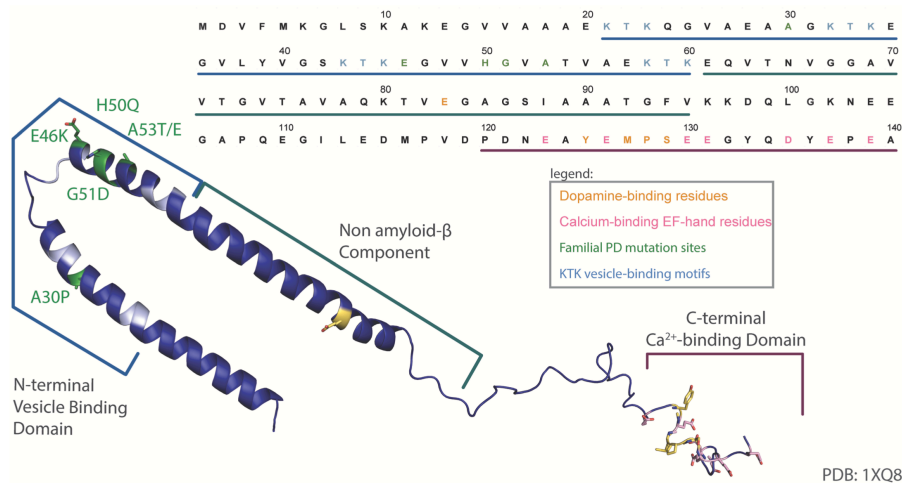


**Figure 4.** Human  $\alpha$ -syn structure.

Annotated structure of human micelle-bound  $\alpha$ -syn solved by solution NMR<sup>64</sup> and sequence have been color coded to highlight the lipid motifs (cyan), common familial PD mutations (green),  $\text{Ca}^{2+}$ -binding motif (pink), and the dopamine-binding residues (yellow).<sup>65</sup>

### 1.2.2 $\alpha$ -synuclein misfolding and aggregation

While unstructured or only partially folded under physiological conditions,  $\alpha$ -syn can undergo structural rearrangement into  $\beta$ -sheet rich secondary structures, leading to the formation of amyloid assemblies<sup>66,67</sup>. Indeed, under certain conditions,  $\alpha$ -syn soluble monomers form metastable oligomeric intermediates, also known as fibril nuclei or seeds<sup>68,69</sup>, which are in a dynamic equilibrium with the monomeric form. Once  $\alpha$ -syn seeds have been formed, they recruit endogenous soluble monomers, providing a template for the formation of highly ordered protein aggregates through a nucleation-dependent mechanism, leading to the formation of protofibrils, that can stack together to form mature amyloid fibrils.

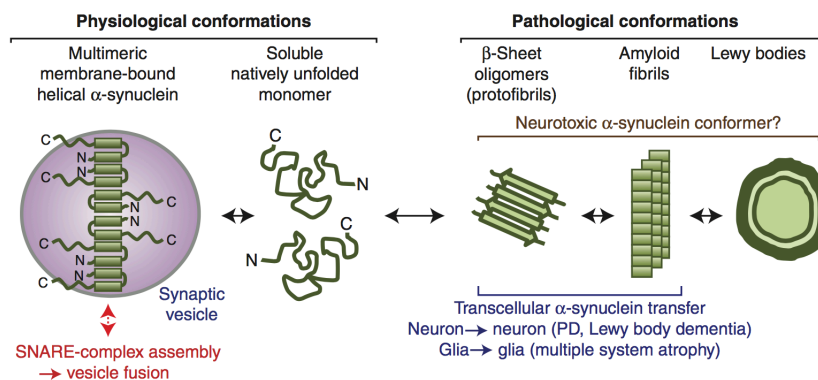


**Figure 5.** Schematic representation  $\alpha$ -syn conformations in physiological and pathological conditions.  $\alpha$ -syn is an intrinsically disordered protein that folds into an amphipathic  $\alpha$ -helix when bound to membranes. Under pathological conditions,  $\alpha$ -syn forms fibrils by converting either all or part of the protein into  $\beta$ -sheet rich secondary structures. Once  $\alpha$ -syn seeds have been formed, they recruit endogenous soluble monomers, providing a template for the formation of highly ordered protein aggregates through a nucleation-dependent mechanism, leading to the formation of protofibrils. Protofibrils can stack together and form mature fibrils and eventually deposit into Lewy bodies. After the seeding, amyloidogenic fibrils are transmitted to other cells where they enhance the aggregation of the endogenous soluble protein as previously reported, leading to the prion-like spreading of the pathology.<sup>70</sup>

During the *in vitro* fibrillization process, heterogeneous species of oligomers and fibrils have been isolated. Spheroidal<sup>71</sup>, annular<sup>72–74</sup> and wreath-shaped oligomers<sup>75</sup> have been reported. Early reports about  $\alpha$ -syn fibrils conformations showed the isolation of twisted and straight filament strands from PD patient brains<sup>76</sup>.

Afterwards, the concept of strain was borrowed from prion research, that in turn derived it from virology<sup>77</sup>. A strain is a genetic variant or subtype of a microorganism responsible for a disease. The concept was adapted to prions, which act as infectious agents themselves. In

particular, a prion strain is a specific type of aggregate with specific biochemical features, disease phenotypes, brain-lesion profiles and incubation periods<sup>78</sup>.

In 2013 Bousset and colleagues generated two different strains, fibrils and ribbons, from the same  $\alpha$ -syn precursor. The resulting assemblies exhibited different grade of toxicity and aggregation and different propensities to bind cell membrane. In addition, both fibrils and ribbons could imprint their structural architecture to endogenous  $\alpha$ -syn *in vivo*<sup>79</sup>, just resembling the behaviour of prion strains. Then Peelaerts and colleagues proved *in vivo* amplification of  $\alpha$ -syn strains after injection in rat brain. Depending on toxicity and seeding capacities, different pathological phenotypes were induced<sup>80</sup>. Afterwards, another group showed that the presence of bacterial endotoxin lipopolysaccharise (LPS) during the *in vitro* fibrillization, led to the formation of a fibril strain with different characteristics from the one obtained without the toxin<sup>81</sup>.

Even though *in vitro*<sup>82-84</sup> and *in vivo*<sup>80,85</sup> studies associate toxic properties to fibrils, several groups support the hypothesis that  $\alpha$ -syn oligomers are the most toxic species<sup>86,87</sup>. For instance, it has been demonstrated that ring-like oligomers can interact with the cytoplasmic membrane and form pores leading to high calcium influx<sup>86</sup>. Peelaerts and colleagues showed that oligomers, ribbons and fibrils can affect neurotransmission after acute exposure, but only fibrillar  $\alpha$ -syn exhibited perpetual behavioral and aggravated neurotoxic phenotypes *in vivo*<sup>80</sup>. Moreover,  $\alpha$ -syn fibrils are able to induce progressive impairments in neuronal network function and excitability leading to neuron death in primary culture<sup>82</sup>. Mahul-Mellier and colleagues demonstrated that neither  $\alpha$ -syn monomers, fibrils nor  $\alpha$ -syn oligomers were able to induce cell death, if used alone. Only the combination of monomers and PFFs induced apoptosis in neuroblastoma cell lines. On the contrary, PFFs have been demonstrated to be toxic by themselves in primary hippocampal neurons and in *ex vivo* hippocampal slice cultures. Moreover, the addition of the monomeric form exacerbated the toxicity. Upon these observations, the process of amyloid formation itself could be detrimental rather than the specific forms of amyloids<sup>88</sup>.

After the seeding, amyloids are transmitted to other cells where they enhance the aggregation of the endogenous soluble protein as previously reported, leading to the prion-like spreading of the pathology.

### 1.2.3 Prion-like spreading

The first evidence supporting the prion-like hypothesis of  $\alpha$ -syn spreading, goes back to ten years ago, when LB-like inclusions were found in embryonic neural tissue grafted to the striatum

of PD patients. In the attempt to replace DA neuron loss, PD patients received intracerebral transplantation of fetal ventral mesencephalic grafts. Postmortem studies carried out 11-16 years after transplantations, showed  $\alpha$ -syn-positive LBs and LNs in grafted neurons<sup>89,90</sup>. These findings corroborated the hypothesis made ahead of time by Braak and colleagues that the nasal and gastric routes might be used by an unidentified pathogen to entry the central nervous system and so develop the pathology<sup>91</sup>.

Many following studies underpinned this speculation, showing not only neuron to neuron but also region to region transmission of pathological  $\alpha$ -syn<sup>92</sup>. In particular, it has been demonstrated that  $\alpha$ -syn PFFs injection into the olfactory bulb (OB) spreads the pathology to the frontal, entorhinal, perirhinal and parietal cortex, striatum, amygdala, SN and hippocampus<sup>93</sup>. Viral vector-mediated  $\alpha$ -syn expression in the rat medulla oblongata (MO), triggered the caudo-rostral diffusion toward pons, midbrain and forebrain<sup>94-96</sup>. The appearance of  $\alpha$ -syn inclusions in widespread brain areas has been reported after injection of  $\alpha$ -syn PFFs into the striatum or cortex of mice and rats<sup>97-99</sup> as well after injection of brain extracts from patients with MSA and probable incidental Lewy body disease (iLBD)<sup>100,101</sup>. Similar spreading patterns were observed from the SN<sup>80,102</sup>. LBs have been described in the enteric nervous system of PD patients. Two studies showed that  $\alpha$ -syn is taken up from the gut and transported retrogradely after injection and the appearance of LBs in the dorsal motor nucleus of the vagus was observed<sup>103,104</sup>.

With regard to the mechanisms of transmission, some evidences indicate that  $\alpha$ -syn is released by exocytosis through an unconventional secretory pathway<sup>105</sup>, in a calcium-dependent manner<sup>106,107</sup> in SH-SY5Y cells. Its release increases after proteasome, lysosome and mitochondrial complex I inhibition<sup>106,108</sup>. In the enteric nervous system instead,  $\alpha$ -syn is secreted through a secretory mechanism likely dependent on ER/Golgi-related vesicular transport and a decrease in release was observed when the sodium channel was blocked<sup>109</sup>.

Once  $\alpha$ -syn has reached the extracellular space, it can be either removed by extracellular enzymes or taken up by recipient cells. Several mechanisms have been proposed. Monomeric  $\alpha$ -syn can easily diffuse across the plasma membrane while aggregated forms, both fibrils and oligomers, enter into cells via receptor-mediated endocytosis. Indeed, when cells were incubated at low temperature, a classical endocytosis blocker, fibrils uptake was significantly reduced. Moreover, the expression of the dominant-negative dynamin-1 K44A, which is GTPase inactive, resulted in the accumulation of the PFFs on the cell surface<sup>110</sup>. Endocytosis inhibitors decreased  $\alpha$ -syn endocytosis in a co-culture of HEK cells expressing  $\alpha$ -syn tagged with either GFP or DsRed.

When dynasore was co-injected with the labelled monomers in mice,  $\alpha$ -syn signal was strongly reduced<sup>111</sup>. Rab5, a small GTPase localized to the early endosome, can mediate  $\alpha$ -syn endocytosis subsequently leading to cell death in neuronal hippocampal cells, while overexpression of GTPase-deficient Rab5A proteins resulted in a significant decrease in the rates of the endocytosis of  $\alpha$ -syn and subsequent cell death<sup>112</sup>.

A recent study showed that  $\alpha$ -syn PFFs endocytosis is mediated by LAG3 (lymphocyte-activation gene 3), a leukocyte immunoglobulin protein also found on the surface of neurons<sup>113</sup>. An involvement of the Cellular Prion Protein (PrP<sup>C</sup>) protein in  $\alpha$ -syn binding and internalization has also been demonstrated<sup>114,115</sup>. PrP<sup>C</sup> expression increased uptake of  $\alpha$ -syn PFFs *in vitro*<sup>115</sup> and increased levels of  $\alpha$ -syn internalization in wild-type and PrP<sup>C</sup> overexpressing mice has been reported<sup>114,115</sup>. Choi and colleagues demonstrated that  $\alpha$ -syn PFFs bind Fc $\gamma$ RIIB and activate its downstream pathway leading to lipid raft-dependent endocytosis and cell transmission of  $\alpha$ -syn<sup>116</sup>. Heparan sulfate proteoglycans (HSPGs) mediate macropinocytosis of  $\alpha$ -syn and tau fibrils<sup>117</sup>, while a previous study showed that GM1 ganglioside is involved in monomeric  $\alpha$ -syn internalization into BV-2 microglial cells<sup>118</sup>.

Finally,  $\alpha$ -syn can transfer between neuron-like cells and primary neurons through tunneling nanotubes (TNTs), which are F-actin containing bridges that allow direct transfer of molecule<sup>119,120</sup>. TNTs are used to spread  $\alpha$ -syn from damaged to healthy astrocytes, when overload of  $\alpha$ -syn lead to ER and mitochondrial stress<sup>121</sup>.

The source of  $\alpha$ -syn in GCIs is still controversial. Healthy oligodendrocytes do not express  $\alpha$ -syn but are able to uptake it from the extracellular space<sup>122</sup>. Therefore, it is widely believed that damaged neurons release  $\alpha$ -syn and internalize it. However, no study is currently available demonstrating GCIs induction after  $\alpha$ -syn uptake<sup>100,123</sup> and there is no evidence that MSA is a naturally occurring transmissible disease among humans<sup>7,124</sup>.

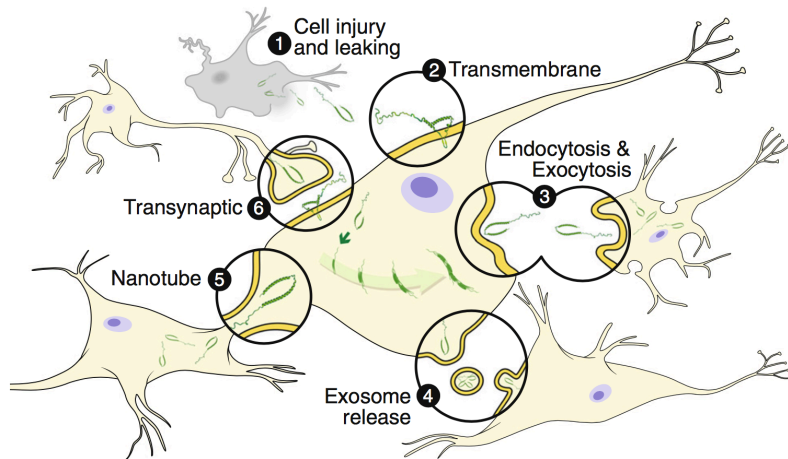


**Figure 6.** Potential mechanisms of  $\alpha$ -syn spreading.

$\alpha$ -syn can be released by damaged cells(1) and by exocytosis (3). Extracellular  $\alpha$ -syn can be taken up by recipient cells by diffusion across the plasma membrane (2), endocytosis (3), exosomes (4), tunneling nanotubes (5) and direct synaptic contact (6). Spreading mechanisms are multiple and can occur via endocytosis, direct penetration, trans-synaptic transmission or membrane receptors. Once inside the host cells,  $\alpha$ -syn aggregates can nucleate aggregation and propagate via the mechanisms described above.

#### 1.2.4 Challenges to the spreading theory and alternative hypotheses

Recent studies demonstrated that the distribution of the pathology in PD brains is not consistent with the aforementioned model of  $\alpha$ -syn spreading.

Retrospective studies suggest that almost half of cases does not follow the ascending pattern of the postulated theory. For instance, LB pathology has been reported in SN but not in the dorsal motor nucleus of the vagus<sup>125</sup>. In other cases, the spinal cord was more affected than the vagus nerve<sup>126</sup>. Even a descending distribution has been reported<sup>127</sup>. Moreover, *in vivo* attempts to correlate metabolic and structural changes in brain with Braak staging failed<sup>128</sup>. The relationship between LBs and neuronal death is also uncertain.

The early manifestation of peripheral symptoms is one of the cornerstones of the spreading theory, while motor symptoms appear only after decades. A possible explanation, opposed to the canonical one, is that the DA neuron circuits are highly developed. Therefore, the complexity of the connections among midbrain, striatal, pallidal, thalamic and cortical nuclei could compensate the initial loss of DA neurons. As a consequence, similar rates of pathology would result in different onset of the symptoms<sup>129</sup>.

Another caveat is that all the studies showing prion-like properties of  $\alpha$ -syn are based on injection and inoculation of fibrils<sup>85,97-99,102</sup> or brain extracts<sup>100-102</sup>. No spreading is observed when  $\alpha$ -syn is overexpressed in different mouse brain areas<sup>130</sup>. It has been speculated that the findings of  $\alpha$ -syn inclusions in embryonic grafts<sup>89,90</sup> could arise from different variables, as transplantation,

cell preparation and surgical technique<sup>129</sup>. Indeed, transplantation of dissociated neurons results in no or rare  $\alpha$ -syn pathology<sup>131,132</sup>.

These and other findings have been reviewed in Surmeier et al.<sup>133</sup>, Engelender and Isacson<sup>129</sup>, Ghiglieri et al.<sup>134</sup>.

In summary, alternative explanations to the spreading theory exist. Moreover, they are not mutually exclusive. It might be hypothesized that synucleinopathies, and more specifically PD, are induced by a combination of all of them.

### 1.2.5 Function

Efforts have been made by the scientific community in order to unveil the physiological function of  $\alpha$ -syn. Although several years have passed from its discovery, there are still unanswered questions.

The structure of  $\alpha$ -syn shares structural homology with, and also binds to, 14-3-3 proteins, a family of ubiquitous cytoplasmic chaperones<sup>135</sup>. Therefore, it has been hypothesized that  $\alpha$ -syn can be considered a molecular chaperone, particularly following the observation of its ability to prevent – under stress condition - the aggregation of non-native conformations of proteins<sup>136–139</sup>.  $\alpha$ -syn binds to tyrosine hydroxylase (TH)<sup>140</sup>, inhibiting its activity<sup>141</sup>. In agreement,  $\alpha$ -syn overexpression reduced TH mRNA and protein levels in rat<sup>142</sup> and human DA cells<sup>143</sup>. Controversial results were obtained in mice. The injection of its monomeric form into the striatum (ST) or SNpc, results in increased DA concentration. TH protein levels were increased in the SNpc and reduced in ST, whereas loss of DA neurons 30 days after administration was observed<sup>144</sup>. Interestingly, phosphorylation at Ser129 enhanced TH activity<sup>145</sup>.

Overall, conflicting results have been observed in knockout and overexpressing mice model addressing whether  $\alpha$ -syn has impact on neurotransmission<sup>146–150</sup>.

In a highly quoted paper, Burré and colleagues showed that  $\alpha$ -syn actively participates to the maintenance of the SNARE-complex structure during the assembly/disassembly cycles. Indeed,  $\alpha$ -syn interacts directly with phospholipids through the N-terminal domain and with synaptobrevin-2 via its C-terminus<sup>146</sup>. Upon membrane binding,  $\alpha$ -syn multimerizes into large homomeric complexes and only in this state, it is able to promote SNARE complex assembly<sup>151</sup>. Moreover,  $\alpha$ -syn multimers cluster synaptic vesicles and restrict their motility<sup>152,153</sup>.

Thanks to its propensity for membrane binding,  $\alpha$ -syn has been proposed to be a curvature-sensing and stabilizing protein, thus negatively or positively affecting exocytosis and endocytosis.

A lot of studies in different organisms showed that its inhibition of ER-Golgi trafficking and increase of Ypt1p/Rab1 production are sufficient to protect against  $\alpha$ -syn related DA neuron loss in animal models<sup>154–157</sup>. In a recent publication, Fang and colleagues showed that  $\alpha$ -syn expression induced endocytic dysfunction by upregulating the level of activated Rab5 and Rab7 and impaired retrograde transport of BDNF, leading to neuronal atrophy in primary cortical neurons<sup>158</sup>. Its role in membrane remodelling and exocytosis and endocytosis is well reviewed in Lautenschläger *et al.*<sup>159</sup>.

### 1.2.6 Post-translational modifications

Although the exact mechanism leading to  $\alpha$ -syn toxicity is still poorly understood, several reports suggest that  $\alpha$ -syn synthesis, aggregation and clearance rate imbalance can result in  $\alpha$ -syn accumulation, triggering the pathology. Moreover, as previously reported, multiplication of *SNCA*, which occurs in some familial forms of parkinsonism, may result in  $\alpha$ -syn accumulation. On the other hand, the smooth functioning of protein removal pathways is fundamental to clear the excess of  $\alpha$ -syn and is considered to be a defensive mechanism against its accumulation.

$\alpha$ -syn has been shown to be degraded by both ubiquitin-proteasome system (UPS) and autophagy-lysosome pathway (ALP). These pathways, extensively reviewed in Xilouri *et al.*<sup>160</sup>, will not be deeply explored in this thesis but many references will be made trying to give a comprehensive view of  $\alpha$ -syn post-translational modifications, some of which are responsible for preferentially targeting the protein toward one path or the other.

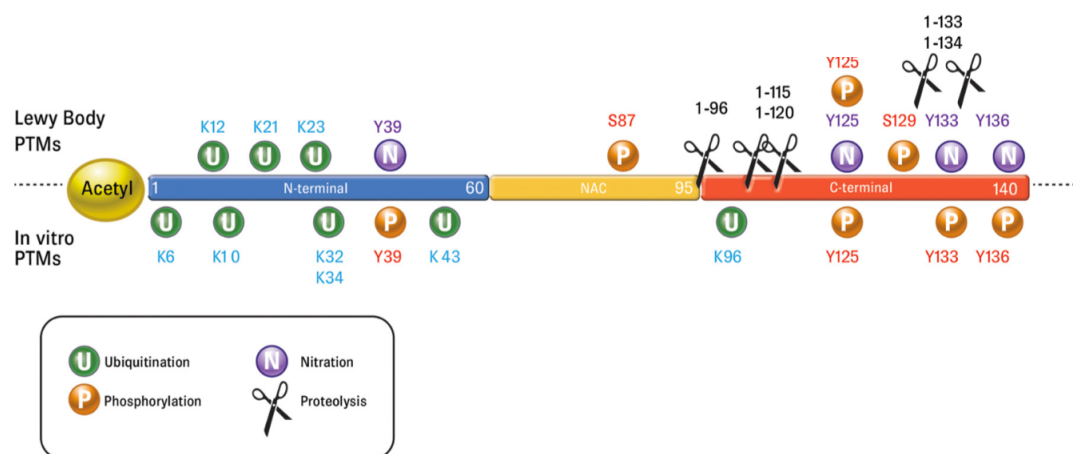


**Figure 7.** Post-translational modifications of  $\alpha$ -syn.

A, the locations of the main  $\alpha$ -syn PTMs (phosphorylation, ubiquitination, nitration, and truncation) are shown. Disease-associated PTMs identified in Lewy bodies are shown in the upper part of the scheme, and those identified from *in vitro* studies are shown below. Modified from Adrien W. Schmid *et al.*<sup>161</sup>

### *Phosphorylation*

Both serine (S129 and S87)<sup>162</sup> and tyrosine (Y125, Y133 and Y135)  $\alpha$ -syn residues are commonly subjected to phosphorylation modification. It preferentially occurs at S129. Indeed, 90% of insoluble  $\alpha$ -syn is phosphorylated, though only 4% of total protein is found phosphorylated under physiological conditions<sup>163–165</sup>. Phosphorylation is thought to be a late event in the pathogenesis of synucleinopathies since several studies reported a strong accumulation of pS129- $\alpha$ -syn at late stages in PD and DLB brains compared to control<sup>165,166</sup>. Phosphorylation enhances the binding affinity to divalent but not trivalent ions<sup>32,167</sup>, while it inhibits  $\alpha$ -syn membrane binding<sup>168,169</sup>. However, a recent study showed that the effect on membrane affinity, as well as internalization, depends on which PD-linked mutation is present<sup>170</sup>.

UPS and ALP inhibition induced increase of pSer129- $\alpha$ -syn<sup>171,172</sup>, while Polo-like kinase 2 (PLK2) overexpression enhanced  $\alpha$ -syn clearance by the autophagic degradation machinery<sup>173</sup>. Furthermore, pSer129- $\alpha$ -syn was found ubiquitinated<sup>164,172,174</sup>, supporting the implication of phosphorylation at Ser129 in the regulation of  $\alpha$ -syn degradation.

Moreover, *in vitro* studies showed controversial results about pSer129 influence on  $\alpha$ -syn inclusions formation<sup>175,176</sup>. Interestingly, overexpression of G protein-coupled receptor kinases (GRKs) enhanced cellular loss in flies<sup>177</sup> and in a mouse model of PD<sup>178</sup>. On the contrary, PLK2 overexpression in rat decreased DA neurons loss<sup>173</sup>.

Phosphorylation at S87 inhibits  $\alpha$ -syn aggregation and seems to be protective against  $\alpha$ -syn-induced toxicity in a rat model of PD<sup>179</sup>. Tyrosine 39 and 125 are phosphorylated by c-Abl kinase. c-Abl inhibition promotes autophagic degradation of  $\alpha$ -syn *in vitro*, increases DA level and improves motor performance *in vivo*<sup>180</sup> while it may also affect the proteasome system<sup>181</sup>.

### *Ubiquitination*

Colocalization of  $\alpha$ -syn and ubiquitin has been found in LBs, LNs and GCIs<sup>182–184</sup>. Moreover, two of the four ubiquitin ligases known to ubiquitinate  $\alpha$ -syn, are also associated to PD<sup>185,186</sup>. Phosphorylated synuclein is mono and diubiquitinated<sup>174</sup> and this modification is not dependent on A53T and A30P PD-linked mutations, while fibrillar  $\alpha$ -syn is ubiquitinated to a smaller extent than the soluble one<sup>187</sup>.

### *Sumoylation*

$\alpha$ -syn can be also conjugated to small ubiquitin-like modifier (SUMO) at lysines 96 and 102, but its role in  $\alpha$ -syn induced pathogenicity is still under debate. In particular,  $\alpha$ -syn is primarily

modified by SUMO1, and to a lesser extent, by SUMO2 and SUMO3<sup>188</sup>. Sumoylated  $\alpha$ -syn has been found in LBs of brains from PD and DLB patients<sup>189</sup> and sumoylation improved  $\alpha$ -syn aggregation by blocking its ubiquitin-dependent degradation pathways and promoting its accumulation and aggregation into inclusions<sup>190</sup>. However, mutations of the two lysine residues targets of sumoylation, increase aggregation propensity and cytotoxicity *in vitro* and *in vivo*, thus supporting that sumoylation defects may contribute to aggregation<sup>191</sup>. Moreover, increased formation of aggregates containing sumoylated  $\alpha$ -syn as a result of proteasome inhibition has also been reported<sup>189</sup>.

#### *Nitration and oxidation*

Excessive production of ROS induces saturation of antioxidant signaling pathway, leading, eventually, to nitroxidation of molecules. Several studies showed high oxidative stress in DA neurons in PD brains<sup>192,193</sup> and nitrated  $\alpha$ -syn has been detected in LBs of patients suffering from different synucleinopathies<sup>194,195</sup>. Production of nitrating agents seems to be increase in  $\alpha$ -syn aggregation<sup>196</sup> and nitration of  $\alpha$ -syn promoted the formation of fibrils<sup>197</sup>. Moreover, nitrated  $\alpha$ -syn is cytotoxic to SH-SY5Y cells<sup>198</sup> and primary midbrain DA neurons while injection in rat SN causes severe DA neuron loss<sup>199</sup>. Other effects of  $\alpha$ -syn nitration are reviewed in He *et al.*<sup>200</sup>.

Methionine oxidation, an oxidative stress-related modification, has been demonstrated to inhibit  $\alpha$ -syn fibrillation and to induce the formation of soluble oligomers that are not toxic to DA neurons<sup>201</sup>. On the other hand, Nakaso and colleagues showed that mutating two of the four methionine residues of  $\alpha$ -syn, decreased DA-related toxicity in PC12 cells<sup>202</sup>.

Moreover,  $\alpha$ -syn can undergo di-tyrosine crosslinking at residue 39 under condition of oxidative stress. This is interesting since di-tyrosines were found in LB of PD patients by immunogold electron microscopy<sup>203</sup>.

#### *N-terminal acetylation*

N-terminal acetylation has been reported in both control and PD individuals stabilizing the  $\alpha$ -helix and increasing affinity for membranes and resistance to aggregation<sup>204,205</sup>.

#### *Glycation*

$\alpha$ -syn is mainly glycated at its N-terminal region and it is present both in control and PD brains. Glycation induces  $\alpha$ -syn toxicity in different *in vitro* models and neuronal loss in a mouse model of PD. Moreover, it promotes oligomerization and impairs UPS- and ALP-mediated degradation of  $\alpha$ -syn<sup>206</sup>.

## Truncation

C-terminal truncated species of  $\alpha$ -syn ( $\Delta$ C- $\alpha$ -syn) are highly enriched in LBs, representing 15% of  $\alpha$ -syn in the aggregates<sup>11</sup>. They are also present in GCIs as well as in the brain of control individuals<sup>13–20</sup>. Prasad and colleagues reported the presence of  $\Delta$ C- $\alpha$ -syn in the core of different types of aggregates in PD and Incidental Lewy Body Disease<sup>207</sup>.

In order to understand whether  $\alpha$ -syn truncation may have a role in the pathological process, several studies have been carried out demonstrating that  $\Delta$ C- $\alpha$ -syn aggregates faster than FL- $\alpha$ -syn and increases FL- $\alpha$ -syn aggregation propensity *in vitro*<sup>60,66,208,209</sup> and this effect is exacerbated when FPD-linked mutant  $\alpha$ -syn is used<sup>11,210</sup>.

The influence of  $\Delta$ C- $\alpha$ -syn species on  $\alpha$ -syn toxicity *in vivo* has also been largely investigated. Increasing evidence suggests that the expression of truncated  $\alpha$ -syn is correlated with the formation of pathological inclusions *in vivo* and, interestingly, with reduction in DA levels, deficits in locomotion and in cortical-hippocampal memory tests<sup>37,211–214</sup>. Lack of consistency among studies is reported regarding DA neurons degeneration<sup>211,212,215</sup>. Furthermore, passive immunization against  $\Delta$ C- $\alpha$ -syn ameliorated neurodegeneration and neuroinflammation, reduced the accumulation of  $\Delta$ C- $\alpha$ -syn and improved motor and memory deficits in a mouse model of PD<sup>216</sup>. Moreover, using a double chamber system, Games and colleagues proved that these antibodies were able to block the propagation of FL- $\alpha$ -syn *in vitro*<sup>216</sup>.

Given the importance of  $\Delta$ C- $\alpha$ -syn production, efforts have been made to identify the pathways leading to the truncation. A complex model involving proteasome, lysosomes, intra- and extra-cellular proteases has emerged. Unfolded  $\alpha$ -syn can be degraded by purified 20 S Proteasome giving rise to C-terminal truncated species<sup>11,217</sup>.

As already stated, the autophagy-lysosome pathway (ALP) is in part responsible for  $\alpha$ -syn degradation and several proteins driving this process are dysregulated in PD<sup>218</sup>.

Among them, Cathepsin D (CatD), one of the effectors of the ALP together with other cathepsins, has been found downregulated in SN in PD brains<sup>219</sup> while opposite results were obtained in anterior cingulate cortex in early stage PD<sup>220</sup>. Since cathepsins are the effectors of the ALP, they are the main candidates as involved in  $\alpha$ -syn degradation and, as intermediate step,  $\Delta$ C- $\alpha$ -syn production. *In vitro* experiments demonstrated that CatD degraded FL- $\alpha$ -syn and generated  $\Delta$ C- $\alpha$ -syn species while both inhibition and silencing of CatD prevented  $\alpha$ -syn truncation in different cell systems<sup>221,222</sup>. Interestingly, reduction of Cpn1 activity did not produce the same

effects<sup>221</sup>. Accordingly, reduction of  $\Delta$ C- $\alpha$ -syn and increased  $\alpha$ -syn accumulation were observed in CatD deficient mice<sup>223,224</sup>. In a cell-based model, the partial loss of CatD was responsible for a reduction of exogenous  $\alpha$ -syn clearance, as result of reduced lysosomal activity, and therefore promoted  $\alpha$ -syn aggregation, as result of  $\alpha$ -syn accumulation. No effects were observed on  $\alpha$ -syn endogenous clearance<sup>225</sup>. In CatD deficient mice, mRNA encoding lysosomal cathepsins B, L, F and H were up-regulated<sup>224</sup>. Crabtree and colleagues showed that pharmacological inhibition of CatD, but not Cathepsin B (CatB), led to  $\alpha$ -syn accumulation. Furthermore, overexpression of inactive CatD resulted in increased  $\alpha$ -syn levels and, at the same time, increased CatB activity<sup>226</sup>. Using lysosomal extracts and mass spectrometry analysis, McGlinchey and Lee showed that CatD generates  $\Delta$ C- $\alpha$ -syn fragments, whereas Cathepsin L (CatL) and, to a lesser extent, CatB are responsible for the majority of  $\alpha$ -syn degradation. In particular, CatD degrades membrane-bound  $\alpha$ -syn, while CatL and CatB can degrade both soluble and membrane bound  $\alpha$ -syn<sup>227</sup>.

Another study supports the hypothesis that CatB is the major enzyme involved in  $\alpha$ -syn degradation. Indeed, aggregates formation induced by  $\alpha$ -syn PFFs was inhibited by using a CatB inhibitor but no effect was obtained using a CatD inhibitor and similar results were obtained by CatB knockdown. Moreover, *in vitro* digestion of  $\alpha$ -syn PFFs by CatB formed  $\Delta$ C- $\alpha$ -syn fragments and increased  $\alpha$ -syn seeding propensity<sup>228</sup>.

Evidence suggests that calpain1 (Capn1) could take part to this process and, in fact, Cpn1-cleaved fragments of  $\alpha$ -syn were detected in LBs and LNs in both PD and DLB brains<sup>229</sup>. Calpains are cytoplasmic cysteine proteases that require calcium for their activation. Two calpains exist in mammals,  $\mu$ - or calpain1 and m- or calpain2, that are activated by micromolar and millimolar levels of calcium respectively. They exist in the cytosol in their inactive form and, after an increase in calcium levels, they translocate to the membrane. The physiological function of calpains is still not fully understood and is reviewed in Suzuki *et al*<sup>230</sup>. *In vitro* experiments showed that Capn1 cleavage of recombinant  $\alpha$ -syn lead to several products with cleavage sites inside the NAC region. When fibrillar  $\alpha$ -syn was used, a different pattern was detected. The major cleavage site was inside the C-terminal region and only a small amount of products derived from N-terminal truncation<sup>231</sup>. The cleavage of fibrillar  $\alpha$ -syn resulted in  $\Delta$ C- $\alpha$ -syn fragments that retained their fibrillar structure and induced soluble  $\alpha$ -syn assembly, while products obtained by calpain cleavage of soluble  $\alpha$ -syn inhibited fibrillation<sup>232</sup>. Dufty and colleague demonstrated that Capn1 is able to cleave  $\alpha$ -syn both at the N- and C-terminal ends<sup>229</sup>. Recently, Diepenbroek and colleagues used two mouse models,

one expressing A30P  $\alpha$ -syn and deficient for calpastatin, and the other overexpressing calpastatin, a calpain specific inhibitor. In the first model, enhanced calpain activity led to increased  $\alpha$ -syn truncation. In the latter, reduced calpain activity led to a decrease of  $\alpha$ -syn truncation and inclusion formation with decreased astrogliosis<sup>233</sup>.

Caspases activation is a well-known key step in PD pathogenesis. In fact, oxidative stress, inflammation and ER stress lead to caspases activation and, finally, to DA neurons degeneration<sup>234</sup>. Caspase-1 (Cas1) is mostly activated by inflammatory stimuli<sup>235</sup> and two recent studies shed light on the role of Cas1 in PD and MSA. In one of the two aforementioned studies, inflammasome activators were used in cells and resulted in  $\alpha$ -syn aggregation and  $\Delta$ C- $\alpha$ -syn species production.  $\Delta$ C- $\alpha$ -syn fragments were aggregation-prone while Cas1 inhibition and silencing reduced  $\alpha$ -syn truncation<sup>236</sup>. In the other study, a transgenic mouse model of MSA was used. Truncated  $\alpha$ -syn was identified in GCIs and treatment with VX-765, a specific Cas1 inhibitor, decreased monomeric and oligomeric  $\alpha$ -syn, reduced  $\Delta$ C- $\alpha$ -syn species production and GCIs positive inclusions. All these findings were observed in the striatum but not in cortex<sup>237</sup>.

As previously reported, according to the prion-like spreading of  $\alpha$ -syn, the protein is released into the extracellular space with no well understood mechanisms and, there, can be degraded by extracellular proteases.

Plasmin has been reported to cleave recombinant monomeric and fibrillar  $\alpha$ -syn at the N-terminus<sup>238</sup>.

LBs and GCIs were found positive to neurosin (or KLK6) staining<sup>239,240</sup> and recently the levels of neurosin have been found decreased with increased accumulation of  $\alpha$ -syn in DLB cases and in a mouse model of DLB compared to controls<sup>241</sup>. Lentiviral vector driven expression of neurosin reduced  $\alpha$ -syn accumulation both in neuronal cell cultures and mice and, notably, it also ameliorated neurodegenerative pathology<sup>241</sup>. In a cell-free assay, neurosin cleaved  $\alpha$ -syn<sup>240,242</sup> giving rise to fragments that were not toxic to cells<sup>241</sup> and able to inhibit FL- $\alpha$ -syn polymerization<sup>240</sup>. In cells, Tabete and colleagues reported that neurosin is secreted, activated in the extracellular space, where degrades extracellular  $\alpha$ -syn<sup>243</sup>, while Iwata and colleagues reported that levels of cytosolic neurosin were increased under stress<sup>240</sup>. Other studies demonstrated that secreted  $\alpha$ -syn is not degraded directly by neurosin<sup>244</sup> but neurosin activates MMP-2 as effector for the degradation process<sup>245</sup>.

Among all the matrix metalloproteinases (MMP), MMP-3 degrades  $\alpha$ -syn more efficiently than the other ones at the C-terminal<sup>246,247</sup>. MMP-3 activation causes microglial activation, leading

to DA neuronal degeneration in primary cultures of mouse mesencephalon and enriched microglia, as well as MPTP-injected animal model of PD<sup>248</sup>. Partial cleavage by MMP-1 and MMP-3 increases the tendency of  $\alpha$ -synuclein to aggregate<sup>247,249</sup> and, interestingly, MMP-3 colocalizes with  $\alpha$ -syn in LBs in PD patients<sup>247</sup> and MMP-1, -2 and -3 colocalize with GCIs in MSA brains<sup>250</sup>.

## 1.3 Hemoglobin

### 1.3.1 The globin family

Globins are proteins characterized by the “globin-fold” which consists of a series of  $\alpha$ -helices and a heme group<sup>251</sup>. They are expressed in a highly species- and tissue-specific manner and have different functions (recently reviewed in Burmester and Hankeln<sup>252</sup>) mainly involving O<sub>2</sub> transport and storage, detoxification, sensing and signaling<sup>253</sup>. They have been identified in bacteria, plants, fungi, and animals<sup>254</sup>. Four main components have been discovered in mammals neuroglobin (Ngb), he- moglobin (Hb), myoglobin (Mb), and cytoglobin (Cygb)<sup>255</sup>. Harboring a heme-prosthetic group (Fe-protoporphyrin IX), Hb and Mb are penta-coordinate, whereas Cgb and Ngb display a hexa-coordinate configuration<sup>255</sup>.

Ngb is related to the invertebrate nerve globins, indicating that an ancestral gene was present before the divergence of vertebrates and invertebrates, more than 800 million years ago<sup>256</sup>. It is highly expressed in human and mouse brains<sup>257</sup>. Ngb is a monomer with high affinity for O<sub>2</sub> and carbon monoxide (CO). It is predominantly found in neurons and it is increased by neuronal hypoxia *in vitro* and ischemia *in vivo*<sup>258</sup>. In addition, it seems to be protective in different neurological disorders and may also function as a ROS and Reactive nitrogen species (RNS) scavenger. Ngb function and properties are reviewed in Ascenzi *et al.*<sup>256</sup>.

Mb is a monomeric protein with great ability to store O<sub>2</sub> in cells<sup>259</sup>, mainly found in striated and smooth muscles as well as in cardiac myocytes. Its presence in other locations has been reported in carp and zebrafish under physiological conditions<sup>260,261</sup>, while in mammals it has only been found in cancer cell lines<sup>262</sup>.

Cytb is a more recently identified globin that is ubiquitously expressed as dimer<sup>263</sup> in different tissues including the brain<sup>264</sup>. It localizes to the cytoplasm in fibroblasts, but both nuclear and cytoplasmic localizations have been reported for neurons<sup>265</sup>. Cygb binds O<sub>2</sub> with high affinity and it has been proposed to have a role in O<sub>2</sub> transport, storage, sensing and in NO removal<sup>266</sup>. In the CNS, it has a well-characterized role in response to hypoxia. It is upregulated in mice hypoxic brains, in particular in hippocampus, thalamus and hypothalamus, that are highly responsive to oxidative stress<sup>267,268</sup>. *In vitro* experiments confirmed the upregulation<sup>268</sup>.

In vertebrates, other four globins have been recently discovered: globin X<sup>269</sup>, globin Y<sup>270</sup>, eye-globin or globin E<sup>271</sup> and androglobin<sup>272</sup> (reviewed in Burmester and Hankeln<sup>252</sup>).

Lastly, hemoglobin is well known for its capacity to transport O<sub>2</sub> from the lungs to the periphery of the body and it is found primarily in red blood cells (RCBs). Its structure, functions and involvement in neurodegenerative disorders will be explored in the next sections.

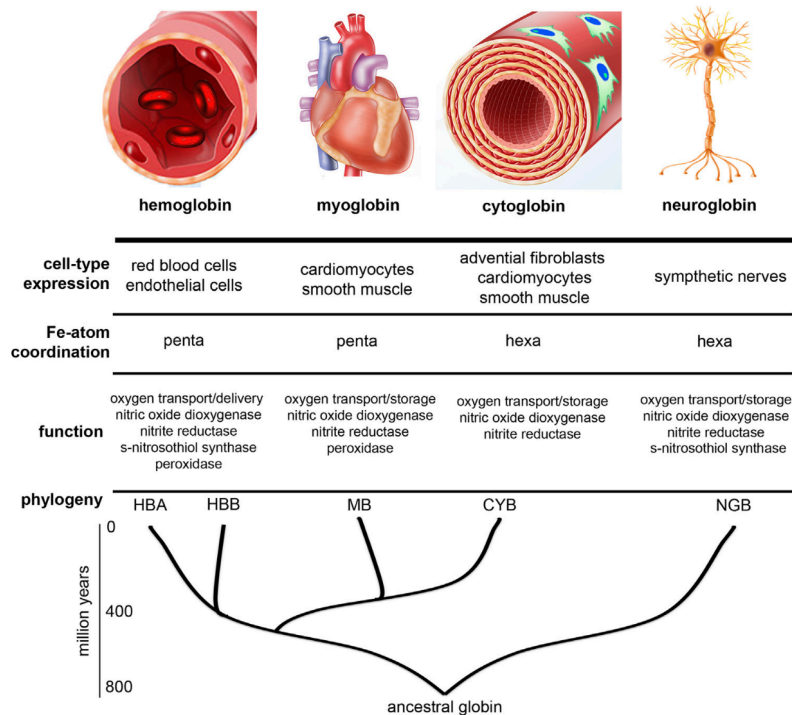


**Figure 7.** Schematic outline of vertebrate globins expression, functions and phylogenetic features.<sup>255</sup>

### 1.3.2 Hemoglobin: from gene to protein

In human,  $\alpha$ - and  $\beta$ -globin chains are encoded by the duplicated HBA1 and HBA2 genes and by the HBB gene, located on chromosome 16 and 11, respectively. They are in clusters with multiple related genes in the same order of their expression during human ontogeny<sup>273</sup>. During the embryonic period, Hb-Gower 1 ( $\zeta_2\varepsilon_2$ ), Hb Gower-2 ( $\alpha_2\varepsilon_2$ ) and Hb Portland-1 ( $\zeta_2\gamma_2$ ) are expressed. Fetal Hb (HbF) ( $\alpha_2\gamma_2$ ) is expressed after the first trimester and predominates until birth<sup>273</sup>.  $\beta$ -globin expression, on the other hand, increases slowly during the second trimester in human, while it is predominant in the fetal liver of mouse and rabbit<sup>274</sup>. The expression gradually switches to HbA, which accounts for >95% of total Hb in adulthood, accompanied by HbA-2 ( $\alpha_2\delta_2$ ) and HbF<sup>275</sup>.

This phenomenon, called  $\beta$ -globin switching, is tightly regulated. In particular,  $\beta$ -globin expression is under the control of a super-enhancer known as locus control region (LCR). The LCR is found several Kb upstream of the HBB gene and, thanks to chromatin looping, it is brought in close proximity to the  $\beta$ -globin gene. Several players participate to the regulation: BCL11A, LRF, SOX6, the GATA family, KLF1 and its competitor DRED. They interact with modulators

of chromatin structure, histone deacetylases, lysine-specific demethylase-1 (LSD1), arginine methyltransferases (PRMTs) and DNA methyltransferase 1 (DNMT1)<sup>276,277</sup>.

The  $\alpha$ -globin gene cluster is very close to the telomere and is regulated by four highly conserved noncoding sequences (MCS-R1 to MCS-R4) and several other conserved cis-acting regulatory elements. Among them, MCS-R2 is the most highly conserved and, in addition, the most critical one. The key transcription factors regulating  $\alpha$ -globin expression are GATA1, KLF1, SCL, E2A, LMO2 and LIM. In cells not expressing  $\alpha$ -globin, the transcriptional repressor polycomb repressive complex (PRC2) exert its silencing effect through the EZH2 histone methyltransferase that increases trimethylation of histone H3 lysine 27 (H3K27me3). When  $\alpha$ -globin gene expression is activated, PRC2 is displaced thanks to demethylases and H3K4me3 increases<sup>278</sup>.

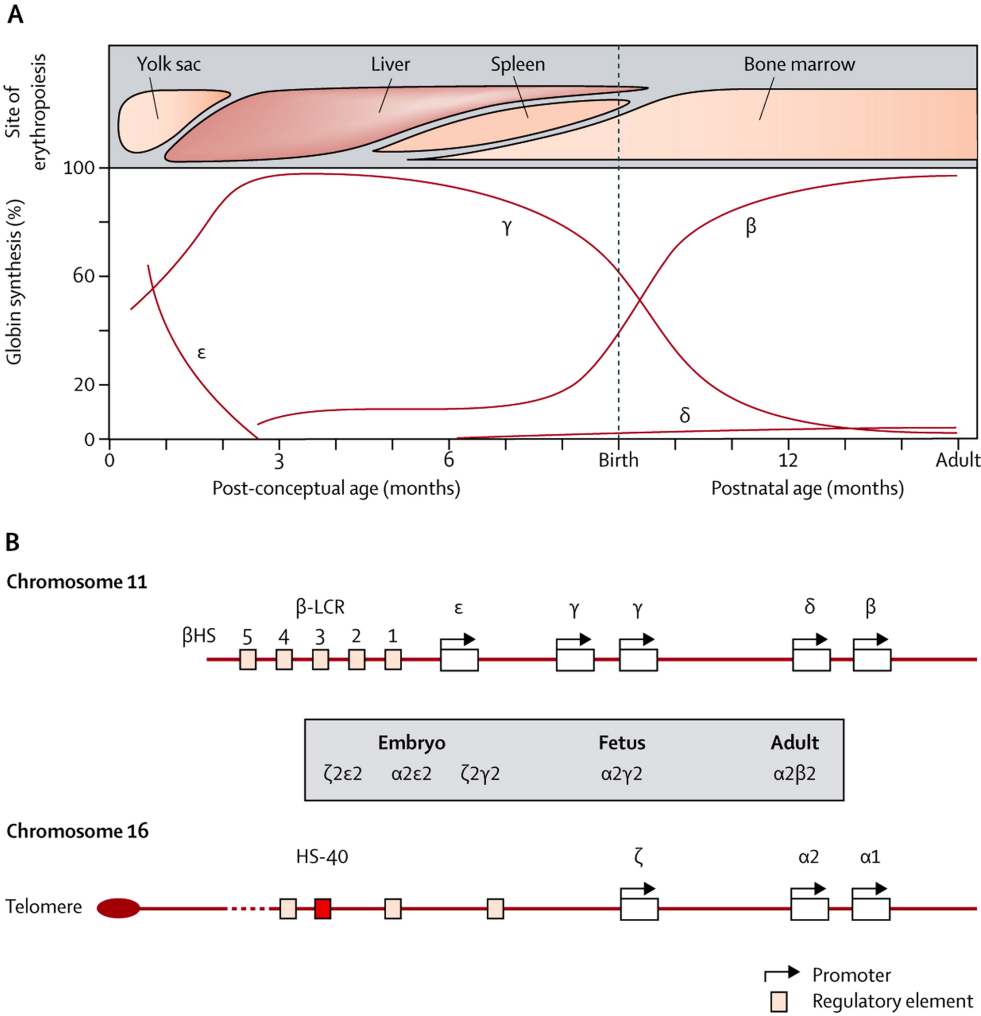


**Figure 8.** Developmental switches in globin expression and  $\alpha$ - and  $\beta$ - globin gene clusters. A. The sites of hemopoiesis at different stages of development and levels of expression of the embryonic, fetal, and adult globin chains at various gestational ages are shown. B. The structure of the  $\alpha$ - and  $\beta$ - globin gene clusters are

shown together with the types of hemoglobin produced at each developmental stage. HS=major upstream regulatory element.  $\beta$ -LCR= $\beta$ -locus control region. Modified from <sup>279</sup>.

For what concerns the protein structure, HbA is a heterotetramer composed of two  $\alpha\beta$  dimers in which each globin binds the other one through the high affinity  $\alpha1\beta1$  interaction. The lower affinity  $\alpha1\beta2$  interaction mediates tetramerization. Each globin binds a heme molecule, that is a porphyrin molecule coordinating iron by the four nitrogen atoms. A covalent bond between iron and the proximal histidine inside helix F8, stabilizes the folding into a globular structure composed of seven ( $\alpha$ -globin) or eight ( $\beta$ -globin) helices. Additional residues stabilize the heme binding through non-covalent interactions<sup>280</sup>. This is the tense deoxygenated state of Hb (T), in which the porphyrin is in a non-planar configuration and iron is oxidized ( $Fe^{3+}$ ) (methemoglobin). Once the iron is reduced ( $Fe^{2+}$ ), it binds  $O_2$  causing  $Fe^{2+}$  to move into the porphyrin plane, so the porphyrin adopts a planar configuration. Oxygen binding destabilizes the  $\alpha1\beta2$  interaction and results in the transition from the T state to the R state (relaxed, oxygenated), in which the binding of the other subunits to  $O_2$  is favored. This property of hemoglobin is known as “cooperative binding” and it is an example of its allosteric regulation that determines its primary function.

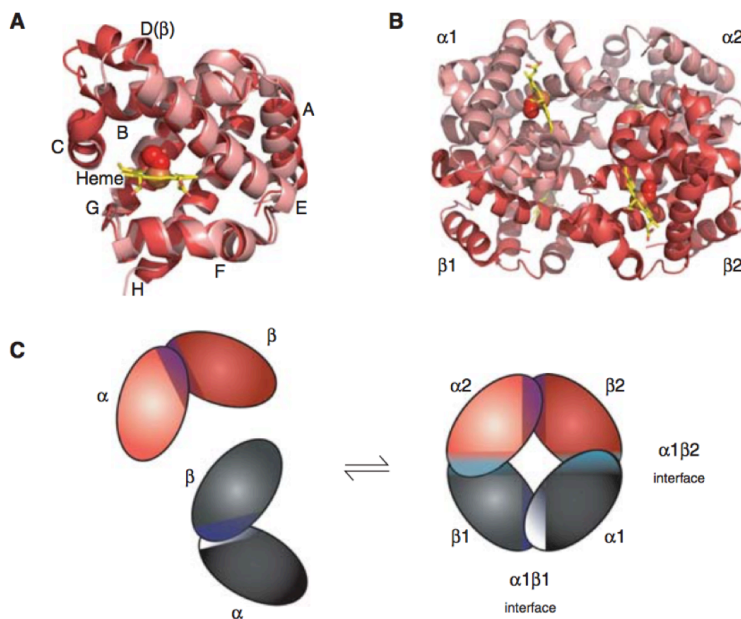


**Figure 9.** Hemoglobin structure.

A. The  $\alpha$ - (pink) and  $\beta$ - (red) Hb subunits. Helices are labeled A–H from the amino terminus. The  $\alpha$ -subunit lacks helix D. B. Quaternary structure of Hb into the R state with  $O_2$  (red spheres) bound at the four heme sites (yellow sticks with central iron atom as orange sphere). C. Two identical  $\alpha\beta$  dimers (shown in red and gray, on the left). In the tetramer (on the right), each subunit makes contact with the unlike chain through a high affinity dimerization  $\alpha1\beta1$  interface and a lower affinity  $\alpha1\beta2$  interface. Modified from Thom *et al.*<sup>280</sup>

### 1.3.3 Function

#### Oxygen

The role of Hb in oxygen delivery and release has been the focus of many studies and, as previously discussed, the structural properties of Hb are fundamental for this function. Indeed, at low oxygen concentration, the T-state is favored, while a progressive increase of the oxygen pressure, shifts the equilibrium to the R-state. This is represented by the characteristic sigmoidal curve of the Hb-O<sub>2</sub> binding. The cooperativity binding of O<sub>2</sub> allows maximal O<sub>2</sub> release over relatively small drops in O<sub>2</sub> pressure. So, in the lungs, where partial pressure of oxygen is high, the Hb binds O<sub>2</sub> and becomes nearly saturated. At the periphery, instead, low O<sub>2</sub> pressure leads to the transition from the R to the T state and, finally, to O<sub>2</sub> release.

Another type of allosteric regulation is the Bohr effect. At the periphery, CO<sub>2</sub> is taken up by red blood cells and metabolized to carbonic acid. The resulting H<sup>+</sup> product binds the β-subunit and stabilizes the T structure of deoxyhemoglobin, thus promoting O<sub>2</sub> release<sup>281</sup>. In tissues, the remaining CO<sub>2</sub> is bound by Hb through the formation of carbamino adducts with the N-terminus of both α- and β-chain. In this way, Hb transport CO<sub>2</sub> to the lungs, where the increase in PO<sub>2</sub>, decreases the CO<sub>2</sub> affinity, determining its exhalation.

2,3-diphosphoglycerate (2,3DPG) is another allosteric regulator of Hb, resulting from glycolysis. It is present in red blood cells, where it binds and stabilizes the Hb T state to facilitate O<sub>2</sub> dissociation<sup>282</sup>.

Altogether, these interactions allow Hb to modulate O<sub>2</sub> binding in response to change in metabolic activity.

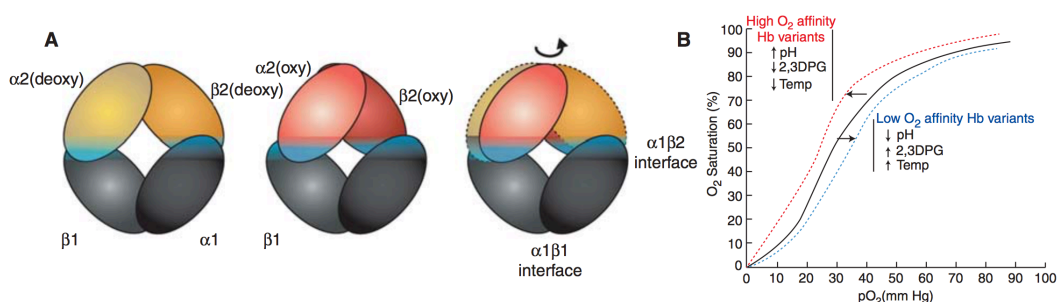


**Figure 10.** Hb-O<sub>2</sub> binding.

A. Conversion from the T state (deoxy) to the R state (oxy) involves a relative rotation of the α1β1 and α2β2 dimers. In this cartoon, the α1β1 dimer is held stationary to reveal the relative motion of the α2β2 dimer in going from the deoxy (orange) to the oxy (red) states. B. The sigmoidal shape of the Hb-O<sub>2</sub> binding curve shows allosteric regulation by changes in pH, temperature, and 2,3DPG. High oxygen affinity variants, high pH, low 2,3DPG, or low temperature induce a “left shift” in the saturation curve (red line). Low oxygen affinity variants, low pH, high 2,3DPG, or high temperature induce a “right shift” (blue line). Modified from Thom *et al.*<sup>280</sup>

### *Nitric oxide*

Nitric oxide (NO) is a vasodilator produced by the endothelium. It binds to soluble guanylyl cyclase in smooth muscle cells and triggers vasodilatation. Heme iron in its reduced state has high affinity for NO. The interaction thus forms methemoglobin (methHb) with ferric iron ( $\text{Fe}^{3+}$ ) and nitrate ions. Therefore, Hb acts as an efficient scavenger of NO, causing vasoconstriction. This is particularly important in two conditions: when endogenous NO levels highly increase and when it is administered by inhalation or by infusion of nitrite ions or other NO donors<sup>283</sup>.

Other two interactions between Hb and NO have been reported. NO can bind both heme  $\text{Fe}^{2+}$ , forming nitrosyl(heme)hemoglobin (NO-Hb), and cysteine at position 93 of the  $\beta$ -chain, forming S-nitrosylhemoglobin (SNO-Hb). The latter can deliver NO in an allosteric-dependent manner and promote vasodilatation in hypoxic tissues<sup>284</sup>. Moreover, SNO-Hb formation is competitive with and/or circumvents the Fe(II)-NO and nitrate-forming reactions<sup>285</sup>. Evidence has been reported that NO-Hb may be capable of releasing NO molecules too<sup>286</sup>.

### *Carbon monoxide*

Carbon monoxide (CO) is a signaling molecule with antioxidant, anti-inflammatory and vaso-relaxing activities<sup>287</sup>. Given its high affinity for transition metals, it binds heme iron at its oxygen binding site, forming carboxyhemoglobin (COHb). In this form, COHb cannot release oxygen from the other heme moieties. In this way, Hb can act as CO scavenger to reduce its physiological impact. At the same time, however, it is incapable of transferring oxygen, becoming highly toxic in higher concentration. In particular, the baseline levels of COHb in man is 0,1–1,0%. When this level reaches and exceeds 30%, syncope, cardiac arrhythmias and death can occur<sup>288</sup>.

### *Antimicrobial activity*

Oxygenated Hb undergoes continuous autoxidation, leading to a cascade of events that results in the production of superoxide, hydrogen peroxide, hydroxyl radical, and oxidation of the ferrous Hb to methHb. Heme dissociates from methHb, due to its low affinity, and reacts with membranes, proteins and lipids<sup>289</sup>. In RBCs, there are enzymes capable of reducing oxidized Hb and neutralize ROS production, like superoxide dismutase, catalase, glutathione peroxidase, and peroxiredoxin-2. In the absence of the erythrocyte's reducing system, cell-free Hb can be highly toxic as results of ROS inactivation. Moreover, free heme has been shown to be involved in atherosclerosis pathogenesis and renal dysfunction<sup>289</sup>. Furthermore, it has been reported that Hb-

catalyzed ROS production can lead to oxidation of a neurotransmitter precursor,  $\beta$ -phenylethylamine (PEA)<sup>290</sup>. Hb antimicrobial activity has been demonstrated against bacteria<sup>291</sup> and fungi<sup>292</sup>. Therefore, it was hypothesized that the aforementioned reaction leading to free heme could be involved. Nevertheless,  $\alpha$ - and  $\beta$ -globin alone exert higher effect than the entire molecule, thus indicating that the presence of heme is not fundamental for the antimicrobial activity of Hb<sup>293</sup>. Later on, Du and co-workers showed that extracellular proteases of an invading microbe cause limited proteolysis of Hb and induce a conformation switch to a more relaxed structure. Thus, produced Hb fragments bind microbes and enhance ROS production by pseudoperoxidase cycle<sup>292</sup>. Therefore, it is conceivable that, in addition to its well-known roles, Hb can function as multi-defence agent against microorganisms.

Other putative functions of Hb, are related to its non-erythroid localization and will be discussed later in this chapter.

#### 1.3.4 Hemoglobin disorders

Hemoglobin disorders can be classified in thalassemia, due to quantitative defect in the synthesis of one subunit, and disorders raising from structural defect of the subunits.

The thalassemia are characterized by the absence or strong decrease of one chain and are called  $\alpha$ - and  $\beta$ -thalassemia depending on the affected subunit. Cases of thalassemia involving  $\delta$ - or  $\gamma$ - subunit have been reported rarely.  $\alpha$ -thalassemia is usually caused by deletion of one or more genes and is classified accordingly in  $\alpha^+$  (one gene),  $\alpha^0$  (two genes), HbH (three genes), hydrops fetalis with Hb Bart's (four genes). The  $\beta$ -thalassemias are divided into  $\beta^0$  if there is no synthesis and  $\beta^+$  when some normal  $\beta$ -chain is produced. More than 200 point mutations have been reported to cause these disorders. A large deletion involving part or the whole gene cluster causes the  $\delta\beta$ -thalassemia, in which the  $\alpha$ - deficiency is partially restored by increased expression of the  $\gamma$ -globin.

Importantly, the substitution of Glutamic acid residue at position six with Valine causes the formation of Sickie Hb, giving rise to Sickie Cell Disorders. This mutation induces the polymerization of deoxy-HbS and fiber formation that change the shape of RBCs, but it can be reverted by reoxygenation cycles.

Other substitutions alter Hb solubility, inducing protein precipitation and therefore reducing the lifespan of the RBCs. Variants with altered oxygen affinity have also been reported. Amino

acids substitutions can result in increased stability of the T state of Hb, with a consequent reduction of its ability to release oxygen.

Methemoglobin variants result from an amino acid substitutions within the heme pocket, that stabilize the heme iron and its oxidized form ( $\text{Fe}^{3+}$ ). Several types of methemoglobins have been reported<sup>280,294</sup>.

### 1.3.5 Expression in nonerythroid locations

Hb was thought to be expressed only in erythroid cells until some decades ago, when this tenet was challenged by the discovery of Hb in different locations.

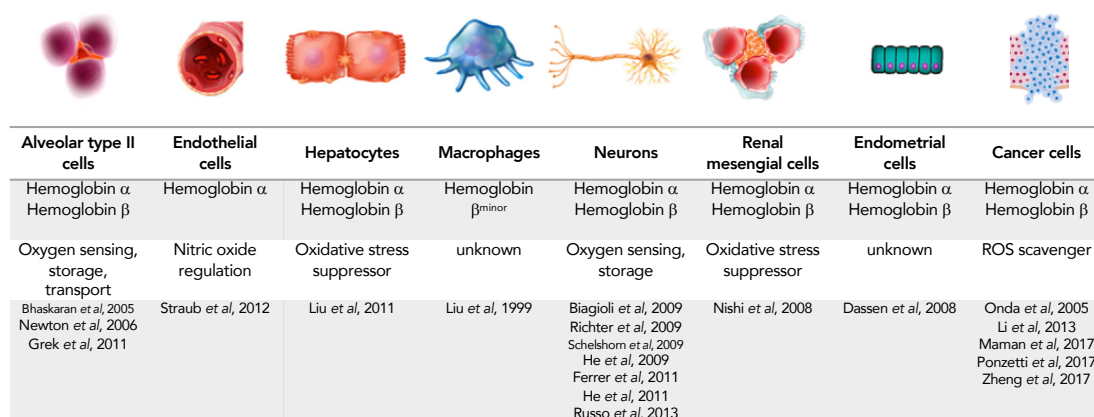


**Figure 11.** Atypical localization of Hb and its putative functions. Modified from Rahaman *et al.*<sup>255</sup>

The first evidence for a nonerythroid location of Hb dates back to 1975, when Groudine and Weintraub reported that embryonic globin RNA accumulated after Rous sarcoma virus infection in chicken fibroblasts<sup>295</sup>. Then, Cheung and co-workers found  $\alpha$ -globin gene activation after herpes simplex virus infection of human fibroblasts and HeLa cells<sup>296</sup>. Later on, Liu and co-workers reported  $\beta^{\text{minor}}$ -globin expression in macrophage RAW264.7 cells and mice peritoneal macrophages after LPS and interferon treatments<sup>297</sup>.

$\alpha$  and  $\beta$ -globin genes expression has been found in alveolar epithelial cells from human and rodents<sup>298,299</sup>, therefore it was speculated that Hb may have a role in oxygen transport across the air-blood barrier,  $\text{O}_2$  or NO scavenging and  $\text{O}_2$  sensing<sup>298</sup>. Moreover, it has been demonstrated that Hb expression increased after hypoxia and, interestingly, that hypoxia inducible factors (HIFs) and the transcription factor GATA-1 play a crucial role. So Hb expression in alveolar cells occurs in similar fashion as in erythrocytes<sup>300</sup>.

Tezel and co-workers found that Hb is the major protein in human retinal pigment epithelium (RPE), possibly linked to RPE cells requirement of high O<sub>2</sub> concentration<sup>301</sup>. Hb was found upregulated in ocular hypertensive rat eyes and glaucomatous human donor eyes<sup>302</sup>. These findings suggest that Hb may act to increase cellular oxygenation, protect cells against hypoxia and act as scavenger of free radicals and nitric oxide, that are increased during glaucomatous injury<sup>303</sup>.

Expression of Hb in hepatocytes has been demonstrated in a study on liver biopsies from non-alcoholic steatohepatitis (NASH) patients, revealing increased Hb levels compared to control. Moreover, Hb overexpression was able to reduce oxidative stress HepG2 cells treated with hydrogen peroxide<sup>304</sup>.

The same protective effect against oxidative stress was reported for both primary rat mesangial cells<sup>305</sup> and human primary vaginal epithelial cells<sup>306,307</sup>.

Recently, a potential role of Hb in cancer has emerged. The first report showed that Hb- $\beta$  gene is downregulated in anaplastic thyroid cancer cell derived from patients<sup>308</sup>. On the other hand, both Hb- $\alpha$  and - $\beta$  genes were found overexpressed in cervical carcinoma compared to normal cervical tissues. Their expression was upregulated by H<sub>2</sub>O<sub>2</sub> in human cervical carcinoma cell lines. Importantly, Hb expression reduced ROS production and improved cell viability<sup>309</sup>. The  $\beta$ -subunit of Hb has also been reported to be upregulated in lungs of micrometastasis-bearing mice and to exert an inhibitory effect on the growth of micrometastatic and macrometastatic neuroblastoma cells<sup>310</sup>. A significantly higher expression of Hb- $\beta$  was observed in invasive human breast cancers vs in situ counterparts. The overall survival rate was lower in patients with increased Hb- $\beta$  expression. Its overexpression in breast cancer cell lines, increased their motility and ability to migrate. Vascular endothelial growth factor (VEGF) expression was also increased and so was the cells' capacity to induce angiogenesis<sup>311</sup>. The authors speculated that Hb could act as ROS scavenger in tumor cells and to prevent their toxicity against the tumor. In a recent study, Zheng and colleagues used single-cell RNA seq data from metastasis-competent circulating tumor cells (CTCs) from breast, prostate and lung cancer. They observed an induction of Hb- $\beta$  in all three tumor types and, at the same time, increased oxidative stress. They also showed that Hb- $\beta$  upregulation in response to ROS and matrix deprivation, is mediated by the transcription factor KLF4. By ChIP they demonstrated the interaction between KLF4 and Hb- $\beta$  promoter. Moreover, they proved that Hb- $\beta$  exerts a protective role against oxidative stress in these cancer cells and

increases their metastatic propensity in a mouse model<sup>312</sup>. These findings support the strong correlation between Hb and cancer and the role of Hb as ROS scavenger in tumor.

#### *Neurons and neurodegenerative disorders*

In 2009, three different groups demonstrated Hb expression in neurons. Biagioli and colleagues showed by cDNA microarrays and nanocage that  $\alpha$ - and  $\beta$ - globin are expressed in A9 DA neurons, cortical and hippocampal astrocytes and mature oligodendrocytes in mice. They confirmed the same expression pattern in rats and human post-mortem brains. These results were suggesting a potential correlation between high Hb expression and DA cells' vulnerability in PD. Moreover, gene expression analyses of MN9D cells overexpressing Hb, showed changes in genes involved in O<sub>2</sub> homeostasis and mitochondrial oxidative phosphorylation, a pathway altered in PD<sup>1</sup>. Richter and co-workers showed  $\alpha$ - and  $\beta$ - globin expression in nigral, cortical and striatal neurons from rats and confirmed the expression in human brains<sup>313</sup>. Interestingly, inhibition of mitochondrial complex I by *in vivo* administration of rotenone, downregulated Hb expression<sup>313</sup>. Schelshorn *et al.* demonstrated that  $\alpha$ -globin is expressed in neurons of cerebral cortex, cerebellum, hippocampus and striatum, but not in astrocytes and oligodendrocytes<sup>314</sup>. Moreover, they showed that erythropoietin induces  $\alpha$ -globin expression and that cells expressing  $\alpha$ -globin display a better oxygenation than normal cells after hypoxia<sup>314</sup>. Interestingly, Russo and colleagues demonstrated that Hb maintains its hetero-tetrameric structure in neurons<sup>315</sup>. Given the strong correlation between Hb structure and its functions, these results opened newsworthy questions regarding Hb functions in the nervous system.

A connection between Hb and neurodegenerative disorders has started emerging lately. Decreased Hb expression in AD brains has been reported<sup>316,317</sup>, while an opposite pattern was reported in a rat model of AD depending on the disease stage, with decreased expression at early stages and increased levels at late pathological stages<sup>318</sup>. Furthermore, Hb was shown to bind A $\beta$ , promote its oligomerization and colocalize with senile plaques<sup>319,320</sup>.

Both upregulation and downregulation of Hb chains have been reported in prion-infected animals and human samples<sup>317,321-324</sup> and different trends have been reported depending on the disease type in humans, suggesting a correlation between Hb gene expression and prion strains<sup>317</sup>.

Increased Hb levels in blood have been associated with an increased risk of PD<sup>325</sup>. In contrast, it has been reported that anaemia is associated with PD and may precede the onset of motor symptoms by decades<sup>326</sup>. Recently, a blood transcriptomic meta-analysis from PD patients

showed a significant downregulation of genes related to Hb and iron metabolism, providing evidence for the impairment of these pathways in PD<sup>327</sup>. Reduced levels of Hb have been reported in DA neurons of SN and other altered neurons with  $\alpha$ -syn deposits in both PD and DLB<sup>316</sup>. The group of Prof. Chakrabarti found that Hb colocalizes with mitochondria and, in particular, with their inner membrane space in both human frontal lobe and SN. It is decreased in mitochondria in degenerating neurons and, importantly, changes in its distribution between cytoplasm and mitochondria during neurodegeneration have been reported<sup>328</sup>. While levels of mitochondrial Hb trend towards a decrease in the cerebellum of females with PD, no change was observed in males. However, Hb content moved from intermembrane space to the outer membrane of the organelle<sup>329</sup>. Finally, the presence of Hb- $\alpha$ -syn complexes in brain and peripheral red blood cells (RBCs) of aging cynomolgus monkeys has recently been demonstrated<sup>3</sup>. Yang *et al.* suggest that increased intracellular  $\alpha$ -syn reduces the pool of free neuronal Hb in mitochondria as a result of Hb- $\alpha$ -syn complex formation. Hb overexpression increased free Hb levels in mitochondria, stabilized mitochondrial membrane potential, and reduced  $\alpha$ -syn-induced apoptosis *in vitro*<sup>3</sup>. In a recent study, our group demonstrated that Hb confers DA cells' susceptibility to MPP<sup>+</sup> and rotenone *in vitro* and its toxicity is O<sub>2</sub>-independent. Moreover, Hb forms insoluble aggregates in the nucleolus of DA neurons and induces nucleolar stress. After injection into mouse SN, Hb forms aggregates and impairs performance associated to motor learning<sup>2</sup>.

Transcriptome profiling analysis of MSA brain revealed increased expression of the alpha and beta hemoglobin genes<sup>330,331</sup>, while Hb- $\alpha$  genes were found downregulated in MSA mouse model<sup>332</sup>.

A connection between mitochondria and Hb seems to be relevant in multiple sclerosis too. Indeed, Hb  $\beta$ -chain is differentially expressed in cortex grey matter of MS patients<sup>333</sup>. Notably, Hb  $\beta$ -chain was enriched in pyramidal neurons in the internal layers of the cortex<sup>334</sup>. Furthermore, it interacts with mitochondrial proteins<sup>334</sup>.

These results provide evidence that Hb may play an important role in neuronal cells' physiology. It may act as oxygen reservoir, available in response to injury, or for mitochondrial homeostasis, and/or as neuroprotective agent against oxidative stress. Furthermore, these data position Hb as a potential player in several neurodegenerative diseases. Studying its role in neuronal dysfunction could lead to further insights into the pathogenesis and to new interesting cues for drug development.

The aim of this study is to clarify Hb involvement in  $\alpha$ -synucleinopathies and, in particular, in PD.

## **2 MATERIALS AND METHODS**

### **2.1 Production of recombinant human $\alpha$ -synuclein**

Expression and purification of human  $\alpha$ -syn were performed as previously described<sup>335</sup>. Briefly,  $\alpha$ -syn gene was cloned in pET-11a vector and expressed in *E. coli* BL21(DE3) strain. Cells were grown in Luria-Bertani medium at 37°C and expression of  $\alpha$ -syn was induced by addition of 0.6 mM isopropyl- $\beta$ -D-thiogalactoside (IPTG) followed by incubation at 37°C for 5 hours. The protein was extracted and purified according to Huang *et al*<sup>336</sup>.

### **2.2 Fibrillation of human $\alpha$ -synuclein**

Lyophilized human  $\alpha$ -syn was resuspended in ddH<sub>2</sub>O, filtered with a 0,22  $\mu$ m syringe filter and the concentration was determined by absorbance measured at 280 nm. Fibrillization reactions were carried out in a 96-well plate (Perkin Elmer) in the presence of a glass bead (3 mm diameter, Sigma) in a final reaction volume of 200  $\mu$ L. Human  $\alpha$ -syn (1.5 mg/ml) was incubated in the presence of 100 mM NaCl, 20 mM TrisHCl pH 7.4 and 10  $\mu$ M Thioflavin T (ThT). Plates were sealed and incubated in BMG FLUOstar Omega plat reader at 37°C with cycles of 50 seconds shaking (400 rpm) and 10 seconds rest. Formation of fibrils was monitored by measuring the fluorescence of ThT (excitation: 450 nm, emission: 480 nm) every 15 minutes. After reaching the plateau phase, the reactions were stopped. Fibrils were collected, centrifuged at 100000g for 1 hour, resuspended in sterile PBS and stored at -80°C for further use. For cell culture experiments, the fibrillization reactions was carried out without ThT.

### **2.3 Atomic Force Microscopy**

Atomic Force Microscopy was performed as previously described<sup>337</sup> by Pietro Parisse, PhD, and Fabio Perissinotto, PhD, at Elettra Sincrotrone Trieste. Three to five  $\mu$ L of fibril solution was deposited onto a freshly cleaved mica surface and left to adhere for 30 minutes. Samples were then washed with distilled water and blow-dried under a flow of nitrogen. Images were collected at a line scan rate of 0.5-2 Hz in ambient conditions. The AFM free oscillation amplitudes ranged from 25 nm to 40 nm, with characteristic set points ranging from 75% to 90% of these free oscillation amplitudes.

## 2.4 Cell line

MN9D-Nurr1<sup>Tet-on</sup> (iMN9D) cell line stably transfected with pBUD-IRES-eGFP (Control cells) or with pBUD- $\beta$ -globin-MYC IRES-eGFP, 2xFLAG- $\alpha$ -globin (Hb cells) were used<sup>1</sup>. Cells were maintained in culture at 37 °C in a humidified CO<sub>2</sub> incubator with DMEM/F12 medium (Gibco by Life Technologies, DMEM GlutaMAX™ Supplement Cat. No. 31966-021; F-12 Nutrient Mix GlutaMAX™ Supplement Cat. No. 31765-027) supplemented with 10% fetal bovine serum (Euroclone, Cat. No. ECS0180L), 100  $\mu$ g/ml penicillin (Sigma–Aldrich), 100  $\mu$ g/ml streptomycin (Sigma-Aldrich), 300  $\mu$ g/ml neomycin (Gibco by Life Technologies, Cat. No 11811-031) and 150  $\mu$ g/ml zeocyn (Invivogen, Cat. No. ant-zn-05) were used for selection.

## 2.5 Transfection

iMN9D cells were plated in 6 cm-plates or 12 well-plates (for immunofluorescence) the day before transfection (6x10<sup>5</sup> cells/plate or 1x10<sup>5</sup> cells/well) and transfected with 8 or 1,6  $\mu$ g of pCDNA3- $\alpha$ -syn using Lipofectamine 2000 (Invitrogen by Life Technologies, Cat. No. 11668019) following manufacturer's instructions. Cells were collected 48 hours after transfection.

## 2.6 Co-immunoprecipitation

The co-immunoprecipitation (co-IP) was performed as previously described<sup>338</sup>. In brief, iMN9D cells were washed two times with D-PBS 1X 48 h after transfection. Then, lysine residues of the interacting proteins were crosslinked by incubation with 1 mM of the cell permeable dithio-bissuccinimidylpropionate (DSP) (Sigma-Aldrich, D3669) at room temperature for 30 min, followed by incubation with quenching solution (20 mM TrisHCl pH 7,4 in D-PBS) at room temperature for 15 min and washed two times with D-PBS 1X. Cells were scraped from dishes on ice with cold IP buffer (300 mM NaCl, 50 mM Tris pH 7.5, 1% Igepal CA-630, 10% glycerol) supplemented with protease inhibitor mixture (Roche Diagnostics, COEDTAF-RO) and then lysed for 30 minutes at 4°C on rotator. Lysates were cleared at 12000 g for 30 minutes and incubated with anti-FLAG M2 Affinity Gel (Sigma–Aldrich, A2220) or anti-MYC antibody (Cell Signaling, 2276) for 2 h at 4 °C on rotator. Lysates incubated with anti-MYC antibody were then incubated with Protein G Sepharose 4 Fast Flow (GE Healthcare, 17-0618-01) for 30 min at 4 °C on rotator. After washing the resin three times with PBS, immunoprecipitated proteins were eluted with SDS

sample buffer 2X containing  $\beta$ -mercaptoethanol, boiled at 95°C for 5 min and analysed by western blot.

## **2.7 Exposure of iMN9D cells to $\alpha$ -syn monomers and fibrils**

iMN9D cells were exposed to 2  $\mu$ M of  $\alpha$ -syn species (2  $\mu$ M equivalent monomer concentration in the case of amyloids) in cell culture media for 24, 48, 96 hours before collection.

For western blot analysis cells were plated in 6 well-plate (6x10<sup>5</sup> cells/plate for 24h collection, 3x10<sup>5</sup> cells/plate for 48h collection, 2x10<sup>5</sup> cells/plate for 96h collection). Additionally, at 96 hours cells were split and maintained for three additional days before collection as Passage 1 (P1). Cells treated with vehicle were used as control (Untreated).

For immunocytochemistry, cells were cultured in 12-well plates with coverslips (3x10<sup>5</sup> cells/well for 24h collection, 1,5x10<sup>5</sup> cells/well for 48h collection, 1x10<sup>5</sup> cells/well for 96h collection).

For MTT analysis, cells were cultured in 96-well plates (4x10<sup>4</sup> cells/well for 24h collection, 2x10<sup>4</sup> cells/well for 48h collection, 1x10<sup>4</sup> cells/well for 96h collection).

## **2.8 Antibodies validation for quantitative western blot**

For antibodies validation, cells were lysed in cold lysis buffer (10 mM TrisHCl pH 8, 150 mM NaCl, 0.5% Igepal CA-630, 0.5% sodium deoxycholate) supplemented with protease inhibitor mixture (Roche Diagnostics, COEDTAF-RO). Lysates were incubated for 30 min at 4°C on rotator and cleared at 12000 g for 20 min at 4°C. Supernatants were transferred in new tubes and total protein content was measured using bicinchoninic acid protein (BCA) quantification kit (Pierce) following the manufacturer's instructions.

## **2.9 Biotinylated fibrils pulldown**

For pulldown experiments,  $\alpha$ -syn PFFs were biotinylated following the manufacturer's instructions (Sigma-Aldrich). iMN9D cells were lysed in cold immunoprecipitation (IP) buffer (50 mM Tris HCl pH 8, 150 mM NaCl, 0.1% Igepal CA-630) containing protease inhibitors (Roche Diagnostics, COEDTAF-RO). Following 30 min incubation at 4 °C on rotator, lysates were cleared at 12000 g for 20 min and incubated with biotinylated fibrils overnight at 4°C on rotator. Biotinylated fibrils were pulled down by binding to NeutrAvidin Agarose Resin (Pierce, 29200).

After 4 h incubation at 4 °C, the resin-bound complexes were washed three times with IP buffer and eluted with SDS sample buffer 2X, boiled at 95°C for 5 min and analyzed by western blot.

## **2.10 Cathepsin D and Calpain inhibitors treatment**

Pepstatin (Pep, Cathepsin D inhibitor, MedChem Express Cat. No. HY-P0018) and Calpain inhibitor III (Santa Cruz Cat. No. SC-201301) were dissolved in dimethylsulfoxide (DMSO) and diluted in cell culture medium to a final concentration respectively of 100 µM and 10 µM. Hb cells were treated with vehicle (DMSO), Calpain inhibitor III and Pepstatin A at the indicated concentrations for 24 h. Medium was then removed and replaced with new one containing  $\alpha$ -syn amyloids, as previously reported, and protease inhibitors to a final concentration respectively of 100 µM and 10 µM, as the day before. Cells were collected at the indicated time points for western blot analysis. Immunoblot of Spectrin  $\alpha$  II was used to monitor Calpain inhibitor activity, while Cathepsin D activity kit was used to monitor Cathepsin D activity.

## **2.11 Cathepsin D activity assay**

Cathepsin D (CatD) activity measurements were performed using the Cathepsin D activity assay kit (BioVision, Cat. N. K143) following manufacturer's instructions. Briefly, cells were washed twice with PBS, collected in culture media and pelleted by centrifugation at 500 g for 5 min. Cells were counted and  $1 \times 10^5$  cells/well were used. Cells were washed once with PBS, pelleted again by centrifugation at 500 g for 5 min and lysed in CD Cell Lysis Buffer incubating samples for 10 min on ice. Cells were then centrifuged at maximum speed for 10 min. As control, untreated cells were incubated with PepA (100 µM final concentration) at 37°C for 10 min prior addition of Reaction Buffer and CD substrate. The reaction was left to proceed at 37°C for 1:30 h in the dark. Fluorescence was read using Thermo Scientific Varioskan® Flash with a 328-nm excitation filter and 460-nm emission filter.

CD activity in relative fluorescence units (RFU) was then normalized to Hb cells treated with vehicle and indicated as % Activity. Each sample was measured in duplicate and measurements were repeated two times.

## 2.12 MTT analysis

Cell viability was assayed using Thiazolyl Blue Tetrazolium Bromide (MTT, Sigma–Aldrich, M5655) following the manufacturer’s instructions. Briefly, 20 µl of MTT solution (5 mg/ml in PBS) were added to each well and incubated at 37°C for 4 h. The medium was then removed and replaced with 200 µl DMSO. Plates were shaken before absorbance measurements. Absorbance was measured at 550 nm wavelength using a microplate ELISA reader (Thermo Scientific).

## 2.13 Western Blot

iMN9D cells were washed 2 times with D-PBS and lysed in 300 µl SDS sample buffer 2X (6 well-plate), briefly sonicated, boiled and 10 µl/sample loaded on 15 % or 8 % (for Spectrin  $\alpha$  II immunoblot) SDS-PAGE gel. For antibodies validation, cells were lysed in cold lysis buffer (10 mM Tris-HCl pH 8, 150 mM NaCl, 0.5% Igepal CA-630, 0.5% sodium deoxycholate) supplemented protease inhibitor mixture (Roche Diagnostics, COEDTAF-RO). Lysates were incubated for 30 minutes at 4 °C on rotator and cleared at 12000 g for 20 minutes at 4 °C. Supernatants were transferred in new tubes and total protein content was measured using bicinchoninic acid protein (BCA) quantification kit (Pierce) following the manufacturer’s instructions. Proteins were transferred to nitrocellulose membrane (Amersham™, Cat. No. GEH10600001) for 1:30 hour at 100V or 16 hours 20V (only for Spectrin  $\alpha$  II immunoblot). Membranes were blocked with 5% non-fat milk or 5% BSA (only for Spectrin  $\alpha$  II immunoblot) in TBST solution (TBS and 0.1% Tween20) for 40 minutes at room temperature. Membranes were then incubated with primary antibodies at room temperature for 2 h or overnight at 4 °C (only for Spectrin  $\alpha$  II immunoblot). The following antibodies were used: anti-FLAG 1:2000 (Sigma–Aldrich, F3165), anti-MYC 1:2000 (Cell Signaling, 2276), anti- $\beta$ -actin 1:5000 (Sigma–Aldrich, A5441), anti-Hemoglobin 1:1000 (Cappel, MP Biomedicals, 55039) and anti-GFP 1:1000 (Clontech, 632380), anti- $\alpha$ -syn 1:1000 (C-20) (Santa Cruz Biotechnology, sc-7011-R), anti- $\alpha$ -syn 1:1000 (SYN-1) (BD Transduction Laboratories, 610787), anti-biotin-HRP (Jackson ImmunoResearch Laboratories), anti Spectrin  $\alpha$  II 1:1000 (Santa Cruz, Cat. No. sc-46696). For development, membranes were incubated with secondary antibodies conjugated with horseradish peroxidase (Dako) for 1 hour at room temperature. For IP and pulldown experiments, membranes were incubated with Protein A antibody conjugated with horseradish peroxidase for 1 hour at room

temperature. Proteins of interest were visualized with the Amersham ECL Detection Reagents (GE Healthcare by SIGMA, Cat. No. RPN2105) or LiteAblot TURBO Extra-Sensitive Chemiluminescent Substrate (EuroClone, Cat. No. EMP012001). Western blotting images were acquired using with Alliance LD2-77WL system (Uvitec, Cambridge) and band intensity was measured UVI-1D software (Uvitec, Cambridge).

## **2.14 Immunocytochemistry**

Cells were washed two times with D-PBS, fixed in 4% paraformaldehyde for 20 minutes, washed two times with PBS 1X and treated with 0.1M glycine for 4 minutes in PBS 1X, washed two times and permeabilized with 0.1% Triton X-100 in PBS 1X for 4 minutes. Cells were then incubated in blocking solution (0.2% BSA, 1% NGS, 0.1% Triton X-100 in PBS 1X), followed by incubation with primary antibodies diluted in blocking solution for 2:30 hours at room temperature. After two washes in PBS 1X, cells were incubated with labelled secondary antibodies and 1 $\mu$ g/ml DAPI (for nuclear staining) for 60 minutes. Cells were washed twice in PBS 1X and once in Milli-Q water and mounted with Vectashield mounting medium (Vector Lab, H-1000). The following antibodies were used: anti-FLAG 1:100 (Sigma–Aldrich, F7425), anti-MYC 1:250 (Cell Signaling, 2276), anti- $\alpha$ -syn (C-20) 1:200 (Santa Cruz Biotechnology, sc-7011-R), anti- $\alpha$ -syn (SYN-1) 1:200 (BD Transduction Laboratories, 610787) and anti- $\alpha$ -syn(phosphoS129) 1:200 (Abcam, ab59264). For detection, Alexa Fluor-488, -594 or -647 (Life Technologies) antibodies were used. Image acquisition was performed using C1 Nikon confocal microscope (60x oil, NA 1.49, 7x zoom-in).

## **2.15 Immunofluorescence with labelled $\alpha$ -syn fibrils**

Human  $\alpha$ -syn fibrils were fluorescently labelled with Alexa-488 succinimidyl ester (Thermo Fisher Scientific, A20000) following manufacturer's instructions and the unbound fluorophore was removed with multiple dialysis steps in sterile PBS. Uptake experiments were performed following standard IF protocol or following the protocol described by Karpowicz *et al*<sup>39</sup>. Briefly, cells seeded on coverslips were incubated with culture medium containing labelled  $\alpha$ -syn fibrils for 24 h. Prior to standard immunocytochemistry protocol, fluorescence from non-internalized fibrils was quenched by incubating with Trypan Blue for 5 minutes. Cells were then fixed in 4% paraformaldehyde for 20 minutes, washed two times and permeabilized with 0.1%

Triton X-100 in PBS 1X for 4 minutes and incubated with HCS Blue Cell Mask 1:1000 for 30 minutes (Thermo Fisher Scientific). Cells were washed twice in PBS 1X and once in Milli-Q water and mounted with Vectashield mounting medium (Vector Lab, H-1000). Images acquisition was performed using C1 Nikon confocal microscope (60x oil, NA 1.49, 7x zoom-in) as z-stacks of 0.5  $\mu\text{m}$ .

## **2.16 Statistical Analysis**

Biostatistical analysis was performed using GraphPad Prism version 7.0. All the data groups were considered as unpaired. Groups were first tested for normality, and then for homogeneity of variance (homoscedasticity). If the normality assumption was not met, data were analyzed by nonparametric Mann-Whitney test. If the normality assumption was met, but homogeneity of variance was not, data were analyzed by unpaired two-tailed t-test followed by Welch's correction. If both assumptions were met, data were analyzed by unpaired two-tailed t-test. With small sample size ( $n < 10$ ), data were directly analyzed by nonparametric Mann-Whitney test. For qPCR analysis,  $\Delta\Delta\text{Ct}$  values were used for the comparison. *P*-values  $< 0.05$  were considered statistically significant.

### 3 RESULTS

#### 3.1 Previous data obtained in the laboratory of Professor Gustincich

While studied for its fundamental function in O<sub>2</sub> transports in red blood cells, hemoglobin (Hb) has been recently found expressed in non-erythroid locations, including neurons. Furthermore, Hb expression has been shown altered in several neurodegenerative diseases.

A previous study in the laboratory of Prof. Gustincich showed that Hb is differentially expressed in mesencephalic DA neurons with a potential correlation between high expression and cells' vulnerability. Furthermore, they showed its presence in oligodendrocytes and selected astrocytes<sup>1</sup>. Then Russo and colleagues showed for the first time that the  $\alpha_2\beta_2$  tetramer structure, that is fundamental for the cooperative property of Hb, is present in iMN9D and N2a cells as well as in mouse mesencephalon<sup>315</sup>. The study of Codrich and colleagues demonstrated that neuronal Hb may contribute to DA cells' dysfunction in PD by sensitizing cells to neurointoxication interfering with pathways involved in neurodegeneration<sup>2</sup>.

These observations prompted us to deepen the mechanisms by which neuronal Hb might act as potential player in PD or, more generally, in  $\alpha$ -synucleinopathies.

To this purpose, we took advantage of iMN9D DA cell line stably overexpressing  $\alpha$ - and  $\beta$ -chains of Hb, previously shown to preserve the  $\alpha_2\beta_2$  tetramer<sup>315</sup>, and of  $\alpha$ -syn preformed fibrils (PFFs), kindly provided by Prof. Legname's group.

### 3.2 Experimental model

In order to study the involvement of neuronal Hb in  $\alpha$ -synucleinopathies pathogenesis, we used iMN9D cells expressing tagged  $\alpha$  and  $\beta$  chains of mouse Hb (Hb cells) and iMN9D cells stably expressing the empty vector (Control cells) (Fig. 12 C). iMN9D cells were maintained in selection and periodically assessed for Hb protein and mRNA expression levels (Fig. 12 A and B). Notably, that Ct values of Hb- $\beta$ -chain in Control cells were often undetermined, indicating very low expression of the transcript.

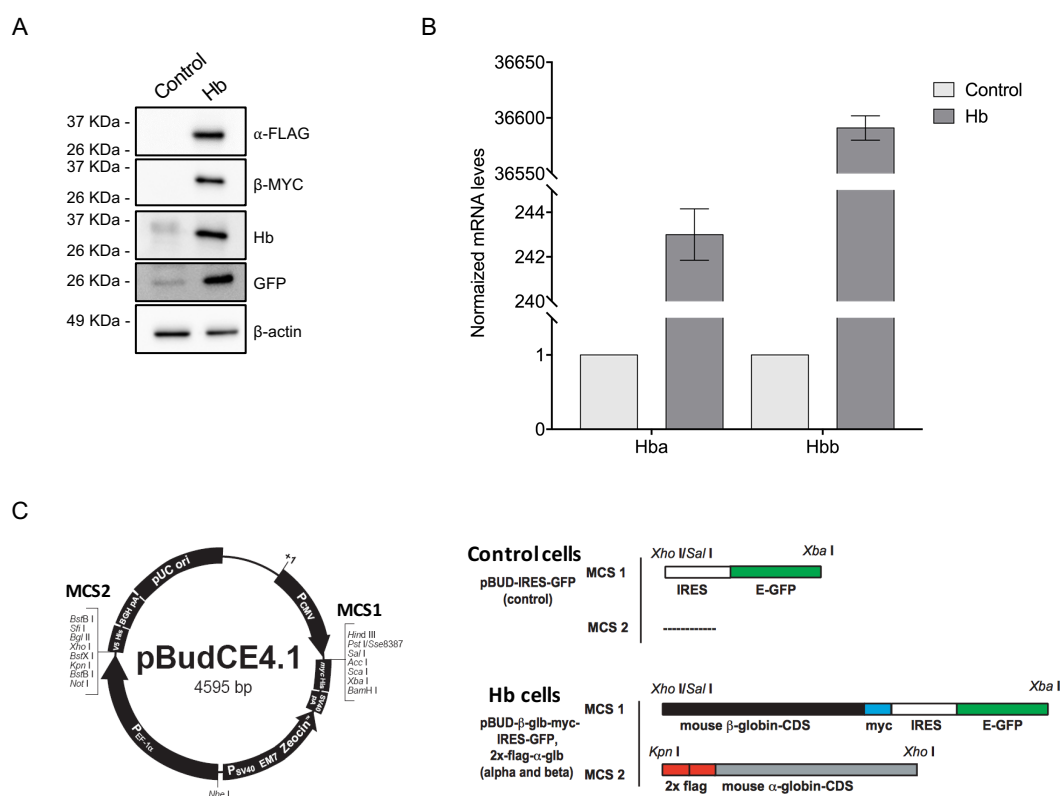


**Figure 12.** Mouse dopaminergic cell line (iMN9D) stably overexpressing  $\alpha$ - and  $\beta$ -chains of Hb. A. Protein levels were analyzed by western blot (WB) with anti-FLAG, -MYC and -Hb antibodies. B. RNA levels were analyzed by qRT-PCR with  $\alpha$ - and  $\beta$ -specific primers. Values are represented as mean  $\pm$  standard error of mean (SEM) (n=5 for Hb- $\alpha$ -chain; n=3 for Hb- $\beta$ -chain). C. Cloning strategy scheme of pBUD-IRES-GFP (empty vector) and pBUD- $\beta$ -glb-Myc-IRES-GFP, 2x-flag- $\alpha$ -glb ( $\alpha$  and  $\beta$  vector), modified from Biagioli et al.<sup>1</sup> Control, iMN9D Control cells; Hb, iMN9D Hb cells.

### 3.3 Hb and $\alpha$ -synuclein interact in transfected cells

It has been previously demonstrated by Yang and colleagues that Hb and  $\alpha$ -syn form complexes in brain and red blood cells of aging cynomolgus monkeys<sup>3</sup>. Therefore we asked whether  $\alpha$ -syn and Hb physically interact in our model. To address this question, we transfected Hb cells with a vector expressing  $\alpha$ -syn and performed co-immunoprecipitation (co-IP)

experiments. 48 hours after transfection cell lysates were immunoprecipitated with both anti-FLAG agarose beads and anti-MYC antibody, the latter followed by incubation with beads. We did not detect any  $\alpha$ -syn signal in the immunoprecipitated fractions.

Therefore, we decided to perform chemical crosslinking prior to co-IP experiments. Indeed, transient or labile interactions are difficult to assess and chemical crosslinkers have been widely used to stabilize weakly interacting partners. In particular, dithio-bissuccinimidylpropionate (DSP) is a cell permeable crosslinker with a spacer arm of 12 Å that reacts with lysine residues, highly abundant in proteins. We performed *in vivo* crosslinking and the reaction was stopped by the addition of a quenching solution, prior to cell lysis, as previously reported<sup>338</sup>. By addition of SDS sample buffer containing  $\beta$ -mercaptoethanol, DSP is then cleaved and the bound molecules are released. In these conditions,  $\alpha$ -syn was detected in the fraction of both FLAG and MYC IP samples, thus indicating that  $\alpha$ -syn interacts with both  $\alpha$  and  $\beta$ -chains of Hb.

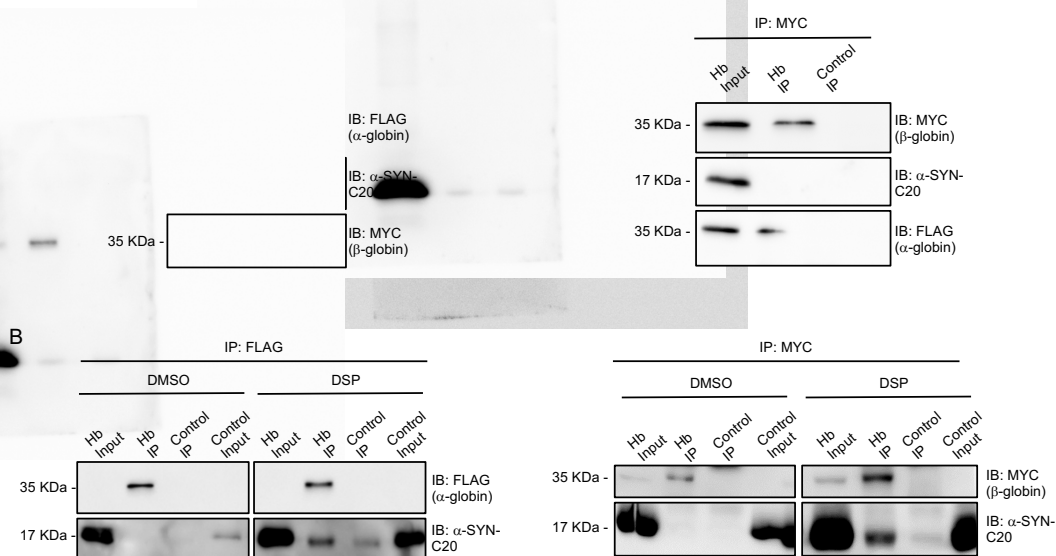


**Figure 13.**  $\alpha$ -syn and Hb binding in iMN9D cells.

Control and Hb cells were transfected with pcDNA3- $\alpha$ -syn for 48h. A. After lysis,  $\alpha$ -globin (IP: FLAG) and  $\beta$ -globin (IP: MYC) were immunoprecipitated (IP) and bound proteins were revealed by immunoblot (IB). After standard co-IP protocol, no  $\alpha$ -syn signal was detected in the immunoprecipitated fraction. B. After treatment with vehicle (DMSO) or 1 mM dithiobissuccinimidylpropionate (DSP) crosslinker,  $\alpha$ -globin (IP: FLAG) and  $\beta$ -globin (IP: MYC) were immunoprecipitated (IP) and bound  $\alpha$ -syn was revealed by immunoblot (IB) with anti- $\alpha$ -syn antibody (C20) (n=3, n=3). Control, iMN9D Control cells; Hb, iMN9D Hb cells; IP, Immuniprecipitated fraction.

### 3.4 Characterization of $\alpha$ -synuclein preparations

$\alpha$ -syn monomers (Ms) and sonicated preformed fibrils (PFFs) were kindly provided by Prof. Legname's group after biochemical analysis and structural characterization.

$\alpha$ -syn fibrillation was monitored by thioflavin T (ThT) fluorescence and fibrils were collected at plateau (long fibrils). Atomic force microscopy (AFM) was performed as previously reported<sup>115</sup> after 5 minutes of sonication to confirm the presence of fibrils (Fig. 14 A and B). Immunoblotting was used to confirm the presence of high molecular weight species in  $\alpha$ -syn PFFs preparation. Species with different molecular weights were detected using two epitope-specific antibodies respectively raised against the  $\alpha$ -syn C-terminal epitope ( $\alpha$ -syn C-20) and the region between the C-terminal and NAC region ( $\alpha$ -syn SYN-1) and different exposure times were used for the same membrane (Fig. 14 D). Both in Ms and PFFs preparations,  $\alpha$ -syn appears monomeric. Moreover, bands corresponding to dimers were also detected in both samples. High molecular weight species were only detected in PFFs preparation as a smear. No signal was observed using the antibody recognizing the phosphorylated Serine 129 of  $\alpha$ -syn (pSer129) (Fig. 14 D).

In addition to Ms and PFFs, western blot (WB) revealed the presence of fragments smaller than the molecular weight of full length  $\alpha$ -syn. A previous work by Vlad and colleagues also reported the presence of  $\alpha$ -syn fragments due to the autoproteolytic activity of the protein<sup>342</sup>.

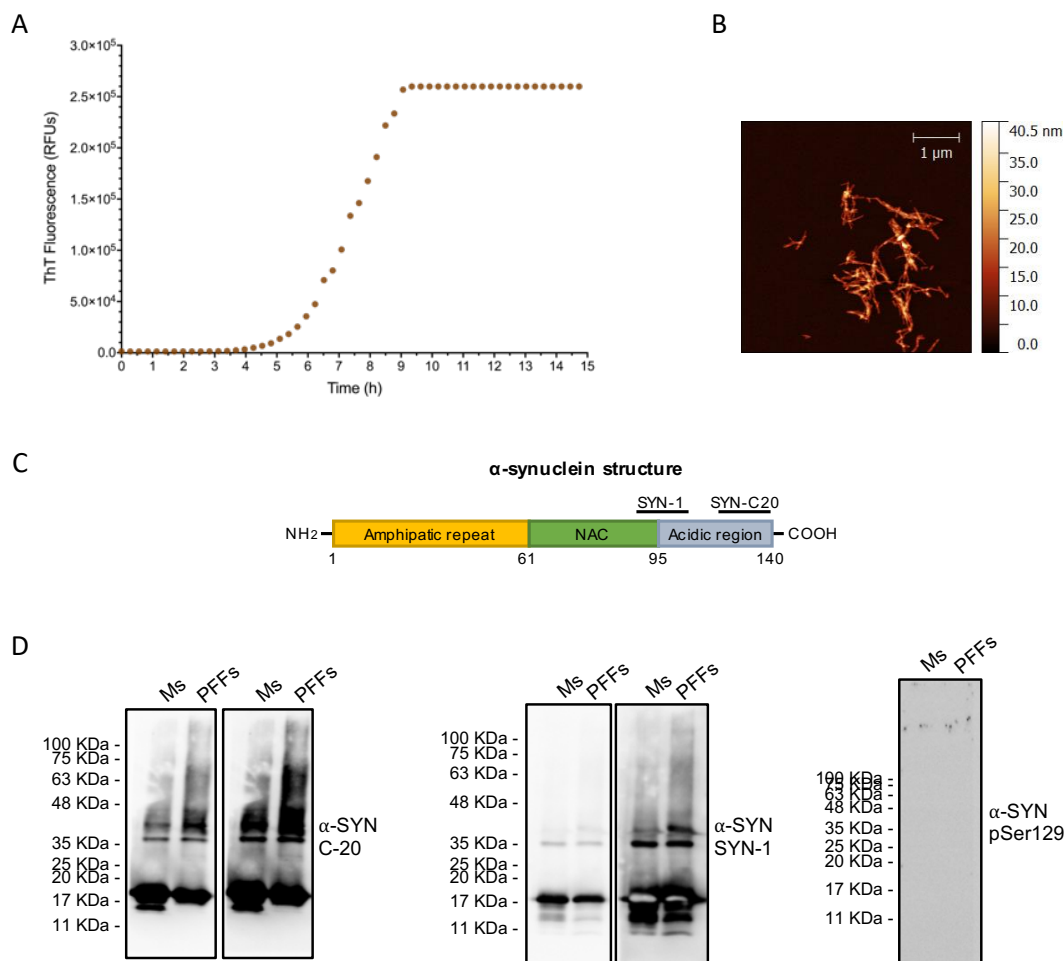


**Figure 14.** Biochemical analysis and structural characterization of  $\alpha$ -syn preparations.

A. Fibrillation curve of recombinant human  $\alpha$ -syn protein analysed using ThT fluorescence assay. Mean of three wells is represented. B. AFM analysis of fibrillary human  $\alpha$ -syn aggregates after 5 min of sonication. C. Domain structure of human  $\alpha$ -syn protein and epitopes of anti- $\alpha$ -syn antibodies used for the study. D. Ms and PFFs preparations were analysed by western blot with three different anti  $\alpha$ -syn antibodies. The same membrane was exposed for a longer period in order to detect high molecular weight species. Ms, monomers; PFFs, sonicated  $\alpha$ -syn-preformed fibrils.

### 3.5 Antibodies validation for quantitative western blot

In order to obtain reproducible and reliable quantification from western blot experiments, it is crucial to work within the linear response range of detection. Indeed, a linear relationship between proteins loaded on gels and the signal (band intensity) recorded by the detector should be observed. Therefore, protein lysates of cells treated with PFFs were measured and 1.25 fold dilution series were prepared and subjected to WB analysis.

Band intensity was quantified for both the housekeeping ( $\beta$ -actin) and target protein ( $\alpha$ -SYN). Within our experimental conditions,  $\beta$ -actin signal was linear up to 16,1  $\mu$ g ( $R^2 = 0,95$ ).

Full length -  $\alpha$ -syn (FL- $\alpha$ -syn) signal was linear within the entire range tested ( $R^2 = 0,95$ ), while the signal from the fragment detected at 11 KDa ( $\Delta C$ - $\alpha$ -syn) was linear up to 20,2  $\mu\text{g}$  ( $R^2 = 0,99$ ). The other points were outside the linear range of detection, meaning that an appropriate quantification is not allowed.

Therefore, we decided to perform our following experiments using an amount of proteins corresponding to the middle of the linear range (11,4  $\mu\text{g}$ ), that we assessed to correspond to 10  $\mu\text{l}$  of lysate (final volume of 300  $\mu\text{l}$  SDS sample buffer 2X from one well of 6 well-plate). For practical purposes, we proceeded with the experiments by lysing directly cells in SDS sample buffer 2X and loading on gels the volume corresponding to the middle of the linear range.

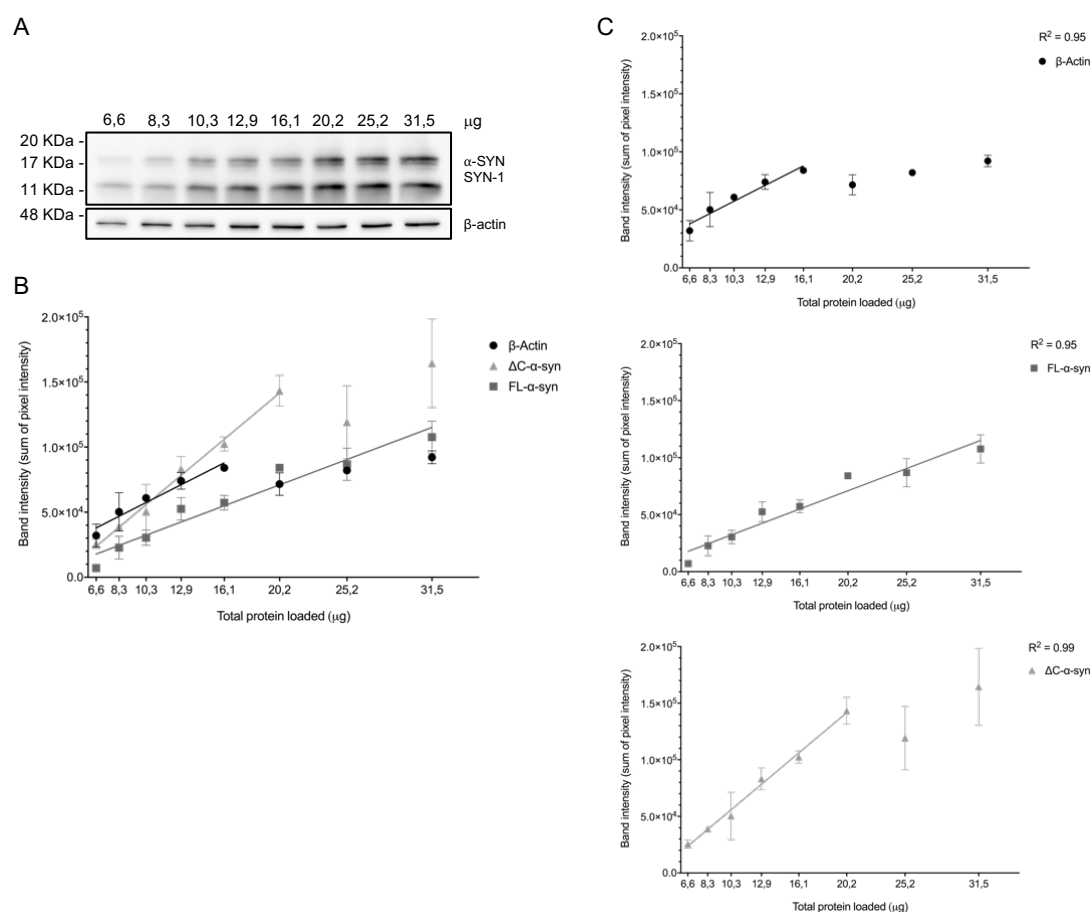


**Figure 15.** Linearity of immunodetection of housekeeping and target proteins in iMN9D cell lysates. A. Representative images of  $\beta$ -actin and  $\alpha$ -SYN staining. Numbers on the top of the images represent the amount of iMN9D cell lysates loaded to each lane in  $\mu\text{g}$ . B. Graph showing band density versus amount of sample loaded for  $\beta$ -actin, FL- $\alpha$ -syn and  $\Delta C$ - $\alpha$ -syn. Each point of the curves represents the average of two data points and is shown as mean  $\pm$  SD. The fitted regression line is superimposed. C. Graphs showing band density versus amount of sample loaded are reported separately for  $\beta$ -actin, FL- $\alpha$ -syn and  $\Delta C$ - $\alpha$ -syn.  $\beta$ -actin and  $\Delta C$ - $\alpha$ -syn were linear up to 16,1 and 20,2  $\mu\text{g}$  respectively. FL- $\alpha$ -syn was linear across the entire range tested.  $R^2$  values are reported.

### **3.6 Sonicated $\alpha$ -synuclein fibrils are internalized by iMN9D cells and are phosphorylated at serine 129**

It has been previously reported that sonicated PFFs are able to enter cells and promote endogenous  $\alpha$ -syn aggregation in SH-SY5Y, GT1 and N2a cells<sup>115,343</sup>. iMN9D cells instead do not express significant levels of  $\alpha$ -syn (verified by both WB and qPCR analysis, *data not shown*).

In order to assess the internalization of exogenously added PFFs, Hb and Control cells were exposed to Alexa-488 labelled PFFs for 24 hours, as added directly to cell medium, and immunofluorescence (IF) and WB analysis were performed.

Serial confocal z-sections demonstrated the uptake of PFFs and showed the intracellular distribution as small punctate structures (Fig. 16 A). To exclude the possibility of interfering signals coming from the extracellular space, the protocol developed by the group of Dr. Virginia M.-Y. Lee was used<sup>339</sup>. Briefly, prior to IF protocol green fluorescence from extracellular fibrils was quenched by incubation with Trypan Blue, a method that has been validated as quantitative assay to measure PFFs uptake<sup>339</sup>. Trypan Blue does not cross the plasma membrane over short time periods and it is widely used to quench extracellular green and red fluorophores. Moreover, it is reported to have affinity for amyloid fold<sup>339</sup>. Serial confocal z-sections were acquired from samples treated with Trypan Blue and confirmed our previous results (Fig. 16 C). Cells not incubated with Alexa-488-labelled PFFs were used to establish autofluorescence levels (Fig 16 B and D). Intracellular accumulation of  $\alpha$ -syn was confirmed by western blot (Fig. 16 E). Monomers-treated cells were used as negative control.

Therefore, we conclude that iMN9D cells internalize  $\alpha$ -syn PFFs.

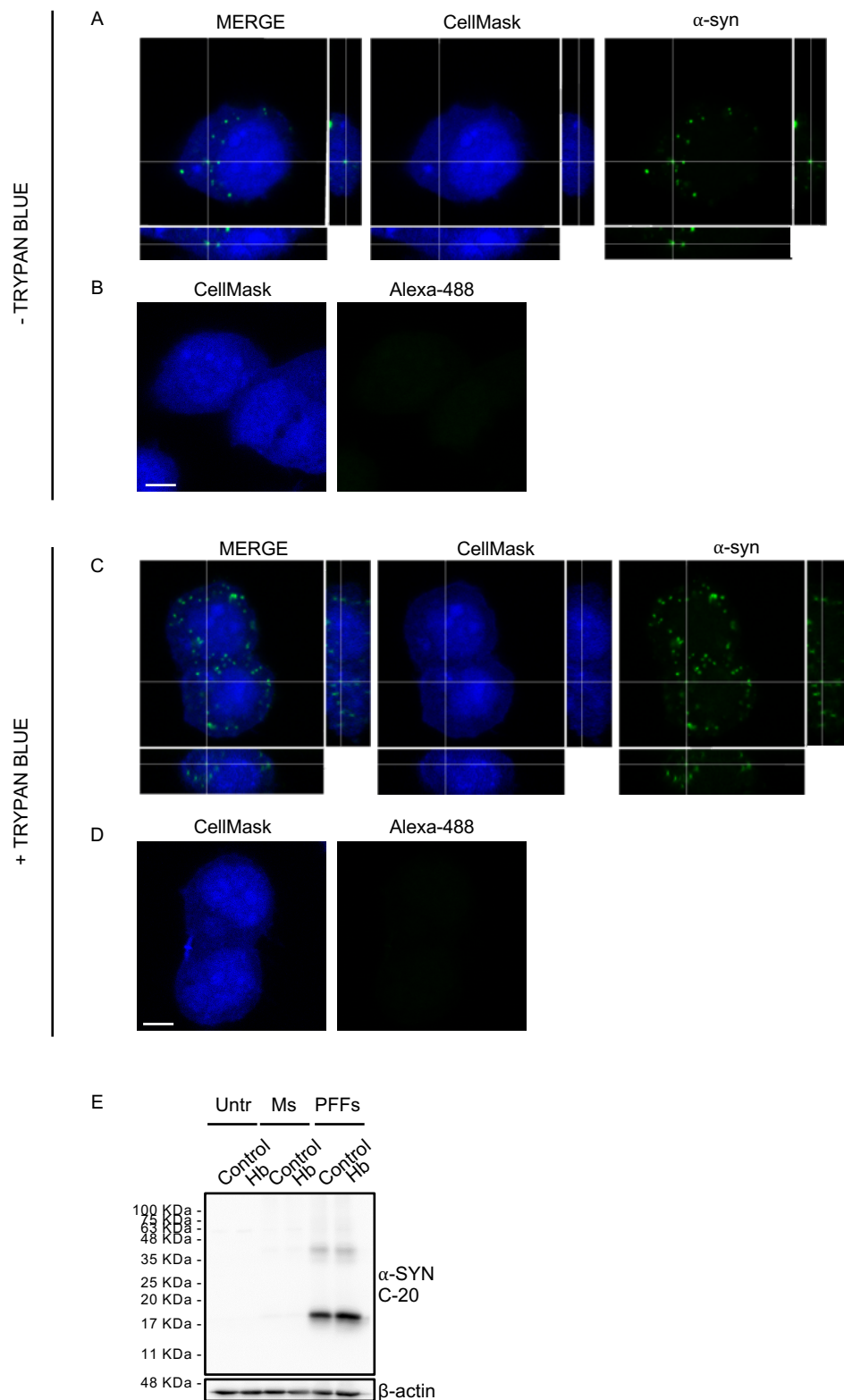


**Figure 16.** Sonicated  $\alpha$ -synuclein fibrils are internalized by iMN9D cells. Representative confocal microscopy images of Hb cells treated with Alexa-488 labelled PFFs for 24 h, without (A) and after (C) Trypan Blue quenching. Cells not incubated with labelled PFFs were used to establish autofluorescence levels (B and D). Entire cells were labelled by CellMask. Scale bar 10  $\mu$ m. E. Immunoblot of lysates from untreated

cells and cells treated with Ms and PFFs for 24 h. Control, iMN9D Control cells; Hb, iMN9D Hb cells, Untreated, untreated cells; Ms, cells treated with monomers; PFFs, cells treated with sonicated  $\alpha$ -syn-preformed fibrils.

We next determined whether  $\alpha$ -syn PFFs inclusions resemble one of the posttranslational modifications considered to be hallmark of LBs, the phosphorylation at Serine 129 of  $\alpha$ -syn (pSer129)<sup>163,164</sup>. Indeed, these inclusions were positively stained by the antibody recognizing pSer129 (Fig. 17), indicating a *de novo* intracellular modification, since WB on purified PFFs confirmed that recombinant  $\alpha$ -syn PFFs are not phosphorylated prior cellular uptake (Fig. 14 D). No staining for phosphorylated  $\alpha$ -syn was detected in cells treated with monomers.

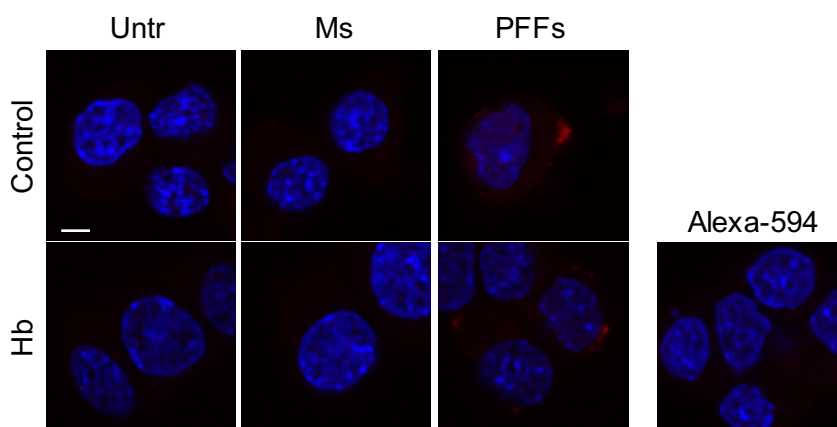


**Figure 17.** iMN9D cells show pSer129 positive inclusions after  $\alpha$ -syn PFFs treatment. Representative confocal microscopy images of Control and Hb cells immunostained for  $\alpha$ -syn phosphorylated at Ser129 (pSer129, Alexa 594, red). Nuclei were stained with DAPI. Scale bar 10  $\mu$ m. Control, iMN9D Control cells; Hb, iMN9D Hb cells; Untreated, untreated cells; Ms, cells treated with monomers; PFFs, cells treated with sonicated  $\alpha$ -syn-preformed fibrils; Alexa-594, cells treated with PFFs and immunostained only with secondary antibody.

### 3.7 Cytotoxicity of $\alpha$ -synuclein preparations

Hb and Control cells were exposed to equal amounts of Ms and PFFs, adding  $\alpha$ -syn preparations directly to cell medium.

We first assessed the cytotoxicity of  $\alpha$ -syn preparations on Hb and Control cells using MTT assay at the 24, 48 and 96 hours and cells treated with vehicle were used as control (Untreated).

Treatment with PFFs reduced the cell viability to 48-65 % in Hb cells and 33-51 % in Control cells and cells, while Ms were only slightly toxic. Interestingly, cell viability of Hb cells treated with PFFs was significantly higher than Control cells at 24 and 96 hours after treatment, likely indicating a possible protective role of Hb against PFFs-induced toxicity in an acute experiment.

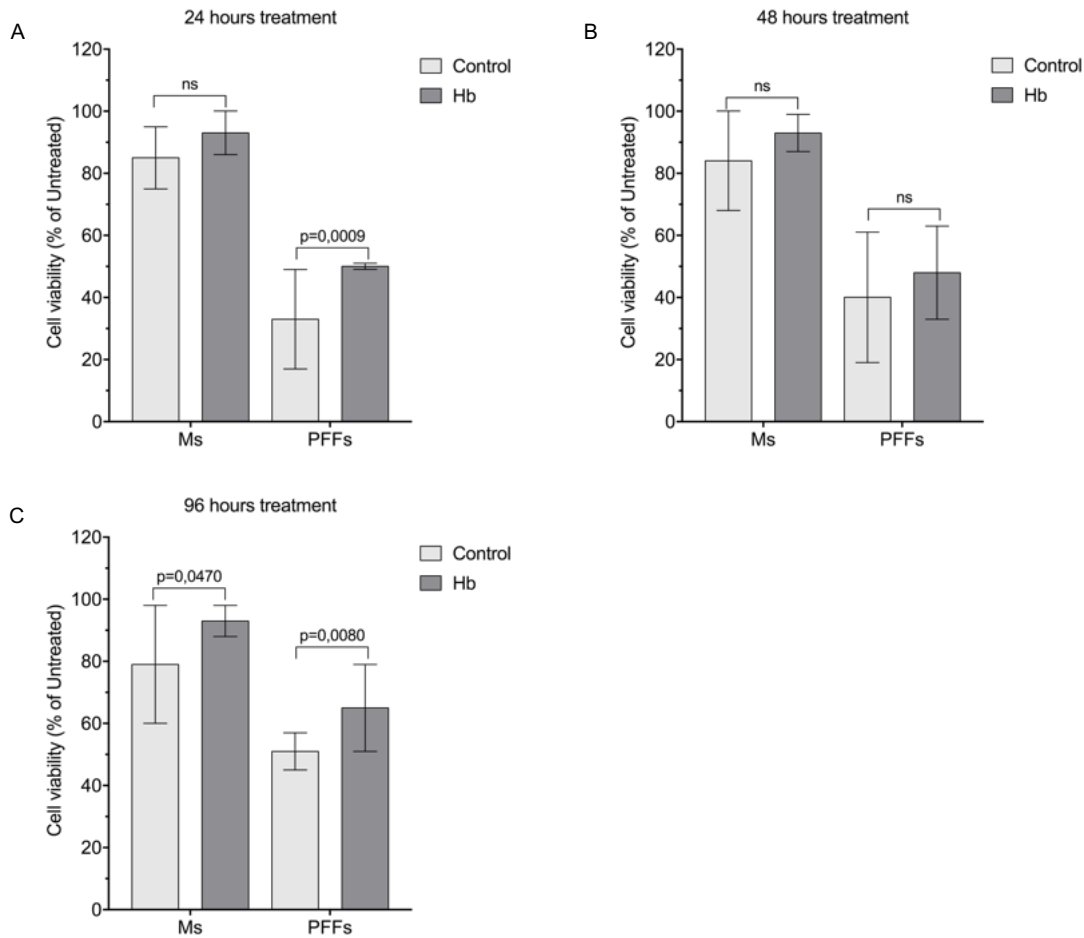


**Figure 18.** Cytotoxicity of  $\alpha$ -syn preparation in iMN9D cells.

Monomers (Ms) or  $\alpha$ -syn amyloids (PFFs) were directly added to cell medium after cell splitting. Cells were treated with Ms and PFFs for A. 24 h, B. 48 h, C. 96 h and cell viability was determined by MTT assay. Results are mean  $\pm$  Standard Deviation (SD) of three independent experiments, each performed in four replicas and are expressed as percentage of untreated Control or untreated Hb cells. Statistical analysis was performed with A. Ms, t-test with Welch's correction; PFFs, Mann-Whitney test; B. Ms, t-test with Welch's correction; PFFs, unpaired t test; C. Ms, t-test with Welch's correction; PFFs, unpaired t test. Control, iMN9D Control cells; Hb, iMN9D Hb cells, Untreated, untreated cells; Ms, cells treated with monomers; PFFs, cells treated with sonicated  $\alpha$ -syn-preformed fibrils; ns, not significant.

### 3.8 Hb triggers the accumulation of a C-terminal truncated form of $\alpha$ -syn

To further characterize  $\alpha$ -syn accumulation in our model, we took advantage of epitope-specific antibodies (Fig. 14 C and D).

iMN9D cells were treated as previously reported and untreated and Ms treated cells were used as control. We performed a time course experiment and cells were collected after 24, 48 and 96 hours and used for WB analysis. SYN-1 antibody recognized an  $\alpha$ -syn cleavage product that was not detected by the C-20 antibody, thus recognizing a C-terminal truncated form of  $\alpha$ -syn ( $\Delta$ C-

$\alpha$ -syn). Since SYN-1 epitope falls within amino acids 83-100<sup>11,18,210,222</sup>, the cleavage occurred approximately after amino acid 100. The levels of full length -  $\alpha$ -syn (FL- $\alpha$ -syn) decreased over time and were almost undetectable at P1, as shown by the staining with both the anti- $\alpha$ -syn antibodies. A concurrent increase of  $\Delta$ C- $\alpha$ -syn was observed up to 96 hours, similarly to findings reported by Sacino and colleagues in neuronal-glia cultures and CHO cells<sup>344</sup>. At P1,  $\Delta$ C- $\alpha$ -syn levels were decreased, probably due to dilution of  $\alpha$ -syn-containing cells after splitting.

Notably,  $\Delta$ C- $\alpha$ -syn was reproducibly more abundant in Hb than Control cells at each time point and the levels of  $\Delta$ C- $\alpha$ -syn normalized to FL- $\alpha$ -syn were higher in Hb than Control cells with a statistically significant difference at each time point (Fig. 19).

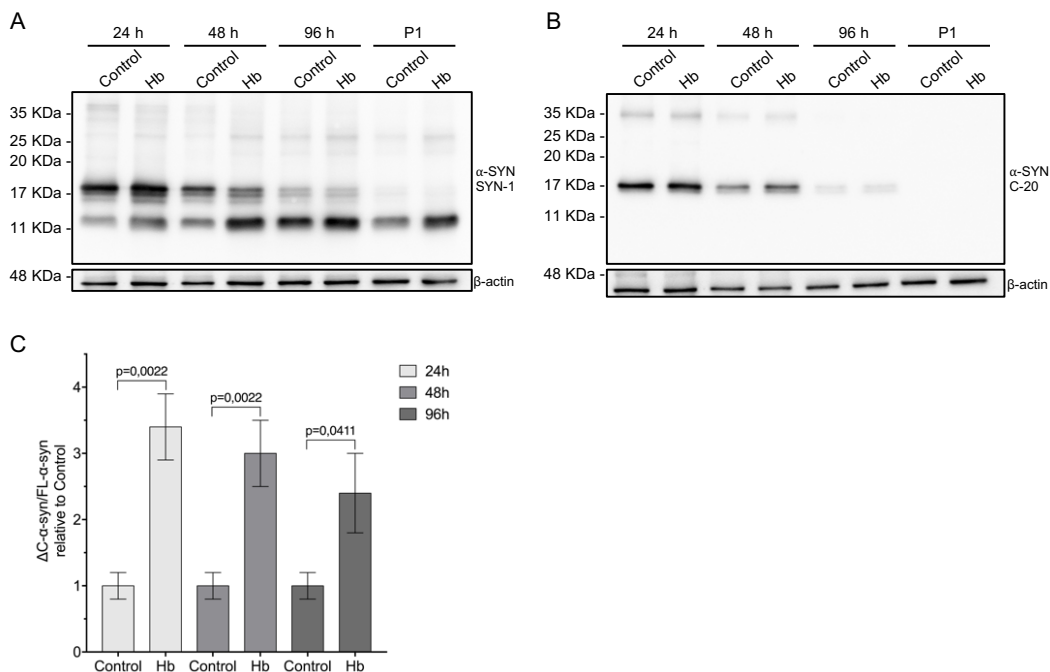


**Figure 19.** C-terminal truncated  $\alpha$ -syn accumulation in the presence of Hb in cell lysates. Control and Hb cells were treated with  $\alpha$ -syn amyloids and collected at the indicated time points. A. Cell lysates were analyzed by immunoblotting with SYN-1 and B. C-20 antibodies. C. Band intensity corresponding to  $\Delta$ C- $\alpha$ -syn and FL- $\alpha$ -syn was quantified and the ratio was calculated. Data indicate mean  $\pm$  SEM and are representative of six independent experiments. Statistical analysis was performed with Mann-Whitney test. Control, iMN9D Control cells; Hb, iMN9D Hb cells; ns, not significant.

We performed the same analysis on cell culture media to which  $\alpha$ -syn PFFs were previously added.  $\alpha$ -syn was relatively stable up to 96 hours following addition to the cultures. Moreover, no  $\alpha$ -syn staining was detected at P1, meaning that  $\alpha$ -syn is not released from cells (Fig 20).

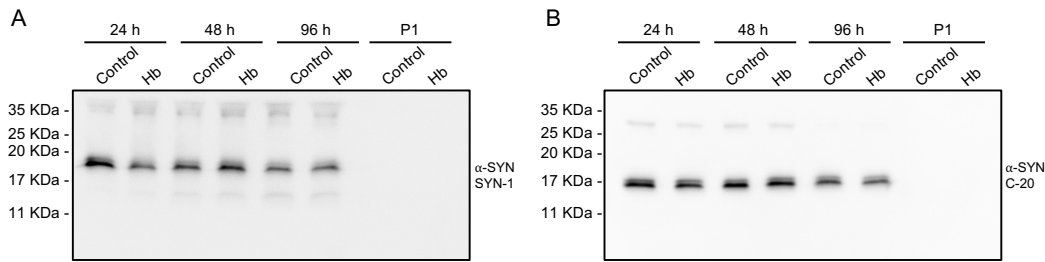


**Figure 20.** C-terminal truncated  $\alpha$ -syn accumulation in the presence of Hb in cell media. Control and Hb cells were treated with  $\alpha$ -syn amyloids and cell medium was collected at the indicated time points. A. Cell medium was analyzed by immunoblotting with SYN-1 and B. C-20 antibodies. Control, iMN9D Control cells; Hb, iMN9D Hb cells.

Given the strong  $\Delta$ C- $\alpha$ -syn signal detected from lysates compared to media, we conclude that  $\alpha$ -syn is actively processed inside the cells, whereas  $\Delta$ C- $\alpha$ -syn in cell media is presumably arising from the autoproteolytic activity of the protein (Fig. 14 D).

Therefore, we asked whether Hb might mediate  $\Delta$ C- $\alpha$ -syn accumulation through a direct interaction and whether intracellular proteases might be involved in  $\alpha$ -syn processing.

### 3.9 $\Delta$ C- $\alpha$ -syn accumulation is not mediated by Hb binding

In order to assess Hb and  $\alpha$ -syn PFFs interaction, iMN9D cell lysates were incubated with biotinylated PFFs and fibrils were pulled-down through NeutrAvidin resin. Western blot analysis revealed that PFFs do not interact with Hb. Therefore, we concluded that  $\Delta$ C- $\alpha$ -syn accumulation is not mediated by a direct interaction. These results are not in accordance to our previous co-IP experiments performed on transfected cells, apparently. We reasoned that, first, pull-down experiments were performed after PFFs addition to cell lysate other than the cell medium. Most importantly, no chemical crosslinking was performed. Therefore, if Hb- $\alpha$ -syn interaction is labile, it is plausible that we do not detect any interaction in these conditions. Nevertheless, it is possible that Hb binding sites are inside the fibrils core and therefore are not available for the interaction.

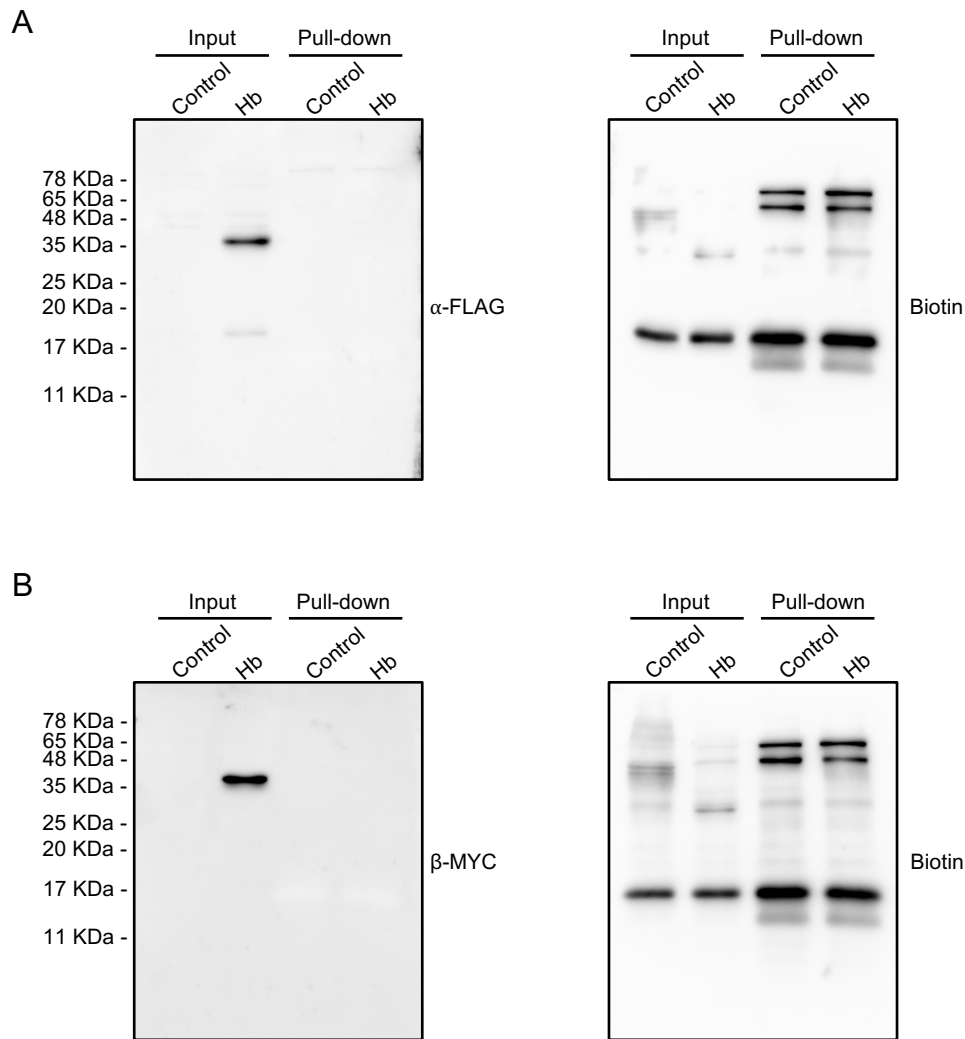


**Figure 21.** Pull down of biotinylated PFFs in iMND cell lysate. Both Control and Hb cell lysates were incubated with biotinylated fibrils and pulled down samples were revealed by immunoblot with anti-FLAG (A) and anti MYC (B) antibodies. Samples were also revealed with anti-biotin antibody as control of the experiment.

### 3.10 Effect of Calpains inhibition on $\alpha$ -syn C-terminal truncated species accumulation

We decided to focus our attention on Calpains and Cathepsins since a preliminary experiment with RT-PCR failed to show expression of Caspase 1. To investigate whether Calpains are involved in  $\alpha$ -syn processing in our model, we used Calpain inhibitor III (CI-III), a cell-permeable inhibitor of Capn1 and 2, and monitored its effects on  $\alpha$ -syn truncation.

In details, Hb cells were treated with vehicle (DMSO) and CI-III at the indicated concentrations for 24 hours. Medium was then removed and replaced with new one containing  $\alpha$ -syn amyloids, as previously reported, and protease inhibitors at the same concentrations. Cells

were collected after 24 and 48 hours for the analysis. Inhibition efficiency of CI-III was monitored by an antibody against  $\alpha$ -spectrin, a well-known calpain-substrate. Immunoblot of treated cells (+) showed an increase of the full-length protein (245 KDa) compared to vehicle treated cells (-) (Fig. 19 D), indicating that the inhibition assay works properly.

The ratio between  $\Delta$ C- $\alpha$ -syn and FL- $\alpha$ -syn was measured as previously reported. While no difference was detected at 24 hours, 48 hours treatment results in a statistically significant decrease of the ratio. From immunoblot performed with anti-SYN1 antibody, a slight increase in FL- $\alpha$ -syn was observed, as opposite to  $\Delta$ C- $\alpha$ -syn. These results indicate that in our cell model Calpains are involved in  $\alpha$ -syn truncation in our model.

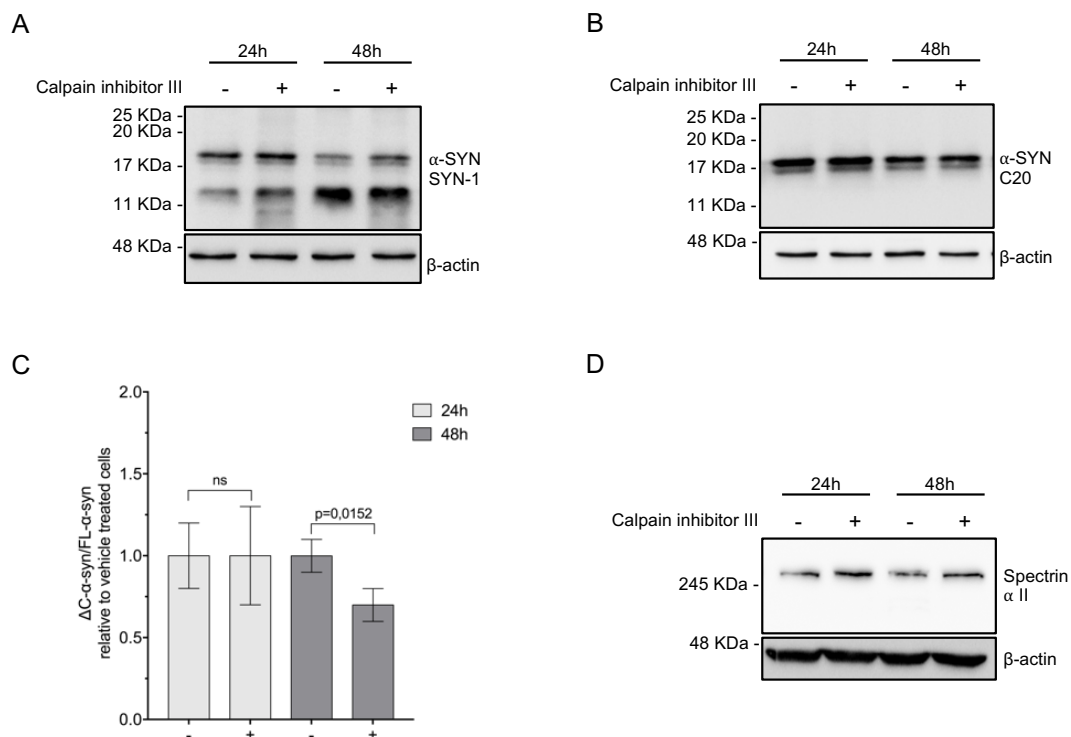


**Figure 22.** Effect of Calpains inhibition on  $\alpha$ -syn C-terminal truncated species accumulation in Hb cells. A. Cell lysates of DMSO (-) and Calpain inhibitor III 10  $\mu$ m (+) Hb cells treated were analysed by immunoblotting with SYN-1 and B. C-20 antibodies. C. Band intensity corresponding to  $\Delta$ C- $\alpha$ -syn and FL- $\alpha$ -syn was quantified and the ratio was calculated. D. Cell lysates of Hb cells DMSO (-) and CI-III (+) treated were analysed by immunoblotting with anti-Spectrin  $\alpha$  II antibody. Data indicate mean  $\pm$  SEM and are representative of six independent experiments. Statistical analysis was performed with Mann-Whitney test. ns, not significant.

### **3.11 Effect of Cathepsin D inhibition on the accumulation of $\alpha$ -syn C-terminal truncated species**

Then, we asked whether Cathepsin D (CatD) may be implicated in  $\alpha$ -syn truncation too.

We performed the experiments as previously reported for Calpains. Cathepsin D inhibition was accomplished by using pepstatin, an inhibitor of acid proteases. The inhibition efficiency was measured by an activity assay. The enzyme activity of cells treated with vehicle (-) were assigned values of 100 % and the activity in the lysate of cells treated with pepstatin (+) was accordingly normalized. To assess the test validity, a sample of lysate from untreated cells was incubated with pepstatin (100  $\mu$ M final concentration) at 37°C for 10 min prior addition of Reaction Buffer and CatD substrate and included as positive control of the experiment. The enzyme activity of the control sample was 3 % and 6 % respectively, indicating that the assay worked correctly (Fig. 20 D). After 24 hours treatment, CatD activity was reduced by approximately 30 %, while only a 20 % reduction was achieved after 48 hours treatment (Fig. 20 D). Even though the inhibition was only partially achieved, increase in cell mortality has not allowed us to test pepstatin concentrations higher than 100  $\mu$ M.

Nevertheless, the ratio between  $\Delta$ C- $\alpha$ -syn and FL- $\alpha$ -syn increased at both time points but the difference was not statistically significant (Fig. 20 C).

Accordingly, we conclude that Cathepsin D is not mainly involved in  $\alpha$ -syn processing, although this result could reflect the low inhibition efficiency.

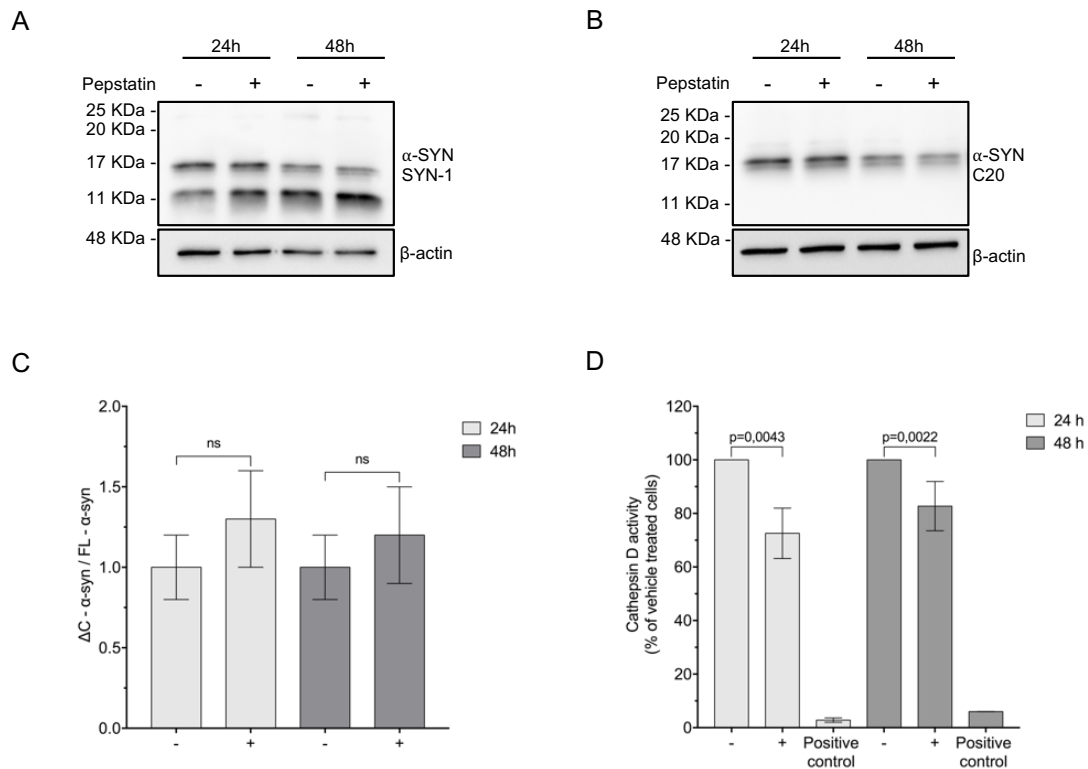


**Figure 23.** Effect of Cathepsin D inhibition on  $\alpha$ -syn C-terminal truncated species accumulation in Hb cells. A. Cell lysates of DMSO (-) and pepstatin 100  $\mu$ m (+) treated Hb cells were analysed by immunoblotting with SYN-1 and B. C-20 antibodies. C. Band intensity corresponding to  $\Delta$ C- $\alpha$ -syn and FL- $\alpha$ -syn was quantified and the ratio was calculated. Data indicate mean  $\pm$  SEM and are representative of five independent experiments. D. Cell lysates of Hb cells DMSO (-) and pepstatin (+) treated were analysed by Cathepsin D activity assay. Data indicate mean  $\pm$  SD and are representative of two independent experiments, each performed in three replicas and are expressed as percentage of vehicle treated cells. Statistical analysis was performed with Mann-Whitney test. ns, not significant.

## DISCUSSION

Hb is well known for its fundamental role as oxygen carrier from the lungs to the periphery in red blood cells. Newly functions have been recently ascribed to the protein, including NO scavenger and defense agent against microorganisms. Moreover, some decades ago the scientific community was left puzzled by the discovery of Hb expression in nonerythroid cells and, most importantly, in neurons. These findings opened the field to striking questions about its functional role. Indeed, several efforts have been made to answer this interesting biological question but Hb function in the central nervous system is still a matter of debate. Gene expression profiling has allowed researchers to identify Hb dysregulation in neurodegenerative diseases<sup>316,317,332,318,321–324,327,330,331</sup>. Although both up- and down-regulation have been reported, it is widely accepted that Hb may play a crucial role in neuronal physiology, possibly acting as oxygen storage during hypoxia, or in mitochondrial homeostasis. Iron metabolism impairment has been observed in neurodegenerative diseases and iron accumulation in the central nervous system is a key feature of synucleinopathies. Therefore, a putative role of Hb in iron homeostasis in these diseases should not be excluded. PD is a neurodegenerative disorder of unknown aetiology affecting about 10 million people worldwide. Its most evident manifestation is the selective vulnerability of DA neurons of SNpc and  $\alpha$ -syn inclusion formation. Despite the large amount of studies, the molecular mechanisms underlying the pathology have been only partially elucidated.

In this context, we aimed to better understand the function of Hb in PD and its relevance, eventually, to the pathology. To this purpose, we took advantage of iMN9D cells overexpressing  $\alpha$  and  $\beta$  chains of Hb, previously shown to maintain Hb tetrameric structure<sup>315</sup> and, moreover, shown to represent a useful model to study DA cell dysfunction.

We mainly focused our attention on elucidating the potential interplay between Hb and  $\alpha$ -syn, by using  $\alpha$ -syn PFFs. These have been shown to induce robust inclusion formation when added in culture or injected in mice. Thus, this model allowed to study the impact of Hb on misfolded  $\alpha$ -syn. In cells expressing endogenous  $\alpha$ -syn, fibrils addition to cell cultures results in endogenous  $\alpha$ -syn recruitment to the core of the inclusions. These inclusions resemble many features of Lewy bodies found in PD brains, as they are filamentous, hyperphosphorylated, ubiquitinated and insoluble in anionic detergent. Unfortunately, iMN9D cells do not express significant levels of  $\alpha$ -syn. Therefore, to overcome this limitation, we used 2  $\mu$ M of  $\alpha$ -syn species even though MTT assay revealed significant cell mortality.

In this particular condition, we demonstrate that  $\alpha$ -syn PFFs are internalized by iMN9D cells and, in addition, are phosphorylated at serine 129. Fibrils addition is cytotoxic to cells and the presence of Hb seems to be protective, in line with previous data from our laboratory showing the protective effects of Hb against MPP<sup>+</sup> insults in undifferentiated conditions (*data not shown*).

Different post-translational modifications have been proposed to contribute to  $\alpha$ -syn pathogenicity. Among these,  $\alpha$ -syn truncation has been demonstrated to enhance full-length  $\alpha$ -syn aggregation *in vitro* and form toxic inclusions *in vivo*. Moreover, C-terminal truncated species of  $\alpha$ -syn are found enriched in LBs. Here, we show that a C-terminal truncated fragment of 11 KDa ( $\Delta$ C- $\alpha$ -syn) is produced in iMN9D cells with a cleavage site between amino acids 83 and 100. Notably, as the levels of FL- $\alpha$ -syn decrease over time, there is a concomitant increase in the cleaved C-terminal fragment, that is much more evident than the decrease. Moreover, we demonstrate that levels of  $\Delta$ C- $\alpha$ -syn normalized to FL- $\alpha$ -syn are about three times more abundant in Hb cells than Control. In cell culture media, instead, we did not observe significant results.

These findings lead us to speculate that Hb may be able to either interfere with  $\alpha$ -syn clearance or induce protease activity involved in  $\alpha$ -syn truncation, inducing in both cases  $\Delta$ C- $\alpha$ -syn accumulation.

It has been demonstrated that the ubiquitin-proteasome system (UPS), the autophagy-lysosome pathway (ALP) and several proteases are involved in the clearance of  $\alpha$ -syn. Even though the importance of the UPS in the pathogenesis of PD is strengthened by the genetic basis of this pathology, few reports have actually shown that the proteasome could be responsible for the truncation of unfolded  $\alpha$ -syn<sup>11,217</sup>. Conversely, the majority of studies showed an involvement of ALP and cytoplasmic proteases, in line with the findings that aggregated proteins are a poor proteasome substrate.

Therefore, we asked whether calpains and cathepsin D are involved in this process. We used specific inhibitors in Hb cells and found that, after 48 hours treatment, calpain inhibitor reduced the ratio between  $\Delta$ C- $\alpha$ -syn and FL- $\alpha$ -syn, due to an increase in FL- $\alpha$ -syn. We did not observe any statistically significant results using pepstatin, a cathepsin D inhibitor. It must be noted that, although inhibitors provide a useful tool to study proteases activity, the inhibition was only partially achieved. Therefore, our results suggest that calpains are, at least partially, involved in  $\alpha$ -syn truncation. However, a knockdown experiment selectively targeting cathepsin D and calpain 1 and 2 would induce a stronger inhibition and, therefore, provide further insights into the mechanism of  $\alpha$ -syn truncation Hb dependent.

Calpains are cytoplasmic proteases shown to be activated by micromolar or millimolar levels of calcium. Calcium homeostasis is fundamental for cells and it is tightly regulated by channels, mitochondria and endoplasmic reticulum storage and by lysosomes, as recently reported<sup>345</sup>. Dysregulation of  $\text{Ca}^{2+}$  homeostasis is frequently observed in PD models. It has been reported that upon  $\text{MPP}^+$  exposure, cytosolic and mitochondria  $\text{Ca}^{2+}$  levels are higher in SN DA neurons compared to VTA DA neurons, possibly contributing to their selective vulnerability to stress and  $\alpha$ -syn toxicity<sup>346</sup>. Moreover  $\text{Ca}^{2+}$  binds  $\alpha$ -syn in its C-terminal region and promotes  $\alpha$ -syn pore-like oligomers formation<sup>347</sup>, their localization to the membrane mediating  $\text{Ca}^{2+}$  entry. Oxidative stress and raised calcium induce  $\alpha$ -syn aggregation in cells<sup>348</sup>. Additionally,  $\text{Ca}^{2+}$  increase leads to mitochondrial stress and impairment of autophagic response. Therefore, intracellular  $\text{Ca}^{2+}$  increase could lead to calpains activation and C-terminal truncated  $\alpha$ -syn accumulation, exacerbating PD pathology. In this context, it is important to consider that Hb cells have autophagy impaired, potentially contributing to the accumulation of  $\Delta\text{C-}\alpha$ -syn.

In summary, this study provides evidence supporting a pivotal role of Hb in  $\alpha$ -syn processing mediated by calpains. A biochemical characterization of  $\Delta\text{C-}\alpha$ -syn should be considered as next step to address the exact cleavage site and the aggregation propensity of the truncated form of  $\alpha$ -syn. It would be intriguing to strengthen our findings by performing knockdown experiments on calpains and, possibly, moving to primary culture or *in vivo* model to deepen the relationship between Hb,  $\alpha$ -syn, calpain and calcium.

## BIBLIOGRAPHY

1. Biagioli, M. *et al.* Unexpected expression of  $\alpha$ - and  $\beta$ -globin in mesencephalic dopaminergic neurons and glial cells. *Proc. Natl. Acad. Sci.* **106**, 15454 LP-15459 (2009).
2. Codrich, M. *et al.* Neuronal hemoglobin affects dopaminergic cells' response to stress. *Cell Death Dis.* **8**, e2538 (2017).
3. Yang, W., Li, X., Li, X., Li, X. & Yu, S. Neuronal hemoglobin in mitochondria is reduced by forming a complex with  $\alpha$ -synuclein in aging monkey brains. *Oncotarget* **7**, 7441–7454 (2016).
4. Lee, A. & Gilbert, R. M. Epidemiology of Parkinson Disease. *Neurol. Clin.* **34**, 955–965 (2016).
5. Kane, J. P. M. *et al.* Clinical prevalence of Lewy body dementia. *Alzheimers. Res. Ther.* **10**, 19 (2018).
6. Halliday, G. M., Holton, J. L., Revesz, T. & Dickson, D. W. Neuropathology underlying clinical variability in patients with synucleinopathies. *Acta Neuropathol.* **122**, 187–204 (2011).
7. Stefanova, N. & Wenning, G. K. Review: Multiple system atrophy: emerging targets for interventional therapies. *Neuropathol. Appl. Neurobiol.* **42**, 20–32 (2016).
8. Fellner, L. & Stefanova, N. The role of glia in alpha-synucleinopathies. *Mol. Neurobiol.* **47**, 575–586 (2013).
9. Spillantini, M. G. & Goedert, M. The alpha-synucleinopathies: Parkinson's disease, dementia with Lewy bodies, and multiple system atrophy. *Ann. N. Y. Acad. Sci.* **920**, 16–27 (2000).
10. Goedert, M., Jakes, R. & Spillantini, M. G. The Synucleinopathies: Twenty Years On. *J. Parkinsons. Dis.* **7**, S51–S69 (2017).
11. Liu, C.-W. *et al.* A precipitating role for truncated alpha-synuclein and the proteasome in alpha-synuclein aggregation: implications for pathogenesis of Parkinson disease. *J. Biol. Chem.* **280**, 22670–22678 (2005).
12. Wakabayashi, K. & Takahashi, H. Cellular pathology in multiple system atrophy. *Neuropathology* **26**, 338–345 (2006).
13. Baba, M. *et al.* Aggregation of alpha-synuclein in Lewy bodies of sporadic Parkinson's disease and dementia with Lewy bodies. *Am. J. Pathol.* **152**, 879–884 (1998).
14. Culvenor, J. G. *et al.* Non-Abeta component of Alzheimer's disease amyloid (NAC) revisited. NAC and alpha-synuclein are not associated with Abeta amyloid. *Am. J. Pathol.* **155**, 1173–1181 (1999).
15. Campbell, B. C. *et al.* Accumulation of insoluble alpha-synuclein in dementia with Lewy bodies. *Neurobiol. Dis.* **7**, 192–200 (2000).
16. Campbell, B. C. *et al.* The solubility of alpha-synuclein in multiple system atrophy differs from that of dementia with Lewy bodies and Parkinson's disease. *J. Neurochem.* **76**, 87–96 (2001).
17. Giasson, B. I. *et al.* Neuronal alpha-synucleinopathy with severe movement disorder in mice expressing A53T human alpha-synuclein. *Neuron* **34**, 521–533 (2002).
18. Ohrfelt, A. *et al.* Identification of novel alpha-synuclein isoforms in human brain tissue by using an online nanoLC-ESI-FTICR-MS method. *Neurochem. Res.* **36**, 2029–2042 (2011).
19. Muntane, G., Ferrer, I. & Martinez-Vicente, M. alpha-synuclein phosphorylation and truncation are normal events in the adult human brain. *Neuroscience* **200**, 106–119 (2012).
20. Gai, W. P., Power, J. H., Blumbergs, P. C., Culvenor, J. G. & Jensen, P. H. Alpha-synuclein immunoisolation

- of glial inclusions from multiple system atrophy brain tissue reveals multiprotein components. *J. Neurochem.* **73**, 2093–2100 (1999).
21. McCann, H., Stevens, C. H., Cartwright, H. & Halliday, G. M.  $\alpha$ -Synucleinopathy phenotypes. *Parkinsonism Relat. Disord.* **20**, S62–S67 (2014).
  22. Dirnberger, G. & Jahanshahi, M. Executive dysfunction in Parkinson's disease: a review. *J. Neuropsychol.* **7**, 193–224 (2013).
  23. Bellucci, A. *et al.* Review: Parkinson's disease: from synaptic loss to connectome dysfunction. *Neuropathol. Appl. Neurobiol.* **42**, 77–94 (2016).
  24. Sumikura, H. *et al.* Distribution of alpha-synuclein in the spinal cord and dorsal root ganglia in an autopsy cohort of elderly persons. *Acta Neuropathol. Commun.* **3**, 57 (2015).
  25. Braak, H., de Vos, R. A. I., Bohl, J. & Del Tredici, K. Gastric alpha-synuclein immunoreactive inclusions in Meissner's and Auerbach's plexuses in cases staged for Parkinson's disease-related brain pathology. *Neurosci. Lett.* **396**, 67–72 (2006).
  26. Olanow, C. W., Perl, D. P., DeMartino, G. N. & McNaught, K. S. P. Lewy-body formation is an aggresome-related process: a hypothesis. *Lancet. Neurol.* **3**, 496–503 (2004).
  27. Wong, Y. C. & Krainc, D. alpha-synuclein toxicity in neurodegeneration: mechanism and therapeutic strategies. *Nat. Med.* **23**, 1–13 (2017).
  28. Lim, S., Chun, Y., Lee, J. S. & Lee, S.-J. Neuroinflammation in Synucleinopathies. *Brain Pathol.* **26**, 404–409 (2016).
  29. Gerhard, A. *et al.* [<sup>11</sup>C](R)-PK11195 PET imaging of microglial activation in multiple system atrophy. *Neurology* **61**, 686–689 (2003).
  30. Ishizawa, K. *et al.* Microglial activation parallels system degeneration in multiple system atrophy. *J. Neuropathol. Exp. Neurol.* **63**, 43–52 (2004).
  31. Lingor, P., Carboni, E. & Koch, J. C. Alpha-synuclein and iron: two keys unlocking Parkinson's disease. *J. Neural Transm.* **124**, 973–981 (2017).
  32. Lu, Y., Prudent, M., Fauvet, B., Lashuel, H. A. & Girault, H. H. Phosphorylation of alpha-Synuclein at Y125 and S129 alters its metal binding properties: implications for understanding the role of alpha-Synuclein in the pathogenesis of Parkinson's Disease and related disorders. *ACS Chem. Neurosci.* **2**, 667–675 (2011).
  33. Hare, D. J. & Double, K. L. Iron and dopamine: a toxic couple. *Brain* **139**, 1026–1035 (2016).
  34. Dexter, D. T., Jenner, P., Schapira, A. H. & Marsden, C. D. Alterations in levels of iron, ferritin, and other trace metals in neurodegenerative diseases affecting the basal ganglia. The Royal Kings and Queens Parkinson's Disease Research Group. *Ann. Neurol.* **32 Suppl**, S94-100 (1992).
  35. Pouloupoulos, M., Levy, O. A. & Alcalay, R. N. The neuropathology of genetic Parkinson's disease. *Mov. Disord.* **27**, 831–842 (2012).
  36. Chai, C. & Lim, K.-L. Genetic insights into sporadic Parkinson's disease pathogenesis. *Curr. Genomics* **14**, 486–501 (2013).
  37. Tofaris, G. K., Goedert, M. & Spillantini, M. G. The Transcellular Propagation and Intracellular Trafficking of alpha-Synuclein. *Cold Spring Harb. Perspect. Med.* **7**, (2017).

38. Karimi-Moghadam, A., Charsouei, S., Bell, B. & Jabalameli, M. R. Parkinson Disease from Mendelian Forms to Genetic Susceptibility: New Molecular Insights into the Neurodegeneration Process. *Cell. Mol. Neurobiol.* **38**, 1153–1178 (2018).
39. Maraganore, D. M. *et al.* UCHL1 is a Parkinson's disease susceptibility gene. *Ann. Neurol.* **55**, 512–521 (2004).
40. Weil, R. S., Lashley, T. L., Bras, J., Schrag, A. E. & Schott, J. M. Current concepts and controversies in the pathogenesis of Parkinson's disease dementia and Dementia with Lewy Bodies. *F1000Research* **6**, 1604 (2017).
41. Ogaki, K. *et al.* Analysis of COQ2 gene in multiple system atrophy. *Mol. Neurodegener.* **9**, 44 (2014).
42. Langston, J. W. & Ballard, P. A. J. Parkinson's disease in a chemist working with 1-methyl-4-phenyl-1,2,5,6-tetrahydropyridine. *The New England journal of medicine* **309**, 310 (1983).
43. Tanner, C. M. *et al.* Rotenone, paraquat, and Parkinson's disease. *Environ. Health Perspect.* **119**, 866–872 (2011).
44. Iwai, A. *et al.* The precursor protein of non-A beta component of Alzheimer's disease amyloid is a presynaptic protein of the central nervous system. *Neuron* **14**, 467–475 (1995).
45. Weinreb, P. H., Zhen, W., Poon, A. W., Conway, K. A. & Lansbury, P. T. J. NACP, a protein implicated in Alzheimer's disease and learning, is natively unfolded. *Biochemistry* **35**, 13709–13715 (1996).
46. Uversky, V. N., Li, J. & Fink, A. L. Evidence for a partially folded intermediate in alpha-synuclein fibril formation. *J. Biol. Chem.* **276**, 10737–10744 (2001).
47. Bartels, T., Choi, J. G. & Selkoe, D. J. alpha-Synuclein occurs physiologically as a helically folded tetramer that resists aggregation. *Nature* **477**, 107–110 (2011).
48. Wang, W. *et al.* A soluble alpha-synuclein construct forms a dynamic tetramer. *Proc. Natl. Acad. Sci. U. S. A.* **108**, 17797–17802 (2011).
49. Davidson, W. S., Jonas, A., Clayton, D. F. & George, J. M. Stabilization of alpha-synuclein secondary structure upon binding to synthetic membranes. *J. Biol. Chem.* **273**, 9443–9449 (1998).
50. Perrin, R. J., Woods, W. S., Clayton, D. F. & George, J. M. Interaction of human alpha-Synuclein and Parkinson's disease variants with phospholipids. Structural analysis using site-directed mutagenesis. *J. Biol. Chem.* **275**, 34393–34398 (2000).
51. Munishkina, L. A., Phelan, C., Uversky, V. N. & Fink, A. L. Conformational behavior and aggregation of alpha-synuclein in organic solvents: modeling the effects of membranes. *Biochemistry* **42**, 2720–2730 (2003).
52. Jao, C. C., Der-Sarkissian, A., Chen, J. & Langen, R. Structure of membrane-bound alpha-synuclein studied by site-directed spin labeling. *Proc. Natl. Acad. Sci. U. S. A.* **101**, 8331–8336 (2004).
53. Pfefferkorn, C. M., Jiang, Z. & Lee, J. C. Biophysics of alpha-synuclein membrane interactions. *Biochim. Biophys. Acta* **1818**, 162–171 (2012).
54. Bussell, R. J. & Eliezer, D. A structural and functional role for 11-mer repeats in alpha-synuclein and other exchangeable lipid binding proteins. *J. Mol. Biol.* **329**, 763–778 (2003).
55. Bussell, R. J., Ramlall, T. F. & Eliezer, D. Helix periodicity, topology, and dynamics of membrane-associated alpha-synuclein. *Protein Sci.* **14**, 862–872 (2005).

56. Chandra, S., Chen, X., Rizo, J., Jahn, R. & Sudhof, T. C. A broken alpha -helix in folded alpha -Synuclein. *J. Biol. Chem.* **278**, 15313–15318 (2003).
57. Bodles, A. M., Guthrie, D. J., Harriott, P., Campbell, P. & Irvine, G. B. Toxicity of non- $\beta$  component of Alzheimer's disease amyloid, and N-terminal fragments thereof, correlates to formation of beta-sheet structure and fibrils. *Eur. J. Biochem.* **267**, 2186–2194 (2000).
58. Bodles, A. M., Guthrie, D. J., Greer, B. & Irvine, G. B. Identification of the region of non- $\beta$  component (NAC) of Alzheimer's disease amyloid responsible for its aggregation and toxicity. *J. Neurochem.* **78**, 384–395 (2001).
59. Giasson, B. I., Murray, I. V., Trojanowski, J. Q. & Lee, V. M. A hydrophobic stretch of 12 amino acid residues in the middle of alpha-synuclein is essential for filament assembly. *J. Biol. Chem.* **276**, 2380–2386 (2001).
60. Murray, I. V. J. *et al.* Role of alpha-synuclein carboxy-terminus on fibril formation in vitro. *Biochemistry* **42**, 8530–8540 (2003).
61. Wang, G.-F., Li, C. & Pielak, G. J. 19F NMR studies of alpha-synuclein-membrane interactions. *Protein Sci.* **19**, 1686–1691 (2010).
62. Alderson, T. R. & Markley, J. L. Biophysical characterization of alpha-synuclein and its controversial structure. *Intrinsically Disord. proteins* **1**, 18–39 (2013).
63. Bisaglia, M., Tessari, I., Mammi, S. & Bubacco, L. Interaction Between  $\alpha$ -Synuclein and Metal Ions, Still Looking for a Role in the Pathogenesis of Parkinson's Disease. *NeuroMolecular Med.* **11**, 239–251 (2009).
64. Ulmer, T. S., Bax, A., Cole, N. B. & Nussbaum, R. L. Structure and dynamics of micelle-bound human alpha-synuclein. *J. Biol. Chem.* **280**, 9595–9603 (2005).
65. Post, M. R., Lieberman, O. J. & Mosharov, E. V. Can Interactions Between  $\alpha$ -Synuclein, Dopamine and Calcium Explain Selective Neurodegeneration in Parkinson's Disease? *Front. Neurosci.* **12**, 161 (2018).
66. Serpell, L. C., Berriman, J., Jakes, R., Goedert, M. & Crowther, R. A. Fiber diffraction of synthetic alpha-synuclein filaments shows amyloid-like cross-beta conformation. *Proc. Natl. Acad. Sci. U. S. A.* **97**, 4897–4902 (2000).
67. Qin, Z., Hu, D., Han, S., Hong, D.-P. & Fink, A. L. Role of different regions of alpha-synuclein in the assembly of fibrils. *Biochemistry* **46**, 13322–13330 (2007).
68. Wood, S. J. *et al.* alpha-synuclein fibrillogenesis is nucleation-dependent. Implications for the pathogenesis of Parkinson's disease. *J. Biol. Chem.* **274**, 19509–19512 (1999).
69. Bhak, G., Lee, J.-H., Hahn, J.-S. & Paik, S. R. Granular assembly of alpha-synuclein leading to the accelerated amyloid fibril formation with shear stress. *PLoS One* **4**, e4177 (2009).
70. Burre, J., Sharma, M. & Sudhof, T. C. Cell Biology and Pathophysiology of alpha-Synuclein. *Cold Spring Harb. Perspect. Med.* **8**, (2018).
71. Hoshi, M. *et al.* Spherical aggregates of beta-amyloid (amylospheroid) show high neurotoxicity and activate tau protein kinase I/glycogen synthase kinase-3 $\beta$ . *Proc. Natl. Acad. Sci. U. S. A.* **100**, 6370–6375 (2003).
72. Lashuel, H. A., Overk, C. R., Oueslati, A. & Masliah, E. The many faces of alpha-synuclein: from structure and toxicity to therapeutic target. *Nature reviews. Neuroscience* **14**, 38–48 (2013).
73. Ding, T. T., Lee, S.-J., Rochet, J.-C. & Lansbury, P. T. J. Annular alpha-synuclein protofibrils are produced

- when spherical protofibrils are incubated in solution or bound to brain-derived membranes. *Biochemistry* **41**, 10209–10217 (2002).
74. Hong, D.-P., Han, S., Fink, A. L. & Uversky, V. N. Characterization of the non-fibrillar alpha-synuclein oligomers. *Protein Pept. Lett.* **18**, 230–240 (2011).
  75. Giehm, L., Svergun, D. I., Otzen, D. E. & Vestergaard, B. Low-resolution structure of a vesicle disrupting &alpha;-synuclein oligomer that accumulates during fibrillation. *Proc. Natl. Acad. Sci. U. S. A.* **108**, 3246–3251 (2011).
  76. Vilar, M. *et al.* The fold of alpha-synuclein fibrils. *Proc. Natl. Acad. Sci. U. S. A.* **105**, 8637–8642 (2008).
  77. Prusiner, S. B. Molecular biology of prion diseases. *Science* **252**, 1515–1522 (1991).
  78. Morales, R. Prion strains in mammals: Different conformations leading to disease. *PLoS Pathog.* **13**, e1006323 (2017).
  79. Bousset, L. *et al.* Structural and functional characterization of two alpha-synuclein strains. *Nat. Commun.* **4**, 2575 (2013).
  80. Peelaerts, W. *et al.* alpha-Synuclein strains cause distinct synucleinopathies after local and systemic administration. *Nature* **522**, 340–344 (2015).
  81. Kim, C. *et al.* Exposure to bacterial endotoxin generates a distinct strain of alpha-synuclein fibril. *Sci. Rep.* **6**, 30891 (2016).
  82. Volpicelli-Daley, L. A. *et al.* Exogenous alpha-synuclein fibrils induce Lewy body pathology leading to synaptic dysfunction and neuron death. *Neuron* **72**, 57–71 (2011).
  83. Pieri, L., Madiona, K., Bousset, L. & Melki, R. Fibrillar alpha-synuclein and huntingtin exon 1 assemblies are toxic to the cells. *Biophys. J.* **102**, 2894–2905 (2012).
  84. Pieri, L., Madiona, K. & Melki, R. Structural and functional properties of prefibrillar alpha-synuclein oligomers. *Sci. Rep.* **6**, 24526 (2016).
  85. Osterberg, V. R. *et al.* Progressive aggregation of alpha-synuclein and selective degeneration of lewy inclusion-bearing neurons in a mouse model of parkinsonism. *Cell Rep.* **10**, 1252–1260 (2015).
  86. Danzer, K. M. *et al.* Different species of alpha-synuclein oligomers induce calcium influx and seeding. *J. Neurosci.* **27**, 9220–9232 (2007).
  87. Winner, B. *et al.* In vivo demonstration that  $\alpha$ -synuclein oligomers are toxic. *Proc. Natl. Acad. Sci.* **108**, 4194 LP-4199 (2011).
  88. Mahul-Mellier, A.-L. *et al.* Fibril growth and seeding capacity play key roles in alpha-synuclein-mediated apoptotic cell death. *Cell Death Differ.* **22**, 2107–2122 (2015).
  89. Kordower, J. H., Chu, Y., Hauser, R. A., Freeman, T. B. & Olanow, C. W. Lewy body-like pathology in long-term embryonic nigral transplants in Parkinson’s disease. *Nat. Med.* **14**, 504–506 (2008).
  90. Li, J.-Y. *et al.* Lewy bodies in grafted neurons in subjects with Parkinson’s disease suggest host-to-graft disease propagation. *Nat. Med.* **14**, 501–503 (2008).
  91. Braak, H., Rub, U., Gai, W. P. & Del Tredici, K. Idiopathic Parkinson’s disease: possible routes by which vulnerable neuronal types may be subject to neuroinvasion by an unknown pathogen. *J. Neural Transm.* **110**, 517–536 (2003).

92. Steiner, J. A., Quansah, E. & Brundin, P. The concept of alpha-synuclein as a prion-like protein: ten years after. *Cell Tissue Res.* **373**, 161–173 (2018).
93. Rey, N. L. *et al.* Widespread transneuronal propagation of alpha-synucleinopathy triggered in olfactory bulb mimics prodromal Parkinson's disease. *J. Exp. Med.* **213**, 1759–1778 (2016).
94. Ulusoy, A. *et al.* Caudo-rostral brain spreading of alpha-synuclein through vagal connections. *EMBO Mol. Med.* **5**, 1119–1127 (2013).
95. Ulusoy, A. *et al.* Neuron-to-neuron alpha-synuclein propagation in vivo is independent of neuronal injury. *Acta Neuropathol. Commun.* **3**, 13 (2015).
96. Helwig, M. *et al.* Brain propagation of transduced alpha-synuclein involves non-fibrillar protein species and is enhanced in alpha-synuclein null mice. *Brain* **139**, 856–870 (2016).
97. Luk, K. C. *et al.* Pathological alpha-synuclein transmission initiates Parkinson-like neurodegeneration in nontransgenic mice. *Science* **338**, 949–953 (2012).
98. Luk, K. C. *et al.* Intracerebral inoculation of pathological alpha-synuclein initiates a rapidly progressive neurodegenerative alpha-synucleinopathy in mice. *J. Exp. Med.* **209**, 975–986 (2012).
99. Paumier, K. L. *et al.* Intrastratial injection of pre-formed mouse alpha-synuclein fibrils into rats triggers alpha-synuclein pathology and bilateral nigrostriatal degeneration. *Neurobiol. Dis.* **82**, 185–199 (2015).
100. Watts, J. C. *et al.* Transmission of multiple system atrophy prions to transgenic mice. *Proc. Natl. Acad. Sci. U. S. A.* **110**, 19555–19560 (2013).
101. Bernis, M. E. *et al.* Prion-like propagation of human brain-derived alpha-synuclein in transgenic mice expressing human wild-type alpha-synuclein. *Acta Neuropathol. Commun.* **3**, 75 (2015).
102. Masuda-Suzukake, M. *et al.* Prion-like spreading of pathological alpha-synuclein in brain. *Brain* **136**, 1128–1138 (2013).
103. Holmqvist, S. *et al.* Direct evidence of Parkinson pathology spread from the gastrointestinal tract to the brain in rats. *Acta Neuropathol.* **128**, 805–820 (2014).
104. Uemura, N. *et al.* Inoculation of alpha-synuclein preformed fibrils into the mouse gastrointestinal tract induces Lewy body-like aggregates in the brainstem via the vagus nerve. *Mol. Neurodegener.* **13**, 21 (2018).
105. Lee, H.-J. *et al.* Autophagic failure promotes the exocytosis and intercellular transfer of alpha-synuclein. *Exp. Mol. Med.* **45**, e22 (2013).
106. Lee, H.-J., Patel, S. & Lee, S.-J. Intravesicular localization and exocytosis of alpha-synuclein and its aggregates. *J. Neurosci.* **25**, 6016–6024 (2005).
107. Emmanouilidou, E. *et al.* Cell-produced alpha-synuclein is secreted in a calcium-dependent manner by exosomes and impacts neuronal survival. *J. Neurosci.* **30**, 6838–6851 (2010).
108. Jang, A. *et al.* Non-classical exocytosis of alpha-synuclein is sensitive to folding states and promoted under stress conditions. *J. Neurochem.* **113**, 1263–1274 (2010).
109. Paillusson, S., Clairembault, T., Biraud, M., Neunlist, M. & Derkinderen, P. Activity-dependent secretion of alpha-synuclein by enteric neurons. *J. Neurochem.* **125**, 512–517 (2013).
110. Lee, H.-J. *et al.* Assembly-dependent endocytosis and clearance of extracellular alpha-synuclein. *Int. J. Biochem. Cell Biol.* **40**, 1835–1849 (2008).

111. Hansen, C. *et al.*  $\alpha$ -Synuclein propagates from mouse brain to grafted dopaminergic neurons and seeds aggregation in cultured human cells. *J. Clin. Invest.* **121**, 715–725 (2011).
112. Sung, J. Y. *et al.* Induction of Neuronal Cell Death by Rab5A-dependent Endocytosis of  $\alpha$ -Synuclein. *J. Biol. Chem.* **276**, 27441–27448 (2001).
113. Mao, X. *et al.* Pathological alpha-synuclein transmission initiated by binding lymphocyte-activation gene 3. *Science* **353**, (2016).
114. Urrea, L. *et al.* Involvement of Cellular Prion Protein in alpha-Synuclein Transport in Neurons. *Mol. Neurobiol.* **55**, 1847–1860 (2018).
115. Aulić, S. *et al.*  $\alpha$ -Synuclein Amyloids Hijack Prion Protein to Gain Cell Entry, Facilitate Cell-to-Cell Spreading and Block Prion Replication. *Sci. Rep.* **7**, 10050 (2017).
116. Choi, Y. R. *et al.* Prion-like Propagation of alpha-Synuclein Is Regulated by the Fc $\gamma$ RIIB-SHP-1/2 Signaling Pathway in Neurons. *Cell Rep.* **22**, 136–148 (2018).
117. Holmes, B. B. *et al.* Heparan sulfate proteoglycans mediate internalization and propagation of specific proteopathic seeds. *Proc. Natl. Acad. Sci.* **110**, E3138 LP-E3147 (2013).
118. Park, J.-Y. *et al.* On the mechanism of internalization of  $\alpha$ -synuclein into microglia: roles of ganglioside GM1 and lipid raft. *J. Neurochem.* **110**, 400–411 (2009).
119. Abounit, S. *et al.* Tunneling nanotubes spread fibrillar alpha-synuclein by intercellular trafficking of lysosomes. *EMBO J.* **35**, 2120–2138 (2016).
120. Dieriks, B. V. *et al.* alpha-synuclein transfer through tunneling nanotubes occurs in SH-SY5Y cells and primary brain pericytes from Parkinson’s disease patients. *Sci. Rep.* **7**, 42984 (2017).
121. Rostami, J. *et al.* Human Astrocytes Transfer Aggregated Alpha-Synuclein via Tunneling Nanotubes. *J. Neurosci.* **37**, 11835–11853 (2017).
122. Reyes, J. F. *et al.* Alpha-synuclein transfers from neurons to oligodendrocytes. *Glia* **62**, 387–398 (2014).
123. Stefanova, N. *et al.* Striatal transplantation for multiple system atrophy--are grafts affected by alpha-synucleinopathy? *Exp. Neurol.* **219**, 368–371 (2009).
124. Prusiner, S. B. *et al.* Evidence for alpha-synuclein prions causing multiple system atrophy in humans with parkinsonism. *Proc. Natl. Acad. Sci. U. S. A.* **112**, E5308-17 (2015).
125. Kalaitzakis, M. E., Graeber, M. B., Gentleman, S. M. & Pearce, R. K. B. The dorsal motor nucleus of the vagus is not an obligatory trigger site of Parkinson’s disease: a critical analysis of alpha-synuclein staging. *Neuropathol. Appl. Neurobiol.* **34**, 284–295 (2008).
126. Jellinger, K. A. A critical reappraisal of current staging of Lewy-related pathology in human brain. *Acta Neuropathol.* **116**, 1–16 (2008).
127. Beach, T. G. *et al.* Multi-organ distribution of phosphorylated alpha-synuclein histopathology in subjects with Lewy body disorders. *Acta Neuropathol.* **119**, 689–702 (2010).
128. Brooks, D. J. Examining Braak’s hypothesis by imaging Parkinson’s disease. *Mov. Disord.* **25 Suppl 1**, S83-8 (2010).
129. Engelender, S. & Isacson, O. The Threshold Theory for Parkinson’s Disease. *Trends Neurosci.* **40**, 4–14 (2017).

130. Sastry, N. *et al.* No apparent transmission of transgenic alpha-synuclein into nigrostriatal dopaminergic neurons in multiple mouse models. *Transl. Neurodegener.* **4**, 23 (2015).
131. Mendez, I. *et al.* Dopamine neurons implanted into people with Parkinson's disease survive without pathology for 14 years. *Nat. Med.* **14**, 507 (2008).
132. Hallett, P. J. *et al.* Long-Term Health of Dopaminergic Neuron Transplants in Parkinson's Disease Patients. *Cell Rep.* **7**, 1755–1761 (2014).
133. Surmeier, D. J., Obeso, J. A. & Halliday, G. M. Parkinson's Disease Is Not Simply a Prion Disorder. *J. Neurosci.* **37**, 9799–9807 (2017).
134. Ghiglieri, V., Calabrese, V. & Calabresi, P. Alpha-Synuclein: From Early Synaptic Dysfunction to Neurodegeneration. *Front. Neurol.* **9**, 295 (2018).
135. Ostrerova, N. *et al.* alpha-Synuclein shares physical and functional homology with 14-3-3 proteins. *J. Neurosci.* **19**, 5782–5791 (1999).
136. Ahn, M., Kim, S., Kang, M., Ryu, Y. & Kim, T. D. Chaperone-like activities of alpha-synuclein: alpha-synuclein assists enzyme activities of esterases. *Biochem. Biophys. Res. Commun.* **346**, 1142–1149 (2006).
137. Rekas, A. *et al.* Interaction of the molecular chaperone alphaB-crystallin with alpha-synuclein: effects on amyloid fibril formation and chaperone activity. *J. Mol. Biol.* **340**, 1167–1183 (2004).
138. Souza, J. M., Giasson, B. I., Lee, V. M. & Ischiropoulos, H. Chaperone-like activity of synucleins. *FEBS Lett.* **474**, 116–119 (2000).
139. Kim, T. D., Paik, S. R., Yang, C. H. & Kim, J. Structural changes in alpha-synuclein affect its chaperone-like activity in vitro. *Protein Sci.* **9**, 2489–2496 (2000).
140. Ichimura, T. *et al.* Molecular cloning of cDNA coding for brain-specific 14-3-3 protein, a protein kinase-dependent activator of tyrosine and tryptophan hydroxylases. *Proc. Natl. Acad. Sci. U. S. A.* **85**, 7084–7088 (1988).
141. Perez, R. G. *et al.* A role for alpha-synuclein in the regulation of dopamine biosynthesis. *J. Neurosci.* **22**, 3090–3099 (2002).
142. Yu, S. *et al.* Inhibition of tyrosine hydroxylase expression in alpha-synuclein-transfected dopaminergic neuronal cells. *Neurosci. Lett.* **367**, 34–39 (2004).
143. Baptista, M. J. *et al.* Co-ordinate transcriptional regulation of dopamine synthesis genes by alpha-synuclein in human neuroblastoma cell lines. *J. Neurochem.* **85**, 957–968 (2003).
144. Wawer, A. *et al.* Exogenous alpha-Synuclein Monomers Alter Dopamine Metabolism in Murine Brain. *Neurochem. Res.* **41**, 2102–2109 (2016).
145. Wu, B. *et al.* Phosphorylation of alpha-synuclein upregulates tyrosine hydroxylase activity in MN9D cells. *Acta Histochem.* **113**, 32–35 (2011).
146. Burre, J. *et al.* Alpha-synuclein promotes SNARE-complex assembly in vivo and in vitro. *Science* **329**, 1663–1667 (2010).
147. Anwar, S. *et al.* Functional alterations to the nigrostriatal system in mice lacking all three members of the synuclein family. *J. Neurosci.* **31**, 7264–7274 (2011).
148. Chandra, S. *et al.* Double-knockout mice for alpha- and beta-synucleins: effect on synaptic functions. *Proc.*

- Natl. Acad. Sci. U. S. A.* **101**, 14966–14971 (2004).
149. Wu, N., Joshi, P. R., Cepeda, C., Masliah, E. & Levine, M. S. Alpha-synuclein overexpression in mice alters synaptic communication in the corticostriatal pathway. *J. Neurosci. Res.* **88**, 1764–1776 (2010).
  150. Vargas, K. J. *et al.* Synucleins regulate the kinetics of synaptic vesicle endocytosis. *J. Neurosci.* **34**, 9364–9376 (2014).
  151. Burre, J., Sharma, M. & Sudhof, T. C. alpha-Synuclein assembles into higher-order multimers upon membrane binding to promote SNARE complex formation. *Proc. Natl. Acad. Sci. U. S. A.* **111**, E4274-83 (2014).
  152. Wang, L. *et al.* alpha-synuclein multimers cluster synaptic vesicles and attenuate recycling. *Curr. Biol.* **24**, 2319–2326 (2014).
  153. Diao, J. *et al.* Native alpha-synuclein induces clustering of synaptic-vesicle mimics via binding to phospholipids and synaptobrevin-2/VAMP2. *Elife* **2**, e00592 (2013).
  154. Cooper, A. A. *et al.* Alpha-synuclein blocks ER-Golgi traffic and Rab1 rescues neuron loss in Parkinson's models. *Science* **313**, 324–328 (2006).
  155. Soper, J. H. *et al.* Alpha-synuclein-induced aggregation of cytoplasmic vesicles in *Saccharomyces cerevisiae*. *Mol. Biol. Cell* **19**, 1093–1103 (2008).
  156. Thayanidhi, N. *et al.* Alpha-synuclein delays endoplasmic reticulum (ER)-to-Golgi transport in mammalian cells by antagonizing ER/Golgi SNAREs. *Mol. Biol. Cell* **21**, 1850–1863 (2010).
  157. Lee, H. J., Kang, S. J., Lee, K. & Im, H. Human alpha-synuclein modulates vesicle trafficking through its interaction with prenylated Rab acceptor protein 1. *Biochem. Biophys. Res. Commun.* **412**, 526–531 (2011).
  158. Fang, F. *et al.* Synuclein impairs trafficking and signaling of BDNF in a mouse model of Parkinson's disease. *Sci. Rep.* **7**, 3868 (2017).
  159. Lautenschlager, J., Kaminski, C. F. & Kaminski Schierle, G. S. alpha-Synuclein - Regulator of Exocytosis, Endocytosis, or Both? *Trends Cell Biol.* **27**, 468–479 (2017).
  160. Xilouri, M., Brekk, O. R. & Stefanis, L. alpha-Synuclein and protein degradation systems: a reciprocal relationship. *Mol. Neurobiol.* **47**, 537–551 (2013).
  161. Schmid, A. W., Fauvet, B., Moniatte, M. & Lashuel, H. A. Alpha-synuclein Post-translational Modifications as Potential Biomarkers for Parkinson Disease and Other Synucleinopathies. *Mol. & Cell. Proteomics* **12**, 3543 LP-3558 (2013).
  162. Okochi, M. *et al.* Constitutive phosphorylation of the Parkinson's disease associated alpha-synuclein. *J. Biol. Chem.* **275**, 390–397 (2000).
  163. Fujiwara, H. *et al.* alpha-Synuclein is phosphorylated in synucleinopathy lesions. *Nat. Cell Biol.* **4**, 160–164 (2002).
  164. Anderson, J. P. *et al.* Phosphorylation of Ser-129 is the dominant pathological modification of alpha-synuclein in familial and sporadic Lewy body disease. *J. Biol. Chem.* **281**, 29739–29752 (2006).
  165. Zhou, J. *et al.* Changes in the solubility and phosphorylation of alpha-synuclein over the course of Parkinson's disease. *Acta Neuropathol.* **121**, 695–704 (2011).
  166. Walker, D. G. *et al.* Changes in properties of serine 129 phosphorylated alpha-synuclein with progression of Lewy-type histopathology in human brains. *Exp. Neurol.* **240**, 190–204 (2013).

167. Liu, L. L. & Franz, K. J. Phosphorylation-dependent metal binding by alpha-synuclein peptide fragments. *J. Biol. Inorg. Chem.* **12**, 234–247 (2007).
168. Pronin, A. N., Morris, A. J., Surguchov, A. & Benovic, J. L. Synucleins are a novel class of substrates for G protein-coupled receptor kinases. *J. Biol. Chem.* **275**, 26515–26522 (2000).
169. Nubling, G. S. *et al.* Modelling Ser129 phosphorylation inhibits membrane binding of pore-forming alpha-synuclein oligomers. *PLoS One* **9**, e98906 (2014).
170. Samuel, F. *et al.* Effects of Serine 129 Phosphorylation on alpha-Synuclein Aggregation, Membrane Association, and Internalization. *J. Biol. Chem.* **291**, 4374–4385 (2016).
171. Chau, K.-Y., Ching, H. L., Schapira, A. H. V & Cooper, J. M. Relationship between alpha synuclein phosphorylation, proteasomal inhibition and cell death: relevance to Parkinson's disease pathogenesis. *J. Neurochem.* **110**, 1005–1013 (2009).
172. Machiya, Y. *et al.* Phosphorylated alpha-synuclein at Ser-129 is targeted to the proteasome pathway in a ubiquitin-independent manner. *J. Biol. Chem.* **285**, 40732–40744 (2010).
173. Oueslati, A., Schneider, B. L., Aebischer, P. & Lashuel, H. A. Polo-like kinase 2 regulates selective autophagic alpha-synuclein clearance and suppresses its toxicity in vivo. *Proc. Natl. Acad. Sci. U. S. A.* **110**, E3945–54 (2013).
174. Hasegawa, M. *et al.* Phosphorylated alpha-synuclein is ubiquitinated in alpha-synucleinopathy lesions. *J. Biol. Chem.* **277**, 49071–49076 (2002).
175. Smith, W. W. *et al.* Alpha-synuclein phosphorylation enhances eosinophilic cytoplasmic inclusion formation in SH-SY5Y cells. *J. Neurosci.* **25**, 5544–5552 (2005).
176. Luk, K. C. *et al.* Exogenous alpha-synuclein fibrils seed the formation of Lewy body-like intracellular inclusions in cultured cells. *Proc. Natl. Acad. Sci. U. S. A.* **106**, 20051–20056 (2009).
177. Chen, L. & Feany, M. B. Alpha-synuclein phosphorylation controls neurotoxicity and inclusion formation in a *Drosophila* model of Parkinson disease. *Nat. Neurosci.* **8**, 657–663 (2005).
178. Sato, H. *et al.* Authentically phosphorylated alpha-synuclein at Ser129 accelerates neurodegeneration in a rat model of familial Parkinson's disease. *J. Neurosci.* **31**, 16884–16894 (2011).
179. Oueslati, A., Paleologou, K. E., Schneider, B. L., Aebischer, P. & Lashuel, H. A. Mimicking phosphorylation at serine 87 inhibits the aggregation of human alpha-synuclein and protects against its toxicity in a rat model of Parkinson's disease. *J. Neurosci.* **32**, 1536–1544 (2012).
180. Hebron, M. L., Lonskaya, I. & Moussa, C. E.-H. Nilotinib reverses loss of dopamine neurons and improves motor behavior via autophagic degradation of alpha-synuclein in Parkinson's disease models. *Hum. Mol. Genet.* **22**, 3315–3328 (2013).
181. Mahul-Mellier, A.-L. *et al.* c-Abl phosphorylates alpha-synuclein and regulates its degradation: implication for alpha-synuclein clearance and contribution to the pathogenesis of Parkinson's disease. *Hum. Mol. Genet.* **23**, 2858–2879 (2014).
182. Mezey, E. *et al.* Alpha synuclein is present in Lewy bodies in sporadic Parkinson's disease. *Mol. Psychiatry* **3**, 493–499 (1998).
183. Dickson, D. W. *et al.* Widespread alterations of alpha-synuclein in multiple system atrophy. *Am. J. Pathol.*

- 155**, 1241–1251 (1999).
184. Gomez-Tortosa, E., Newell, K., Irizarry, M. C., Sanders, J. L. & Hyman, B. T. alpha-Synuclein immunoreactivity in dementia with Lewy bodies: morphological staging and comparison with ubiquitin immunostaining. *Acta Neuropathol.* **99**, 352–357 (2000).
  185. Leroy, E. *et al.* The ubiquitin pathway in Parkinson's disease. *Nature* **395**, 451–452 (1998).
  186. Shimura, H. *et al.* Familial Parkinson disease gene product, parkin, is a ubiquitin-protein ligase. *Nat. Genet.* **25**, 302–305 (2000).
  187. Nonaka, T., Iwatsubo, T. & Hasegawa, M. Ubiquitination of alpha-synuclein. *Biochemistry* **44**, 361–368 (2005).
  188. Dorval, V. & Fraser, P. E. Small ubiquitin-like modifier (SUMO) modification of natively unfolded proteins tau and alpha-synuclein. *J. Biol. Chem.* **281**, 9919–9924 (2006).
  189. Kim, Y. M. *et al.* Proteasome inhibition induces alpha-synuclein SUMOylation and aggregate formation. *J. Neurol. Sci.* **307**, 157–161 (2011).
  190. Rott, R. *et al.* SUMOylation and ubiquitination reciprocally regulate alpha-synuclein degradation and pathological aggregation. *Proc. Natl. Acad. Sci. U. S. A.* **114**, 13176–13181 (2017).
  191. Krumova, P. *et al.* Sumoylation inhibits alpha-synuclein aggregation and toxicity. *J. Cell Biol.* **194**, 49–60 (2011).
  192. Alam, Z. I. *et al.* Oxidative DNA damage in the parkinsonian brain: an apparent selective increase in 8-hydroxyguanine levels in substantia nigra. *J. Neurochem.* **69**, 1196–1203 (1997).
  193. Floor, E. & Wetzel, M. G. Increased protein oxidation in human substantia nigra pars compacta in comparison with basal ganglia and prefrontal cortex measured with an improved dinitrophenylhydrazine assay. *J. Neurochem.* **70**, 268–275 (1998).
  194. Duda, J. E. *et al.* Widespread nitration of pathological inclusions in neurodegenerative synucleinopathies. *Am. J. Pathol.* **157**, 1439–1445 (2000).
  195. Giasson, B. I. *et al.* Oxidative damage linked to neurodegeneration by selective alpha-synuclein nitration in synucleinopathy lesions. *Science* **290**, 985–989 (2000).
  196. Paxinou, E. *et al.* Induction of alpha-synuclein aggregation by intracellular nitrative insult. *J. Neurosci.* **21**, 8053–8061 (2001).
  197. Hodara, R. *et al.* Functional consequences of alpha-synuclein tyrosine nitration: diminished binding to lipid vesicles and increased fibril formation. *J. Biol. Chem.* **279**, 47746–47753 (2004).
  198. Liu, Y., Qiang, M., Wei, Y. & He, R. A novel molecular mechanism for nitrated {alpha}-synuclein-induced cell death. *J. Mol. Cell Biol.* **3**, 239–249 (2011).
  199. Yu, Z. *et al.* Nitrated alpha-synuclein induces the loss of dopaminergic neurons in the substantia nigra of rats. *PLoS One* **5**, e9956 (2010).
  200. He, Y., Yu, Z. & Chen, S. Alpha-Synuclein Nitration and Its Implications in Parkinson's Disease. *ACS Chem. Neurosci.* (2018). doi:10.1021/acchemneuro.8b00288
  201. Zhou, W. *et al.* Methionine oxidation stabilizes non-toxic oligomers of alpha-synuclein through strengthening the auto-inhibitory intra-molecular long-range interactions. *Biochim. Biophys. Acta* **1802**, 322–330 (2010).

202. Nakaso, K. *et al.* Dopamine-mediated oxidation of methionine 127 in alpha-synuclein causes cytotoxicity and oligomerization of alpha-synuclein. *PLoS One* **8**, e55068 (2013).
203. Al-Hilaly, Y. K. *et al.* The involvement of dityrosine crosslinking in alpha-synuclein assembly and deposition in Lewy Bodies in Parkinson's disease. *Sci. Rep.* **6**, 39171 (2016).
204. Bartels, T., Kim, N. C., Luth, E. S. & Selkoe, D. J. N-alpha-acetylation of alpha-synuclein increases its helical folding propensity, GM1 binding specificity and resistance to aggregation. *PLoS One* **9**, e103727 (2014).
205. Dikiy, I. & Eliezer, D. N-terminal acetylation stabilizes N-terminal helicity in lipid- and micelle-bound alpha-synuclein and increases its affinity for physiological membranes. *J. Biol. Chem.* **289**, 3652–3665 (2014).
206. Vicente Miranda, H. *et al.* Glycation potentiates alpha-synuclein-associated neurodegeneration in synucleinopathies. *Brain* **140**, 1399–1419 (2017).
207. Prasad, K., Beach, T. G., Hedreen, J. & Richfield, E. K. Critical role of truncated alpha-synuclein and aggregates in Parkinson's disease and incidental Lewy body disease. *Brain Pathol.* **22**, 811–825 (2012).
208. Hoyer, W., Cherny, D., Subramaniam, V. & Jovin, T. M. Impact of the acidic C-terminal region comprising amino acids 109-140 on alpha-synuclein aggregation in vitro. *Biochemistry* **43**, 16233–16242 (2004).
209. Crowther, R. A., Jakes, R., Spillantini, M. G. & Goedert, M. Synthetic filaments assembled from C-terminally truncated alpha-synuclein. *FEBS Lett.* **436**, 309–312 (1998).
210. Li, W. *et al.* Aggregation promoting C-terminal truncation of alpha-synuclein is a normal cellular process and is enhanced by the familial Parkinson's disease-linked mutations. *Proc. Natl. Acad. Sci. U. S. A.* **102**, 2162–2167 (2005).
211. Daher, J. P. L. *et al.* Conditional transgenic mice expressing C-terminally truncated human alpha-synuclein (alphaSyn119) exhibit reduced striatal dopamine without loss of nigrostriatal pathway dopaminergic neurons. *Mol. Neurodegener.* **4**, 34 (2009).
212. Wakamatsu, M. *et al.* Selective loss of nigral dopamine neurons induced by overexpression of truncated human alpha-synuclein in mice. *Neurobiol. Aging* **29**, 574–585 (2008).
213. Ulusoy, A., Febbraro, F., Jensen, P. H., Kirik, D. & Romero-Ramos, M. Co-expression of C-terminal truncated alpha-synuclein enhances full-length alpha-synuclein-induced pathology. *Eur. J. Neurosci.* **32**, 409–422 (2010).
214. Hall, K., Yang, S., Sauchanka, O., Spillantini, M. G. & Anichtchik, O. Behavioural deficits in transgenic mice expressing human truncated (1-120 amino acid) alpha-synuclein. *Exp. Neurol.* **264**, 8–13 (2015).
215. Michell, A. W. *et al.* The effect of truncated human alpha-synuclein (1-120) on dopaminergic cells in a transgenic mouse model of Parkinson's disease. *Cell Transplant.* **16**, 461–474 (2007).
216. Games, D. *et al.* Reducing C-terminal-truncated alpha-synuclein by immunotherapy attenuates neurodegeneration and propagation in Parkinson's disease-like models. *J. Neurosci.* **34**, 9441–9454 (2014).
217. Lewis, K. A., Yaeger, A., DeMartino, G. N. & Thomas, P. J. Accelerated formation of alpha-synuclein oligomers by concerted action of the 20S proteasome and familial Parkinson mutations. *J. Bioenerg. Biomembr.* **42**, 85–95 (2010).
218. Toulorge, D., Schapira, A. H. V & Hajj, R. Molecular changes in the postmortem parkinsonian brain. *J. Neurochem.* **139 Suppl**, 27–58 (2016).

219. Chu, Y., Dodiya, H., Aebischer, P., Olanow, C. W. & Kordower, J. H. Alterations in lysosomal and proteasomal markers in Parkinson's disease: relationship to alpha-synuclein inclusions. *Neurobiol. Dis.* **35**, 385–398 (2009).
220. Murphy, K. E. *et al.* Reduced glucocerebrosidase is associated with increased alpha-synuclein in sporadic Parkinson's disease. *Brain* **137**, 834–848 (2014).
221. Sevlever, D., Jiang, P. & Yen, S.-H. C. Cathepsin D is the main lysosomal enzyme involved in the degradation of alpha-synuclein and generation of its carboxy-terminally truncated species. *Biochemistry* **47**, 9678–9687 (2008).
222. Takahashi, M. *et al.* Oxidative stress-induced phosphorylation, degradation and aggregation of alpha-synuclein are linked to upregulated CK2 and cathepsin D. *Eur. J. Neurosci.* **26**, 863–874 (2007).
223. Cullen, V. *et al.* Cathepsin D expression level affects alpha-synuclein processing, aggregation, and toxicity in vivo. *Mol. Brain* **2**, 5 (2009).
224. Qiao, L. *et al.* Lysosomal enzyme cathepsin D protects against alpha-synuclein aggregation and toxicity. *Mol. Brain* **1**, 17 (2008).
225. Bae, E.-J. *et al.* Haploinsufficiency of cathepsin D leads to lysosomal dysfunction and promotes cell-to-cell transmission of alpha-synuclein aggregates. *Cell Death Dis.* **6**, e1901 (2015).
226. Crabtree, D. *et al.* Over-expression of an inactive mutant cathepsin D increases endogenous alpha-synuclein and cathepsin B activity in SH-SY5Y cells. *J. Neurochem.* **128**, 950–961 (2014).
227. McGlinchey, R. P. & Lee, J. C. Cysteine cathepsins are essential in lysosomal degradation of alpha-synuclein. *Proc. Natl. Acad. Sci. U. S. A.* **112**, 9322–9327 (2015).
228. Tsujimura, A. *et al.* Lysosomal enzyme cathepsin B enhances the aggregate forming activity of exogenous alpha-synuclein fibrils. *Neurobiol. Dis.* **73**, 244–253 (2015).
229. Dufty, B. M. *et al.* Calpain-cleavage of alpha-synuclein: connecting proteolytic processing to disease-linked aggregation. *Am. J. Pathol.* **170**, 1725–1738 (2007).
230. Suzuki, K., Hata, S., Kawabata, Y. & Sorimachi, H. Structure, activation, and biology of calpain. *Diabetes* **53 Suppl 1**, S12-8 (2004).
231. Mishizen-Eberz, A. J. *et al.* Distinct cleavage patterns of normal and pathologic forms of alpha-synuclein by calpain I in vitro. *J. Neurochem.* **86**, 836–847 (2003).
232. Mishizen-Eberz, A. J. *et al.* Cleavage of alpha-synuclein by calpain: potential role in degradation of fibrillized and nitrated species of alpha-synuclein. *Biochemistry* **44**, 7818–7829 (2005).
233. Diepenbroek, M. *et al.* Overexpression of the calpain-specific inhibitor calpastatin reduces human alpha-Synuclein processing, aggregation and synaptic impairment in [A30P]alphaSyn transgenic mice. *Hum. Mol. Genet.* **23**, 3975–3989 (2014).
234. Venderova, K. & Park, D. S. Programmed cell death in Parkinson's disease. *Cold Spring Harb. Perspect. Med.* **2**, (2012).
235. Denes, A., Lopez-Castejon, G. & Brough, D. Caspase-1: is IL-1 just the tip of the ICEberg? *Cell Death Dis.* **3**, e338 (2012).
236. Wang, W. *et al.* Caspase-1 causes truncation and aggregation of the Parkinson's disease-associated protein

- alpha-synuclein. *Proc. Natl. Acad. Sci. U. S. A.* **113**, 9587–9592 (2016).
237. Bassil, F. *et al.* Reducing C-terminal truncation mitigates synucleinopathy and neurodegeneration in a transgenic model of multiple system atrophy. *Proc. Natl. Acad. Sci. U. S. A.* **113**, 9593–9598 (2016).
  238. Kim, K. S. *et al.* Proteolytic cleavage of extracellular alpha-synuclein by plasmin: implications for Parkinson disease. *J. Biol. Chem.* **287**, 24862–24872 (2012).
  239. Ogawa, K. *et al.* Localization of a novel type trypsin-like serine protease, neurosin, in brain tissues of Alzheimer's disease and Parkinson's disease. *Psychiatry Clin. Neurosci.* **54**, 419–426 (2000).
  240. Iwata, A. *et al.* Alpha-synuclein degradation by serine protease neurosin: implication for pathogenesis of synucleinopathies. *Hum. Mol. Genet.* **12**, 2625–2635 (2003).
  241. Spencer, B. *et al.* Lentivirus mediated delivery of neurosin promotes clearance of wild-type alpha-synuclein and reduces the pathology in an alpha-synuclein model of LBD. *Mol. Ther.* **21**, 31–41 (2013).
  242. Kasai, T. *et al.* Cleavage of normal and pathological forms of alpha-synuclein by neurosin in vitro. *Neurosci. Lett.* **436**, 52–56 (2008).
  243. Tatebe, H. *et al.* Extracellular neurosin degrades alpha-synuclein in cultured cells. *Neurosci. Res.* **67**, 341–346 (2010).
  244. Ximerakis, M. *et al.* Resistance of naturally secreted alpha-synuclein to proteolysis. *FASEB J. Off. Publ. Fed. Am. Soc. Exp. Biol.* **28**, 3146–3158 (2014).
  245. Pampalakis, G. *et al.* KLK6 proteolysis is implicated in the turnover and uptake of extracellular alpha-synuclein species. *Oncotarget* **8**, 14502–14515 (2017).
  246. Sung, J. Y. *et al.* Proteolytic cleavage of extracellular secreted {alpha}-synuclein via matrix metalloproteinases. *J. Biol. Chem.* **280**, 25216–25224 (2005).
  247. Choi, D.-H. *et al.* Role of matrix metalloproteinase 3-mediated alpha-synuclein cleavage in dopaminergic cell death. *J. Biol. Chem.* **286**, 14168–14177 (2011).
  248. Kim, Y. S. Y. J. *et al.* A pivotal role of matrix metalloproteinase-3 activity in dopaminergic neuronal degeneration via microglial activation. *FASEB J. Off. Publ. Fed. Am. Soc. Exp. Biol.* **21**, 179–187 (2007).
  249. Levin, J. *et al.* Increased alpha-synuclein aggregation following limited cleavage by certain matrix metalloproteinases. *Exp. Neurol.* **215**, 201–208 (2009).
  250. Bassil, F. *et al.* Region-Specific Alterations of Matrix Metalloproteinase Activity in Multiple System Atrophy. *Mov. Disord.* **30**, 1802–1812 (2015).
  251. Hendgen-Cotta, U. B., Kelm, M. & Rassaf, T. Myoglobin functions in the heart. *Free Radic. Biol. Med.* **73**, 252–259 (2014).
  252. Burmester, T. & Hankeln, T. Function and evolution of vertebrate globins. *Acta Physiol. (Oxf).* **211**, 501–514 (2014).
  253. Vinogradov, S. N. & Moens, L. Diversity of globin function: enzymatic, transport, storage, and sensing. *J. Biol. Chem.* **283**, 8773–8777 (2008).
  254. Hardison, R. C. A brief history of hemoglobins: plant, animal, protist, and bacteria. *Proc. Natl. Acad. Sci. U. S. A.* **93**, 5675–5679 (1996).
  255. Rahaman, M. M. & Straub, A. C. The emerging roles of somatic globins in cardiovascular redox biology and

- beyond. *Redox Biol.* **1**, 405–410 (2013).
256. Ascenzi, P. *et al.* Neuroglobin: From structure to function in health and disease. *Mol. Aspects Med.* **52**, 1–48 (2016).
  257. Burmester, T., Weich, B., Reinhardt, S. & Hankeln, T. A vertebrate globin expressed in the brain. *Nature* **407**, 520–523 (2000).
  258. Schmidt-Kastner, R., Haberkamp, M., Schmitz, C., Hankeln, T. & Burmester, T. Neuroglobin mRNA expression after transient global brain ischemia and prolonged hypoxia in cell culture. *Brain Res.* **1103**, 173–180 (2006).
  259. Wittenberg, J. B. & Wittenberg, B. A. Myoglobin function reassessed. *J. Exp. Biol.* **206**, 2011–2020 (2003).
  260. Cossins, A. R., Williams, D. R., Foulkes, N. S., Berenbrink, M. & Kipar, A. Diverse cell-specific expression of myoglobin isoforms in brain, kidney, gill and liver of the hypoxia-tolerant carp and zebrafish. *J. Exp. Biol.* **212**, 627–638 (2009).
  261. Fraser, J. *et al.* Hypoxia-inducible myoglobin expression in nonmuscle tissues. *Proc. Natl. Acad. Sci. U. S. A.* **103**, 2977–2981 (2006).
  262. Flonta, S. E., Arena, S., Pisacane, A., Michieli, P. & Bardelli, A. Expression and functional regulation of myoglobin in epithelial cancers. *Am. J. Pathol.* **175**, 201–206 (2009).
  263. de Sanctis, D. *et al.* Crystal structure of cytoglobin: the fourth globin type discovered in man displays heme hexa-coordination. *J. Mol. Biol.* **336**, 917–927 (2004).
  264. Burmester, T., Ebner, B., Weich, B. & Hankeln, T. Cytoglobin: a novel globin type ubiquitously expressed in vertebrate tissues. *Mol. Biol. Evol.* **19**, 416–421 (2002).
  265. Schmidt, M. *et al.* Cytoglobin is a respiratory protein in connective tissue and neurons, which is up-regulated by hypoxia. *J. Biol. Chem.* **279**, 8063–8069 (2004).
  266. Oleksiewicz, U., Liloglou, T., Field, J. K. & Xinarianos, G. Cytoglobin: biochemical, functional and clinical perspective of the newest member of the globin family. *Cell. Mol. Life Sci.* **68**, 3869–3883 (2011).
  267. Mammen, P. P. A. *et al.* Cytoglobin is a stress-responsive hemoprotein expressed in the developing and adult brain. *J. Histochem. Cytochem.* **54**, 1349–1361 (2006).
  268. Fordel, E. *et al.* Cytoglobin expression is upregulated in all tissues upon hypoxia: an in vitro and in vivo study by quantitative real-time PCR. *Biochem. Biophys. Res. Commun.* **319**, 342–348 (2004).
  269. Roesner, A., Fuchs, C., Hankeln, T. & Burmester, T. A globin gene of ancient evolutionary origin in lower vertebrates: evidence for two distinct globin families in animals. *Mol. Biol. Evol.* **22**, 12–20 (2005).
  270. Fuchs, C., Burmester, T. & Hankeln, T. The amphibian globin gene repertoire as revealed by the *Xenopus* genome. *Cytogenet. Genome Res.* **112**, 296–306 (2006).
  271. Kugelstadt, D., Haberkamp, M., Hankeln, T. & Burmester, T. Neuroglobin, cytoglobin, and a novel, eye-specific globin from chicken. *Biochem. Biophys. Res. Commun.* **325**, 719–725 (2004).
  272. Hoogewijs, D. *et al.* Androglobin: a chimeric globin in metazoans that is preferentially expressed in Mammalian testes. *Mol. Biol. Evol.* **29**, 1105–1114 (2012).
  273. Hardison, R. C. Evolution of hemoglobin and its genes. *Cold Spring Harb. Perspect. Med.* **2**, a011627 (2012).
  274. Hardison, R. Hemoglobins from bacteria to man: evolution of different patterns of gene expression. *J. Exp.*

- Biol.* **201**, 1099–1117 (1998).
275. Smith, E. C. & Orkin, S. H. Hemoglobin genetics: recent contributions of GWAS and gene editing. *Hum. Mol. Genet.* **25**, R99–R105 (2016).
  276. Iarovaia, O. V *et al.* Genetic and Epigenetic Mechanisms of beta-Globin Gene Switching. *Biochemistry (Mosc)*. **83**, 381–392 (2018).
  277. Lee, W. S., McColl, B., Maksimovic, J. & Vadolas, J. Epigenetic interplay at the beta-globin locus. *Biochim. Biophys. Acta. Gene Regul. Mech.* **1860**, 393–404 (2017).
  278. Mettananda, S., Gibbons, R. J. & Higgs, D. R. Understanding alpha-globin gene regulation and implications for the treatment of beta-thalassemia. *Ann. N. Y. Acad. Sci.* **1368**, 16–24 (2016).
  279. Higgs, D. R., Engel, J. D. & Stamatoyannopoulos, G. Thalassemia. *Lancet* **379**, 373–383 (2012).
  280. Thom, C. S., Dickson, C. F., Gell, D. A. & Weiss, M. J. Hemoglobin variants: biochemical properties and clinical correlates. *Cold Spring Harb. Perspect. Med.* **3**, a011858 (2013).
  281. Perutz, M. F., Fermi, G. & Shih, T. B. Structure of deoxyhemoglobin Cowtown [His HC3(146) beta----Leu]: origin of the alkaline Bohr effect and electrostatic interactions in hemoglobin. *Proc. Natl. Acad. Sci. U. S. A.* **81**, 4781–4784 (1984).
  282. MacDonald, R. Red cell 2,3-diphosphoglycerate and oxygen affinity. *Anaesthesia* **32**, 544–553 (1977).
  283. Schechter, A. N. Hemoglobin research and the origins of molecular medicine. *Blood* **112**, 3927–3938 (2008).
  284. Gladwin, M. T., Lancaster, J. R. J., Freeman, B. A. & Schechter, A. N. Nitric oxide's reactions with hemoglobin: a view through the SNO-storm. *Nat. Med.* **9**, 496–500 (2003).
  285. Singel, D. J. & Stamler, J. S. Chemical physiology of blood flow regulation by red blood cells: the role of nitric oxide and S-nitrosohemoglobin. *Annu. Rev. Physiol.* **67**, 99–145 (2005).
  286. Schechter, A. N. & Gladwin, M. T. Hemoglobin and the paracrine and endocrine functions of nitric oxide. *N. Engl. J. Med.* **348**, 1483–1485 (2003).
  287. Kim, H.-H. & Choi, S. Therapeutic Aspects of Carbon Monoxide in Cardiovascular Disease. *International Journal of Molecular Sciences* **19**, (2018).
  288. Quaye, I. K. Extracellular hemoglobin: the case of a friend turned foe. *Front. Physiol.* **6**, 96 (2015).
  289. Rifkind, J. M., Mohanty, J. G. & Nagababu, E. The pathophysiology of extracellular hemoglobin associated with enhanced oxidative reactions. *Front. Physiol.* **5**, 500 (2014).
  290. Kawano, T., Pinontoan, R., Hosoya, H. & Muto, S. Monoamine-dependent production of reactive oxygen species catalyzed by pseudoperoxidase activity of human hemoglobin. *Biosci. Biotechnol. Biochem.* **66**, 1224–1232 (2002).
  291. Jiang, N., Tan, N. S., Ho, B. & Ding, J. L. Respiratory protein-generated reactive oxygen species as an antimicrobial strategy. *Nat. Immunol.* **8**, 1114 (2007).
  292. Du, R., Ho, B. & Ding, J. L. Rapid reprogramming of haemoglobin structure-function exposes multiple dual-antimicrobial potencies. *EMBO J.* **29**, 632–642 (2010).
  293. Parish, C. A. *et al.* Broad-spectrum antimicrobial activity of hemoglobin. *Bioorg. Med. Chem.* **9**, 377–382 (2001).
  294. Forget, B. G. & Bunn, H. F. Classification of the disorders of hemoglobin. *Cold Spring Harb. Perspect. Med.*

- 3**, a011684 (2013).
295. Groudine, M. & Weintraub, H. Rous sarcoma virus activates embryonic globin genes in chicken fibroblasts. *Proc. Natl. Acad. Sci. U. S. A.* **72**, 4464–4468 (1975).
  296. Cheung, P., Panning, B. & Smiley, J. R. Herpes simplex virus immediate-early proteins ICP0 and ICP4 activate the endogenous human alpha-globin gene in nonerythroid cells. *J. Virol.* **71**, 1784 LP-1793 (1997).
  297. Liu, L., Zeng, M. & Stamler, J. S. Hemoglobin induction in mouse macrophages. *Proc. Natl. Acad. Sci. U. S. A.* **96**, 6643–6647 (1999).
  298. Bhaskaran, M., Chen, H., Chen, Z. & Liu, L. Hemoglobin is expressed in alveolar epithelial type II cells. *Biochem. Biophys. Res. Commun.* **333**, 1348–1352 (2005).
  299. Newton, D. A., Rao, K. M. K., Dluhy, R. A. & Baatz, J. E. Hemoglobin is expressed by alveolar epithelial cells. *J. Biol. Chem.* **281**, 5668–5676 (2006).
  300. Grek, C. L., Newton, D. A., Spyropoulos, D. D. & Baatz, J. E. Hypoxia up-regulates expression of hemoglobin in alveolar epithelial cells. *Am. J. Respir. Cell Mol. Biol.* **44**, 439–447 (2011).
  301. Tezel, T. H. *et al.* Synthesis and secretion of hemoglobin by retinal pigment epithelium. *Invest. Ophthalmol. Vis. Sci.* **50**, 1911–1919 (2009).
  302. Tezel, G. *et al.* Hemoglobin expression and regulation in glaucoma: insights into retinal ganglion cell oxygenation. *Invest. Ophthalmol. Vis. Sci.* **51**, 907–919 (2010).
  303. Tezel, G. Oxidative stress in glaucomatous neurodegeneration: mechanisms and consequences. *Prog. Retin. Eye Res.* **25**, 490–513 (2006).
  304. Liu, W., Baker, S. S., Baker, R. D., Nowak, N. J. & Zhu, L. Upregulation of hemoglobin expression by oxidative stress in hepatocytes and its implication in nonalcoholic steatohepatitis. *PLoS One* **6**, e24363 (2011).
  305. Nishi, H. *et al.* Hemoglobin is expressed by mesangial cells and reduces oxidant stress. *J. Am. Soc. Nephrol.* **19**, 1500–1508 (2008).
  306. Saha, D., Koli, S. & Reddy, K. V. R. Transcriptional regulation of Hb-alpha and Hb-beta through nuclear factor E2-related factor-2 (Nrf2) activation in human vaginal cells: A novel mechanism of cellular adaptability to oxidative stress. *Am. J. Reprod. Immunol.* **77**, (2017).
  307. Saha, D., Koli, S., Patgaonkar, M. & Reddy, K. V. R. Expression of hemoglobin-alpha and beta subunits in human vaginal epithelial cells and their functional significance. *PLoS One* **12**, e0171084 (2017).
  308. Onda, M. *et al.* Decreased expression of haemoglobin beta (HBB) gene in anaplastic thyroid cancer and recovery of its expression inhibits cell growth. *Br. J. Cancer* **92**, 2216–2224 (2005).
  309. Li, X. *et al.* Characterization of adult alpha- and beta-globin elevated by hydrogen peroxide in cervical cancer cells that play a cytoprotective role against oxidative insults. *PLoS One* **8**, e54342 (2013).
  310. Maman, S. *et al.* The Beta Subunit of Hemoglobin (HBB2/HBB) Suppresses Neuroblastoma Growth and Metastasis. *Cancer Res.* **77**, 14–26 (2017).
  311. Ponzetti, M. *et al.* Non-conventional role of haemoglobin beta in breast malignancy. *Br. J. Cancer* **117**, 994–1006 (2017).
  312. Zheng, Y. *et al.* Expression of beta-globin by cancer cells promotes cell survival during blood-borne dissemination. *Nat. Commun.* **8**, 14344 (2017).

313. RICHTER, F., MEURERS, B. H., ZHU, C., MEDVEDEVA, V. P. & CHESSELET, M.-F. Neurons Express Hemoglobin  $\alpha$ - and  $\beta$ -Chains in Rat and Human Brains. *J. Comp. Neurol.* **515**, 538–547 (2009).
314. Schelshorn, D. W. *et al.* Expression of Hemoglobin in Rodent Neurons. *J. Cereb. Blood Flow Metab.* **29**, 585–595 (2008).
315. Russo, R. *et al.* Hemoglobin is present as a canonical alpha2beta2 tetramer in dopaminergic neurons. *Biochim. Biophys. Acta* **1834**, 1939–1943 (2013).
316. Ferrer, I. *et al.* Neuronal hemoglobin is reduced in Alzheimer’s disease, argyrophilic grain disease, Parkinson’s disease, and dementia with Lewy bodies. *J. Alzheimers. Dis.* **23**, 537–550 (2011).
317. Vanni, S. *et al.* Hemoglobin mRNA Changes in the Frontal Cortex of Patients with Neurodegenerative Diseases. *Front. Neurosci.* **12**, 8 (2018).
318. Do Carmo, S. *et al.* Hippocampal Proteomic Analysis Reveals Distinct Pathway Deregulation Profiles at Early and Late Stages in a Rat Model of Alzheimer’s-Like Amyloid Pathology. *Mol. Neurobiol.* **55**, 3451–3476 (2018).
319. Wu, C.-W. *et al.* Hemoglobin promotes A $\beta$  oligomer formation and localizes in neurons and amyloid deposits. *Neurobiol. Dis.* **17**, 367–377 (2004).
320. Chuang, J.-Y. *et al.* Interactions between amyloid-beta and hemoglobin: implications for amyloid plaque formation in Alzheimer’s disease. *PLoS One* **7**, e33120 (2012).
321. Booth, S. *et al.* Identification of central nervous system genes involved in the host response to the scrapie agent during preclinical and clinical infection. *J. Gen. Virol.* **85**, 3459–3471 (2004).
322. Kim, H. O. *et al.* Prion disease induced alterations in gene expression in spleen and brain prior to clinical symptoms. *Adv. Appl. Bioinform. Chem.* **1**, 29–50 (2008).
323. Barbisin, M. *et al.* Gene expression profiling of brains from bovine spongiform encephalopathy (BSE)-infected cynomolgus macaques. *BMC Genomics* **15**, 434 (2014).
324. Xerxa, E. *et al.* Whole Blood Gene Expression Profiling in Preclinical and Clinical Cattle Infected with Atypical Bovine Spongiform Encephalopathy. *PLoS One* **11**, e0153425 (2016).
325. Abbott, R. D. *et al.* Late-life hemoglobin and the incidence of Parkinson’s disease. *Neurobiol. Aging* **33**, 914–920 (2012).
326. Savica, R. *et al.* Anemia or low hemoglobin levels preceding Parkinson disease: a case-control study. *Neurology* **73**, 1381–1387 (2009).
327. Santiago, J. A. & Potashkin, J. A. Blood Transcriptomic Meta-analysis Identifies Dysregulation of Hemoglobin and Iron Metabolism in Parkinson’ Disease. *Front. Aging Neurosci.* **9**, 73 (2017).
328. Shephard, F., Greville-Heygate, O., Marsh, O., Anderson, S. & Chakrabarti, L. A mitochondrial location for haemoglobins--dynamic distribution in ageing and Parkinson’s disease. *Mitochondrion* **14**, 64–72 (2014).
329. Shephard, F., Greville-Heygate, O., Liddell, S., Emes, R. & Chakrabarti, L. Analysis of Mitochondrial haemoglobin in Parkinson’s disease brain. *Mitochondrion* **29**, 45–52 (2016).
330. Mills, J. D., Kim, W. S., Halliday, G. M. & Janitz, M. Transcriptome analysis of grey and white matter cortical tissue in multiple system atrophy. *Neurogenetics* **16**, 107–122 (2015).
331. Mills, J. D., Ward, M., Kim, W. S., Halliday, G. M. & Janitz, M. Strand-specific RNA-sequencing analysis

- of multiple system atrophy brain transcriptome. *Neuroscience* **322**, 234–250 (2016).
332. Schafferer, S. *et al.* Changes in the miRNA-mRNA Regulatory Network Precede Motor Symptoms in a Mouse Model of Multiple System Atrophy: Clinical Implications. *PLoS One* **11**, e0150705 (2016).
333. Broadwater, L. *et al.* Analysis of the mitochondrial proteome in multiple sclerosis cortex. *Biochim. Biophys. Acta* **1812**, 630–641 (2011).
334. Brown, N. *et al.* Neuronal Hemoglobin Expression and Its Relevance to Multiple Sclerosis Neuropathology. *J. Mol. Neurosci.* **59**, 1–17 (2016).
335. Biedler, J. L., Helson, L. & Spengler, B. A. Morphology and growth, tumorigenicity, and cytogenetics of human neuroblastoma cells in continuous culture. *Cancer Res.* **33**, 2643–2652 (1973).
336. Huang, C., Ren, G., Zhou, H. & Wang, C. A new method for purification of recombinant human alpha-synuclein in Escherichia coli. *Protein Expr. Purif.* **42**, 173–177 (2005).
337. Latawiec, D. *et al.* Modulation of alpha-synuclein aggregation by dopamine analogs. *PLoS One* **5**, e9234 (2010).
338. Helferich, A. M. *et al.* alpha-synuclein interacts with SOD1 and promotes its oligomerization. *Mol. Neurodegener.* **10**, 66 (2015).
339. Karpowicz, R. J. J. *et al.* Selective imaging of internalized proteopathic alpha-synuclein seeds in primary neurons reveals mechanistic insight into transmission of synucleinopathies. *J. Biol. Chem.* **292**, 13482–13497 (2017).
340. Livak, K. J. & Schmittgen, T. D. Analysis of relative gene expression data using real-time quantitative PCR and the 2<sup>-</sup>(Delta Delta C(T)) Method. *Methods* **25**, 402–408 (2001).
341. Schmittgen, T. D. & Livak, K. J. Analyzing real-time PCR data by the comparative C(T) method. *Nat. Protoc.* **3**, 1101–1108 (2008).
342. Vlad, C. *et al.* Autoproteolytic fragments are intermediates in the oligomerization/aggregation of the Parkinson's disease protein alpha-synuclein as revealed by ion mobility mass spectrometry. *Chembiochem* **12**, 2740–2744 (2011).
343. Aulić, S. *et al.* Defined alpha-synuclein prion-like molecular assemblies spreading in cell culture. *BMC Neurosci.* **15**, 69 (2014).
344. Sacino, A. N. *et al.* Proteolysis of alpha-synuclein fibrils in the lysosomal pathway limits induction of inclusion pathology. *J. Neurochem.* **140**, 662–678 (2017).
345. Xu, H. & Ren, D. Lysosomal physiology. *Annu. Rev. Physiol.* **77**, 57–80 (2015).
346. Lieberman, O. J. *et al.* alpha-Synuclein-Dependent Calcium Entry Underlies Differential Sensitivity of Cultured SN and VTA Dopaminergic Neurons to a Parkinsonian Neurotoxin. *eNeuro* **4**, (2017).
347. Lowe, R., Pountney, D. L., Jensen, P. H., Gai, W. P. & Voelcker, N. H. Calcium(II) selectively induces alpha-synuclein annular oligomers via interaction with the C-terminal domain. *Protein Sci.* **13**, 3245–3252 (2004).
348. Goodwin, J., Nath, S., Engelborghs, Y. & Pountney, D. L. Raised calcium and oxidative stress cooperatively promote alpha-synuclein aggregate formation. *Neurochem. Int.* **62**, 703–711 (2013).